

CASE FILE
COPY

NACA TN 4309

NATIONAL ADVISORY COMMITTEE FOR AERONAUTICS

TECHNICAL NOTE 4309

USE OF SHORT FLAT VANES FOR PRODUCING EFFICIENT WIDE-ANGLE
TWO-DIMENSIONAL SUBSONIC DIFFUSERS

By D. L. Cochran and S. J. Kline

Stanford University

DEC 30 1958

PROPERTY AIRCRAFT
ENGINEERING LIBRARY



Washington

September 1958

NATIONAL ADVISORY COMMITTEE FOR AERONAUTICS

TECHNICAL NOTE 4309

USE OF SHORT FLAT VANES FOR PRODUCING EFFICIENT WIDE-ANGLE

TWO-DIMENSIONAL SUBSONIC DIFFUSERS

By D. L. Cochran and S. J. Kline

SUMMARY

An investigation of the use of flat vanes in two-dimensional subsonic diffusers was made. Using optimum designs of vane installations, high pressure recoveries and steady flows were obtained for diffuser-wall divergence angles up to 42° . Criteria for optimum configurations were developed which indicated that the vanes should be symmetrically arranged in the vicinity of the diffuser throat, that the vane-passage divergence angle should be approximately 7.0° , and that the vanes should have a certain predictable length dependent upon the diffuser geometry.

INTRODUCTION

In virtually all systems involving the motion of fluids the need arises to accelerate or decelerate the flow. In general, a flow acceleration (or nozzle process) results in a smooth flow with high effectiveness, low loss, and good velocity profiles. On the other hand, unless considerable care is taken in the design of the passages involved, a flow deceleration (or diffusion process) almost always results in unsteady flows with large pulsations, large losses, and highly nonuniform exit velocity profiles. Such a condition is not only undesirable in itself but it also frequently creates even more undesirable effects on the performance of downstream components such as compressors and burners.

This problem becomes particularly aggravated when a space limitation is present as, for example, in jet engines. Since a given deceleration of the flow requires a given area ratio, by continuity, a compact subsonic diffuser must necessarily incorporate large angles of divergence of the walls, but such geometries are precisely those that create the most unsteady flow, the largest losses, and the most unpredictable behavior. Thus, the discovery of a means for production of wide-angle diffusers of high performance, stable flow, and predictable behavior is a problem of considerable concern. The study of a promising solution to this problem by the use of well-designed, short, flat vanes is one of the primary purposes of the present investigation.

The basic cause of the poor flows found in diffusers has been known for many years to lie in the effect of an adverse pressure gradient (pressure increasing in the direction of the flow) on the boundary layer which inevitably occurs on the walls in any real fluid flow. Since diffusion, by definition, involves an adverse pressure gradient and since in almost all applications of interest the boundary layer on the walls is turbulent in character, the problem of diffuser flows is inextricably connected with the problem of the flow of a turbulent boundary layer in an adverse pressure gradient and, hence, with the problem of stall or separation. These problems have been the object of a great deal of theoretical and experimental effort over the past 50 years, but despite this, sufficient understanding has not been gained. Consequently, no means are available for advance theoretical prediction of even the overall basic flow pattern that will occur in a given diffuser, and it is therefore necessary not only to measure performance but also to study the basic flow mechanisms if any real understanding of diffuser behavior is to be obtained. Thus, the second principal objective of the present investigation is to add to the available knowledge concerning the flow mechanisms in diffusers, that is, flows with adverse pressure gradients.

Both of these objectives are being pursued as a portion of a continuing research program in the Mechanical Engineering Laboratory at Stanford University. The experimental work on vanes in wide-angle diffusers in itself constitutes a rather extensive research program; therefore, the emphasis of the present report has been placed on the presentation of the experimental results; description of the flows, and discussion of a means for the design of vaned wide-angle diffusers having good flow characteristics and high performance. This report is based primarily on the work of Cochran (ref. 1). Certain additional information concerning performance calculations and future work is also contained in reference 1. The present results cover a wide range of geometries but are limited in respect to inlet Mach number and variation in both inlet flow geometry and condition. Discussion of the flow mechanisms is given as needed, but it was beyond the scope of the present work to attempt a presentation of their details and full implications. However, as an outgrowth of the experimental results and observations of the continuing overall research program, Kline has written a report on the topic of basic flow mechanisms (ref. 2). Reference 2 has been written to integrate with the present report, and Kline not only rationalizes the results found in vaned and unvaned diffuser flows but also discusses the entire problem of stall in terms of two new concepts including the introduction of a new flow model which has already been experimentally verified. The reader who is interested in the more basic aspects of stall and of the flow mechanisms in adverse pressure gradients should refer to reference 2; however, it is suggested that the present report be read first since considerable reference is made to the material presented herein.

This investigation was carried out at the Mechanical Engineering Laboratory, Stanford University, under the sponsorship and with the financial assistance of the National Advisory Committee for Aeronautics.

SYMBOLS

Nomenclature involved in diffuser geometry is illustrated in figure 1.

A	area, sq ft
a	minimum spacing between adjacent vanes, in.
b	minimum spacing between diffuser diverging wall and adjacent vane, in.
C_{ER}	energy-recovery coefficient, defined by equation (4)
C_{PR}	pressure-recovery coefficient, defined by equation (11)
c	distance from plane of diffuser throat to plane of vane leading edges, in.
c_p	specific heat at constant pressure, $\frac{\text{ft-lb}}{\text{lb-}^\circ\text{F}}$
c_v	specific heat at constant volume, $\frac{\text{ft-lb}}{\text{lb-}^\circ\text{F}}$
E_k	kinetic energy, $\frac{\text{ft-lb}}{\text{lb}}$
f	length of vanes, in.
G	distance between parallel walls of diffuser, ft
g_c	constant of proportionality in Newton's second law equation, $\frac{\text{lb-ft}}{\text{lb-sec}^2}$
H	boundary-layer shape factor
H_L	head loss, lb/sq ft or in. water
\bar{H}_L	nondimensional head-loss coefficient, H_L/q

j	internal energy, $\frac{\text{ft-lb}}{\text{lb}}$
K	correction factor for compressibility effects
k	ratio of specific heats, c_p/c_v
L	length of diffuser diverging wall measured from throat to exit, in.
n	number of vanes
p	static pressure, lb/sq ft
Q	volumetric flow rate, ft^3/sec
q	dynamic head, $\rho \frac{V^2}{2g_c}$, lb/sq ft or in. H_2O
R	Reynolds number
R_c	gas constant, $\frac{\text{ft-lb}}{\text{lb-}^\circ\text{R}}$
r	radius of curvature, ft or in.
T	temperature, $^\circ\text{R}$
U	free-stream velocity at edge of boundary layer, ft/sec
u	local x-direction velocity in boundary layer, ft/sec
u'	local x-direction turbulence velocity or time-variant component of u , ft/sec
V	velocity, ft/sec
V_{2i}	exit velocity for one-dimensional flow
v	specific volume, ft^3/lb
W	distance between diverging walls normal to geometric axis of diffuser, ft
W_f	flow work, $\frac{\text{ft-lb}}{\text{lb}}$

w	weight flow rate, lb/sec
x,y	length variables, ft or in.
α	total divergence angle between adjacent vanes, deg
$\Delta() = ()_2 - ()_1$	a change in a variable
δ	boundary-layer thickness, in.
δ^*	boundary-layer displacement thickness, $\int_0^\delta \left(1 - \frac{u}{V}\right) dy$, in.
δ^{**}	boundary-layer momentum thickness, $\int_0^\delta \left(1 - \frac{u}{V}\right) \frac{u}{V} dy$, in.
η_p	pressure effectiveness, $C_{PR}/C_{PR_{ideal}}$
θ	half of diffuser total divergence angle, deg
2θ	diffuser total divergence angle, deg
μ	viscosity, lb/hr-ft
ρ	density, lb/cu ft
ψ	normal to a streamline, ft or in.

Subscripts:

1	inlet
2	exit
a	ambient condition
as	appreciable stall
av	average
ϵ	center line
L	diverging wall length

max	maximum
o	outer or stagnation
W	throat width
w	wall

BACKGROUND INFORMATION

The work reported herein is a direct extension of the work of Moore and Kline (refs. 3 and 4). A summary of the status of diffuser research which is pertinent to the present report is given in reference 4. A summary of the available diffuser design data was given by Patterson (ref. 5), and a more recent summary of the data applicable to the present geometry was given by Reid (ref. 6). It therefore seems undesirable, in view of the length of the present report, to repeat these summaries here. It is, however, pertinent to make a few remarks concerning previous investigations of the governing parameters and the overall patterns involved.

Reid (ref. 6) found that the performance of a two-dimensional diffuser was strongly dependent on the total divergence angle and the ratio of wall length to throat width. He also found that, with length ratio held constant, flow separation and pulsations occurred as the divergence angle was increased beyond the point of maximum pressure recovery. Vedernikoff (ref. 7) obtained stable flows for included angles up to approximately 14.0° in a two-dimensional diffuser having a constant length ratio of 10.0. At larger angles vortices formed first along one wall and then along the other, the intensity of the vortices increasing as the angle was increased. In addition, Vedernikoff found that the maximum pressure recovery occurred just prior to the formation of the vortices. Tults (ref. 8) experimented with an asymmetric two-dimensional diffuser of constant length ratio and also found that, with increase of angle, the occurrence of maximum pressure recovery very closely preceded the occurrence of separation. He found further that the angle at which separation occurred did not depend on the inlet Reynolds number but that the amount of separation present increased as the angle was increased. Jones and Binder (ref. 9) investigated the effect of inlet turbulence intensity in a square diffuser and found that the turbulence level influenced both the velocity distributions and the diffuser flow patterns. In addition, they found a complete lack of two-dimensional flow, although the total divergence angle of their diffuser was only 8.0° . Kalinske (ref. 10) studied the effect of turbulence in conical diffusers of constant area ratio. He observed that the effect of turbulence was to produce a

flattening of the velocity profiles and that large-scale turbulence was more effective than fine-grained turbulence.

Moore and Kline (refs. 3 and 4) studied the basic flow mechanisms in diffusers by using two sizes of water-table units incorporating dye injection for flow visualization (see fig. 2). They also investigated a large number of schemes for the production of efficient, wide-angle diffusers using various types of vanes and mixing devices for boundary-layer control. With the exception of aspect ratio, which was shown to be unimportant, the large water-table unit had the same geometry as the air unit used for preliminary tests by Moore and Kline.

Moore and Kline discovered several important new characteristics of unmodified, plane-wall diffusers. Holding all the inlet flow conditions, the wall length, and the throat width constant, they found that four regimes of flow are obtained as the diffuser divergence angle is increased from 0° . These regimes are illustrated in figure 3 which shows typical dye trace photographs (reproduced from ref. 4) and a schematic sketch for each regime of flow. The four regimes are as follows:

- (1) A regime of well-behaved apparently unseparated flow (fig. 3(a)).
- (2) A regime of large transitory stall in which the separation varies in position, size, and intensity with time (fig. 3(b)). (This is the regime of highly pulsating flows noted by Reid, ref. 6, and others.)
- (3) A regime of fully developed stall in which the flow is relatively steady and follows along one wall of the diffuser (fig. 3(c)). The major portion of the diffuser is filled with a large turbulent recirculation region which extends from the diffuser exit almost to the diffuser throat and is roughly triangular in shape. The main flow stream experiences little expansion in passing through the diffuser; hence, little pressure recovery is obtained in this regime.
- (4) A regime of jet flow in which the flow separates from both walls and proceeds through the diffuser similar to a free jet (fig. 3(d)).

Furthermore, it was found that the divergence angles bounding the different flow regimes are not unique but, in fact, depend strongly on the ratio of wall length to throat width and in some instances on the entering free-stream turbulence level. This is clearly illustrated by figure 4 which is taken from reference 4. Figure 4 shows the zones of flow as a function of divergence angle, ratio of wall length to throat width, and inlet free-stream turbulence for constant thin inlet wall boundary layers and nearly constant mean inlet velocity profile. The effect of a change in free-stream turbulence intensity is shown by

comparison of the dashed boundary curves with the solid boundary curves. It should be noted that the definition of the line of appreciable stall, line aa in figure 4, is somewhat subjective. This line was determined experimentally by Moore and Kline as the locus of angles for which a transitory stall was first visible using dye injectors of roughly 1/8 inch in diameter near the wall of the diffuser. However, later investigations led to the conclusion that small transitory stalls probably existed at much lower angles, and this conclusion has been extended and verified experimentally in the work described by Kline in reference 2. Consequently, the name "appreciable stall" is now used in referring to the line aa although it is called "first stall" in references 3 and 4.

Moore and Kline have clearly demonstrated that the flow regime of a simple diffuser depends to an important extent on the following parameters: (1) Total divergence angle; (2) ratio of wall length to throat width; and (3) inlet free-stream turbulence. They also concluded that data available from other sources indicated that the character of the inlet flow, particularly the condition of the boundary layer, also probably had an important effect on performance. In addition, Moore and Kline found that variations in throat-width Reynolds number had little or no effect on flow regime for Reynolds numbers in excess of a few thousand and also that variations in throat aspect ratio had little or no effect on flow regime for all values of aspect ratios normally encountered.

The studies of various boundary-layer control devices in the water-table work reported by Moore and Kline indicated quite clearly that short flat vanes placed somewhat downstream of the throat held more promise than any of the other devices tested. In one case, apparently unseparated flow was obtained at 45.0° in a vaned diffuser which normally, in its simple form, would have entered the regime of fully developed stall at about 15.0° . Preliminary tests using the air apparatus by Moore and Kline confirmed the very high promise of such configurations. Good flow was extended from a typical value of 15.0° to 30.0° , and the pressure recovery at 30.0° was increased in one case from about 18 percent in the unvaned unit to approximately 74 percent in the vaned unit.

The investigation reported herein began at this point. Its primary purpose was to exploit the promise found in the work of Moore and Kline for vaned units. This includes development of simple design criteria for such units over a wide range of geometries and evaluation of typical performance that can be expected using these criteria. The secondary purpose of the investigation was to verify and augment the information on the governing parameters, the overall flow regimes, and the basic flow mechanisms found by Moore and Kline. The portions of the second objective dealing with the governing parameters, with the overall regimes of flow, and with the use of the flow-regime data (shown in fig. 4) for

design purposes are discussed in this report. The portions dealing with the basic mechanisms of the flow are discussed primarily in the report by Kline, reference 2.

EXPERIMENTAL APPARATUS

Several views of the experimental apparatus are shown in figure 5, and a schematic diagram showing nominal dimensions is given in figure 6. The complete system, which is located in a large room in the Mechanical Engineering Laboratory, consists of the two-dimensional diffuser with direct entry through a well-rounded nozzle, an outflow through a plenum chamber, a driving fan, and an exit duct. The diffuser has been oriented vertically downward to provide the necessary aerodynamic clearance. Instrumentation is provided to measure flow rate, pressure recovery, and exit velocity profile. In addition, a large number of access holes are provided for measurement of velocity and pressure profiles throughout the unit. Wall tufts were used for flow visualization in all runs.

Since the fan suction (G) (see fig. 6) was on one side of the large plenum chamber (E), a damping screen (F) having an adequate flow resistance was placed normal to the axis of the diffuser in the cross section of the plenum chamber to prevent skewing the exit flow from the diffuser. The adapter connecting the fan to the discharge-duct transition piece (I) was asymmetric in the vertical plane, but this was remedied by placing an internal baffle (H) in the adapter. An "egg crate" straightener (J) was placed in the circular duct immediately downstream of the transition piece, and a second egg-crate straightener (L) was located $6\frac{1}{2}$ feet downstream of the first straightener. The second straightener had been installed in the duct prior to its use in the present apparatus, but since it was found to be inadequate the straightener (J) was added. Four total head tubes (M) and a wall static tap (N) were installed 8 feet downstream of the first flow straightener. It was necessary to make careful velocity-profile surveys and to use four probes for determining the flow rate because the discharge duct was not long enough to obtain established pipe flow. The two sides of a single inclined manometer (K) were connected to the duct static tap and to the top vertical total-pressure probe, respectively. This manometer was used in setting the flow rate. In preliminary work it was discovered that, because of the fan speed limit, the straight pipe discharge duct prevented the desired maximum flow rate from being obtained. This situation was subsequently remedied by the addition of an available 15° conical diffuser on the duct exit, thereby reducing the overall pressure drop sufficiently to enable the fan to produce the desired maximum flows.

An adjustable sliding total-pressure rake (V), consisting of two rows of seven Kiel probes each, was installed in the two-dimensional plenum chamber (B). Kiel probes were used because of the large flow inclination obtained for wide-angle diffuser settings. The exit rake was operated by a push rod (U) extending through a bushing in the east end of the plenum chamber. The rake was used in this investigation to obtain an approximate quantitative distribution of the flow in the diffuser exit plane and not to determine total-head-loss coefficients.

Pressures were measured with a 33-column, back-light manometer-board (C) and were recorded photographically with a 35-millimeter camera.

A discussion of the more important components of the test apparatus is given below in greater detail.

DETAILS OF DIFFUSER CONSTRUCTION

The diffuser was formed from two parallel, 1/2-inch-thick Plexiglas walls and two diverging aluminum walls 1/2 inch thick.

The diverging walls consisted of a plane section 24 by 24 inches ending in a semicylindrical section having an outside radius of $4\frac{1}{4}$ inches (see fig. 7(a)). They were surface ground and polished resulting in a finished unit having a smooth surface and a gradual transition in curvature from the semicylindrical section to the plane section. The shape of these walls and the manner in which their pivot shafts are secured in the adjustable sliding pillow blocks are shown in figures 7(a) and 7(b). The 1-inch-diameter steel pivot shafts were attached concentrically with the curvature of the cylindrical section so that the diffuser angle could be adjusted without materially altering the inlet geometry.

The five rows of fittings attached to each diverging wall can be seen in figure 7(b). The two outer rows were not used in the present investigation. The other three rows each consist of 22 T-shaped aluminum plugs distributed from the vicinity of the throat to the trailing edge of the diverging wall. A cross-sectional diagram showing the construction of these plugs and the ways in which they are used is given in figure 8. It should be noted that these plugs were securely fastened to the aluminum walls by means of a small machine screw and that their butt ends were surface ground simultaneously with the main plate forming a smooth continuous surface. The longitudinal positions of the plugs are given in table I. The middle row is centered in the wall and the other two are located 6 inches from the edges of the plate. This large number of fittings was installed in the diffuser to provide adequate

flexibility for test work in the unit; it was not intended that the fittings would all be used simultaneously.

The details of both the diffuser and the plenum-chamber side walls are also shown in figure 7. The diffuser side walls are 24 inches wide, extend to a height approximately 9 inches above the tangent plane of the diffuser entrance lips, and terminate in a semicircular arc of about 1 foot radius. Fittings, similar to those described for the diverging walls, are arranged along the vertical center line; their longitudinal positions are given in table II. Identical fittings were symmetrically arranged on a $3/4$ -inch pitch along a horizontal line $1\frac{1}{4}$ inches below the top edge of the plenum-chamber side walls. These fittings were used for the measurement of the exit static pressure because the diffuser height could be adjusted to make the diffuser exit plane coincide with the plane of the fittings; the cornermost fittings were used for each angle setting.

All sliding and fixed joints were sealed with a gasket material approximately $1/32$ inch thick. The gaskets between the parallel and diverging walls also served the purpose of providing the vane end clearance necessary to manipulate the clusters in the diffuser.

DETAILS OF VANES AND CLUSTERS

The vanes were fabricated from 24-inch widths of 12-gage sheet steel (0.110 inch thick). Sets of five vanes each, in lengths of 3, 6, 9, 12, and 15 inches, were manufactured with each set consisting of one center vane and four outer vanes. A diagram showing the end detail of the vanes is given in figure 9. Because of the short length of the 3-inch vanes, it was necessary to add an extension to the center vane in order to obtain good alinement in the diffuser. Assemblies of typical vane clusters are shown in figure 10, and a typical diffuser vane installation is shown in figure 11(a). It is noted that aerodynamic smoothness has been sacrificed for mechanical flexibility in the vane holding mechanisms because a considerable latitude of vane adjustment was required. A diagram of the vane supporting hooks is given in figure 11(b). Two of these hooks were inserted in each parallel wall in place of the appropriate aluminum plug. The position of a cluster, relative to the diffuser, was adjusted in the following ways: (1) Sliding the diffuser side wall, thus centering the cluster with respect to the diverging walls, (2) sliding the supporting hooks in the side-wall holes, thus centering the cluster with respect to the side walls, and (3) adjusting the hook position in the center vane slots, thus obtaining the desired axial location. (The cluster could be moved the distance of

the pitch of the plugs in this manner.) A pair of side braces, which held the clusters in a firm and centered position during flow conditions, can be seen on the diverging walls in figure 11(a).

The clusters were bench assembled using 1/8-inch-diameter steel rods for the main supporting dowels in the upper holes in the vane ends; 1/16-inch-diameter steel welding rods were used to support the vanes in the lower end holes and in comparable upper and lower holes in the vane centers. The rods were rigidly clamped in the vanes by means of small set screws and, when the vanes were adequately adjusted, the butt ends of the rods were ground flush with the outer vane surface. The angle between adjacent vanes was set using accurately cut sheet steel templates, and the throat spacing between adjacent vanes was set using a pair of micrometer adjusted calipers. The vane throat spacing and the vane divergence angle could be adjusted to ± 0.01 inch and $\pm 0.25^\circ$, respectively, on an average throughout a particular cluster.

The limited confines of the diffuser prohibited any significant vane adjustment while the clusters were in the diffuser; consequently, when adjustments were desired it was necessary to remove the clusters. Access to the clusters was obtained by swinging the west wall of the diffuser outward through an angle of approximately 180° .

EXPERIMENTAL METHODS

MEASURING FLOW RATE

The flow unsteadiness and three-dimensional effects that occurred in many of the nonoptimum diffuser configurations made it undesirable to attempt measuring the flow rate in the diffuser itself; instead, the flow rate was measured in the downstream end of the discharge duct. In order to obtain reliable results, an accurate calibration of the duct under a variety of conditions was made. For this purpose the diffuser was set at a divergence angle 2θ of 7° to insure smooth flow, and then the flow conditions described in table III were studied. A flow-rate uncertainty analysis was made using these experimental results. In this analysis the following factors were considered: (1) The uncertainty involved in representing all the expected velocity profiles by an average profile, (2) the uncertainty involved in mechanically positioning the total-pressure probes in the correct radial location in the duct, and (3) the uncertainty involved in using the arithmetic average of the four probe readings as the true flow-average reading. (The probes were positioned to read the average flow velocity on the basis of the measured velocity profiles.) The method of Kline and McClintock (ref. 11) was used to calculate the uncertainty in the flow-rate measurement

attributable to the method employed. This was equal to, at most, 1.25 percent. (A list of the uncertainties involved in all the important measured variables is given in table IV.)

LOCATING DIFFUSER THROAT

The diffuser throat was defined by the point of tangency between the curved surface of the diverging walls and a vertical plane. This point was easily located by using a machinists square referenced to an angle iron placed across the diffuser entrance tangent to the two lips of the diverging walls. Six static-pressure taps were inserted in the diverging-wall fittings which were nearest the diffuser throat. Inspection of table I shows that these static taps could be located to within ± 0.333 inch of the throat. A static-pressure tap was inserted in the top fitting on each parallel wall, but these fittings were approximately $3/8$ of an inch above the throat. Therefore, the latter two static pressures were not used in the calculation of the performance parameters but served only to give a qualitative indication of the flow symmetry.

RECORDING THE DATA

The following pressures were recorded on the 33-column, back-light manometer board: (1) Six diffuser-throat static pressures, (2) two side-wall static pressures near the throat, (3) four diffuser-exit static pressures, (4) fourteen exit-rake total pressures, (5) four flow-rate total pressures, (6) one flow-rate static pressure, and (7) two atmospheric pressures, one in each end column of the manometer. Probe connector tubes of the same length were always used for comparable readings.

Considerable care was exercised in recording the data at the proper time. For many of the configurations tested the flow shifted randomly between two, or more, patterns. In such cases, the frequency of occurrence of the different patterns was observed by watching their respective manometer-board patterns, and the pattern occurring most frequently was selected as being representative of the particular configuration in question. When two stable but distinctly different patterns occurred for a given configuration, data were recorded for each pattern. ("Stable pattern" is used herein to mean a pattern which will remain fixed and can only be changed by deflecting the flow with the hand or a suitable device. Small fluctuations of varying degree occurred for all stable patterns, but their effect did not significantly change the nature of the pattern.)

In view of the relatively slow time response of the manometer it was necessary to wait several seconds while the pattern "held" its position. When the data recorder was satisfied that the manometer had attained equilibrium, a picture was taken. A picture was taken for each exit-rake position that was deemed necessary to traverse adequately the exit flow; and, of course, it was necessary that the same flow pattern was obtained for each position. The number of pictures taken for a given test varied from three to six, depending on the diffuser exit width. However, only one frame was used in calculating the performance parameters with the exception of the exit velocity profile. Several tests were taken at random for which the performance parameters were calculated for two or more frames and very good agreement was always obtained.

It was thought that the damping of the test manometer might produce errors in the measured values of the pressures. A qualitative idea of the degree of damping caused by the manometer was obtained by comparing its time-varying reading with that of a fast time-response manometer connected just below the north-side throat tap. No error of any consequence could be observed when the data-recording procedure just described was used.

In the process of the data reduction, negatives of the photographs were projected on a screen, resulting in an image approximately three times as large as the actual manometer board. Good definition was obtained for this magnification; consequently, it was possible to read the columns to within ± 0.01 inch H_2O .

EXPERIMENTAL PROCEDURE

When the apparatus was started cold, it was allowed to run for at least a half hour to insure good steady-state conditions. During this time the ambient conditions were recorded. (The ambient conditions were measured at least every 4 hours.) Care was exercised to see that all outside doors and windows to the laboratory were closed so that no drafts would occur thus altering the character of the inflow. Since it was necessary to shut down the fan in order to change the axial position of a vane cluster, the flow rate was individually set for every configuration that was tested. The uncertainty analysis of the flow rate indicated, however, that this procedure made no significant change in the total uncertainty of the flow rate.

DIFFUSER INLET FLOW

VELOCITY AND PRESSURE DISTRIBUTIONS

Regardless of whether a diffuser is directly connected to a nozzle, as in the present case, or whether it is connected to a straight duct section, there must be some wall curvature at the juncture of the diverging walls and the entrance section. For such a condition Euler's dynamical equation for the direction normal to the streamline is

$$\frac{\partial p}{\partial \psi} = \rho \frac{v^2}{r}$$

where ψ is the normal to the streamline directed outward from the center of curvature and r is the radius of curvature. Euler's equation thus demonstrates that a local decrease in the static pressure near the walls will occur because of the corresponding curvature of the streamlines outside the boundary layer. Furthermore, Euler's equation written for the flow along a streamline outside the boundary layer

$$d\left(\frac{v^2}{2}\right) = -\frac{dp}{\rho}$$

demonstrates that there will be, of necessity, an increase in the local velocity corresponding to the local decrease in static pressure near the wall. Therefore, it is seen that the diffuser entrance curvature causes variations of the static pressure with corresponding variation in the inlet velocity. Further, these variations are such that the fluid in the boundary layer, on the curved surface downstream of the throat, is subjected to an adverse pressure gradient larger than that which would be predicted from a one-dimensional theory. (It should be noted that the detrimental effects of the intensified positive pressure gradient are somewhat offset by the favorable effect of the reduced static pressure immediately preceding it.) The above statements are true of all diffusers; however, the nature of the velocity and pressure variations that occur depends upon the inlet geometry of the diffuser in question.

It is only logical, then, to question the validity of using the test results obtained from a given diffuser-inlet configuration to predict the performance of other diffuser configurations. This question is of particular importance with regard to the present diffuser because not only do significant pressure and velocity variations occur across the throat width but also small changes in the shape of these profiles occur as either 2θ or W_1 is varied.

Moore and Kline (ref. 4) examined the literature in which changes in entrance velocity profile and changes in inlet shape have been studied. The evidence, they found, suggests that, excluding sharp-edged junctures, no significant change in performance will result so long as the boundary-layer conditions are constant at the throat and the nonuniform profile approximates that of a potential pattern for the remainder of the flow.

Since the present diffuser communicates directly with the ambient surroundings through a nozzle, the entrance flow external to the thin boundary layer very closely approximates that of an ideal nonviscous fluid, and since the ambient total pressure is constant, the total pressure in the diffuser throat is constant outside the boundary layer. Therefore, it is seen that the actual entrance flow to the diffuser closely resembles the potential flow for the given inlet geometry.

Throat velocity and static-pressure profiles, obtained with smooth flow for $W_1 = 3.00$ inches, are shown in figure 12. It can be seen that a better degree of two-dimensionality is obtained for $2\theta = 7^\circ$ than for $2\theta = 42^\circ$; however, even in the latter case the velocity profiles do not differ from a suitably defined average profile by more than ± 2 percent at any point. Also, it can be seen that there is a greater variation in profile for $2\theta = 42^\circ$ than for $2\theta = 7^\circ$. This is as expected since the flow for wider angles more nearly approaches the potential flow between parallel cylinders indicated in figure 12(b). (The solution for the flow between parallel cylinders has been obtained by Moore and Kline, ref. 4.) It is recognized that when large three-dimensional stalls occurred, the approach to two-dimensionality was not so good as it was for the smooth flow shown in figure 12; however, it is believed that an adequate approximation was obtained for all tests.

The character of the inlet boundary layer has been shown by several investigators to have a significant effect on the diffuser performance. (See, e.g., Little and Wilbur, ref. 12.) In the present work it was desired to maintain a relatively constant boundary-layer shape, and the belief that this condition would be obtained with the present entrance section was verified by boundary-layer measurements made in the throat for several different diffuser configurations.

A boundary-layer probe was fabricated from a piece of 0.020-inch-diameter hypodermic tubing by flattening one end and grinding it under a microscope. The resulting tip thickness was approximately 0.010 inch. The probe was referenced to the diffuser wall to within approximately 0.001 inch; it was then positioned with the micrometer-screw traverse mechanism shown installed in the diffuser in figure 13(a). A schematic diagram of the probe is shown in figure 13(b). Measurements were made only for steady flows but, even for some of these flows, minor fluctuations occurred which made it necessary to estimate time average velocity

readings. The fluctuations which occurred, however, were not serious enough to impair the results obtained.

The inlet boundary-layer profiles and values of displacement thickness, momentum thickness, and shape factor are given in figure 14. The first measurements were made without a boundary-layer trip, and the resulting profile is shown in figure 14(a). This profile is definitely of a turbulent character; however, in order to insure that a turbulent boundary layer was obtained for all configurations, a 0.012-inch-diameter trip wire was placed on the curved portion of the diverging walls approximately 3 inches upstream of the throat. The effect of the trip wire is shown in figure 14(a). A comparison of the boundary-layer properties given in figure 14 shows that the overall effect of the trip wire was to produce a slight increase in the displacement thickness with a correspondingly larger increase in the momentum thickness; that is, a decrease in the shape factor. Furthermore, it can be seen that all of the boundary layers obtained with the trip wire installed are of essentially the same size and shape.

In summary, it can be said that the entrance flow of the present diffuser was comparable to that of a straight section in which two-dimensional flow having a constant free-stream total pressure and a thin constant-shape inlet boundary layer was obtained.

FREE-STREAM TURBULENCE

It was shown by Moore and Kline (ref. 4) that the inlet turbulence intensity had a very significant effect upon wide-angle-diffuser performance. This is clearly illustrated by the shift of the boundary between the transitory stall and fully developed stall regimes with change in turbulence intensity as shown in figure 4. It was suspected that a change in the mass-flow rate in the present diffuser, with a consequent change in the ambient velocity field, would result in a change in the entrance turbulence intensity. This was shown to be true by turbulence-intensity measurements made with a hot-wire anemometer installed in the geometric center of the diffuser throat. From the resulting curve shown in figure 15 it can be seen that nearly a three-fold change in intensity occurred over the anticipated range in mass-flow rate from 4 to $7\frac{1}{2}$ lb/sec. Consequently, it was decided to conduct the tests at a constant mass-flow rate which was equivalent to a constant-throat-width Reynolds number since

$$R_{W1} = \frac{\rho_1 W_1 \bar{V}_1}{\mu} = \frac{\rho_1 Q}{\mu G}$$

All of the constant-throat-width tests were easily run with the flow rate selected. However, in the constant-included-angle tests it was necessary to reduce the flow rate because the manometer board could not record the reduced throat pressures and the fan could not handle the required flow commensurate with the desired minimum throat widths. Since these latter tests were run only to show typical results with vanes, no loss of significance results.

EXPERIMENTAL PROGRAM

RESTRICTIONS IMPOSED ON CLUSTER GEOMETRIES

At least four quantities must be specified to describe the location and size of a single flat vane in a two-dimensional diffuser, for example, (1) the distance of the vane leading edge from the diffuser throat, (2) the distance of the vane leading edge from the diffuser center plane, (3) the included angle between the vane surface and the diffuser center plane, and (4) the vane length. Consequently, the number of geometric variables is very great when several vanes are used. Thus, at the expense of some generality, it was necessary to impose restrictions on the vane configurations in order to reduce the total number of independent variables. For any given cluster (see, e.g., fig. 10) the restrictions were as follows:

- (1) All vanes were of the same length f .
- (2) The minimum width a between adjacent vanes was identical.
- (3) The divergence angle α between adjacent vanes was constant.
- (4) The leading edges of the vanes were made tangent to a single plane perpendicular to the longitudinal axis of the diffuser and a distance c downstream from the throat.
- (5) The longitudinal axis of the cluster was made coincident with the longitudinal axis of the diffuser; that is, the vanes were symmetrically disposed with respect to the diffuser.

With these restrictions the cluster geometry was completely specified by the following variables: (1) The number of vanes n , (2) the minimum width a , (3) the divergence angle α , and (4) the vane length f . The location of the cluster in the diffuser was specified by the distance c or by the minimum width b between the outer vanes and the diffuser diverging walls. In other words, with the restrictions imposed,

any given vane configuration was completely specified by no more than five quantities.

OBJECTIVES

Moore and Kline (ref. 4) reached the following conclusions: (1) The best improvement in performance could be obtained with relatively short vanes placed just downstream of the throat, (2) the number of vanes should be selected so that the divergence angle between adjacent vanes is that for optimum efficiency, or approximately 7.0° , and (3) the vanes should be arranged to form small diffuser passages each having the same divergence angle and the same throat spacing. Moore and Kline were unsure about the optimum length of the vanes; they suspected that the lengths should be selected so that the corresponding operation of each passage was at least below the line of appreciable stall (line aa, fig. 4), but further conclusions regarding length had not been reached.

Within the scope of the restrictions imposed on the vane configurations the following questions remained to be answered:

- (1) Precisely how much improvement in performance can be obtained with the type of vane configurations under consideration?
- (2) What is the optimum vane length?
- (3) How far downstream from the throat should the cluster be placed?
- (4) How should the vane spacing be selected?
- (5) If the diffuser total included angle 2θ is not a multiple of approximately 7.0° , how should the number of vanes and their angles of divergence be selected?
- (6) Should the angle α between adjacent vanes and the angle α_0 between the diverging diffuser wall and adjacent vane be identical?
- (7) What is the nature of the flow of a diffuser-vane configuration?

The objectives of the present investigation were to resolve these seven questions.

TEST CONFIGURATIONS

Since Moore and Kline (ref. 4) conducted the majority of their work using a value of L/W_1 of approximately 8.0 and since $L/W_1 = 8.0$ is representative of practical diffusers, this value of length ratio was used in most of the present work.

The uppermost position of a cluster was defined so that the flow cross-sectional area at the vane entrance section was identical to the diffuser-throat cross-sectional area. If the cluster had been placed any farther upstream a blockage of the flow would have resulted.

For the initial testing the vane spacing a was defined by the relation

$$a = \frac{W_1}{n + 1} \quad (1)$$

and the divergence angle α between adjacent vanes was defined by the relation

$$\alpha = \frac{2\theta}{n + 1} \quad (2)$$

It was determined in later tests that a and α as defined by equations (1) and (2), respectively, are actually the most suitable values. Using the value of a from equation (1) the ratio b/a was unity for the uppermost cluster position, where b is the minimum width between the diffuser diverging wall and adjacent vanes.

A systematic series of tests was conducted using the configurations summarized in table V. The configurations are listed in the order in which the included angle was set.

Included in these tests are auxiliary tests designed to evaluate the effect of the following factors on the diffuser performance:

- (1) The placement of a pair of turbulence-generating rods in the low-velocity region of the entrance flow
- (2) The variation of the end clearance between the vanes and parallel walls
- (3) The modification of the vane holding mechanism

A near optimum diffuser-vane configuration was employed for each of these three tests.

EXPERIMENTAL OPTIMIZING TECHNIQUE

Since the number of variables of the basic diffuser plus those of the vane cluster geometry is very large, it was not feasible to take data over the entire region of possible variation of all variables. Consequently, a method was followed in which the optimum value for a given variable, such as the vane length f , was found for several conditions. This optimum value was then used in further tests to determine optimum values of the other variables. Such a method will not, in general, yield precisely the optimum value for all possible configurations, but it will usually provide a rapid means for finding a good approximation of it. In the present case, the good performance found suggests that the design criteria developed do give configurations not too far removed from the optimum configuration possible. However, as will be discussed subsequently, the exit traverses and flow observations indicate that some further improvements in performance of the wide-angle units can be expected by additional refinements of the geometry and by the superposition of other means of boundary-layer control. Thus, the results in this report should be considered as indicative of the sort of performance that can be obtained fairly readily but not as the ultimate possible optimum performance for a very refined design.

DEFINITION AND INTERPRETATION OF PERFORMANCE PARAMETERS

PRESSURE RECOVERY

In most of the literature the diffuser has been considered as a pressure-momentum device with attention being consequently focused on the static-pressure recovery which has generally been expressed in terms of the nondimensional pressure-recovery coefficient defined by the following equation:

$$C_{PR} = \frac{P_2 - P_1}{q_1} \quad (3)$$

In this definition, C_{PR} is the ratio of the actual static-pressure rise to the theoretical, incompressible, isentropic static-pressure rise obtained by stagnating the entrance flow. However, C_{PR} of equation (3) is a satisfactory performance parameter only when the following

conditions prevail: (1) The flow is essentially incompressible; (2) the entrance flow is essentially one-dimensional; and (3) the exit pressure is uniform. Equation (3) may be readily modified to apply to compressible flows by using the theoretical maximum possible static-pressure rise for compressible isentropic flow in place of q_1 . However, even when modified in this way, the resulting expression for C_{PR} is limited to essentially one-dimensional entrance flows and uniform exit pressures. It should be noted that the effect of the entrance transition curvature, discussed previously, can lead to erroneous results because the measured inlet wall static pressure p_1 may be appreciably less than the mean inlet static pressure.

Moore and Kline (ref. 4) recognized the problems of the nonuniform velocity and pressure profiles in considering suitable performance parameters for the present diffuser and inlet geometries. They concluded that the definition of C_{PR} given by equation (3) was meaningless for the present flow conditions; therefore, they considered the diffuser as an energy device and interpreted the performance in terms of an energy-recovery coefficient which is defined by the following equation:

$$C_{ER} = \frac{\text{Flow work out} - \text{Flow work in}}{\text{Inlet kinetic energy}} \quad (4)$$

It is implied that the terms in equation (4) are to be obtained by integration across the inlet and outlet flows.

Moore and Kline used equation (4) only for incompressible-flow calculations, and the results obtained were comparable to what would be expected for an equivalent pressure-recovery coefficient. However, had the flow not been assumed incompressible the resulting calculations would have been very misleading. This arises from the fact that for compressible flows there is a "coupling" between the change in flow work and change in internal energy which produces a surprising difference between the value of C_{ER} and the expected comparable value of C_{PR} . This is readily illustrated by considering a simple, steady-state, one-dimensional, isentropic compressible flow of air through an ideal, two-dimensional diffuser (fig. 16).

A first-law analysis of this diffuser flow yields the following expression:

$$\frac{V_1^2}{2g_c} - \frac{V_2^2}{2g_c} = p_2 v_2 - p_2 v_1 + j_2 - j_1 \quad (5)$$

or its equivalent

$$-\Delta E_k = \Delta W_f + \Delta j \quad (5a)$$

From equations (5) and (5a) it is readily seen that the ratio of the change in flow work to the change in internal energy may be written as

$$\frac{\Delta W_f}{\Delta j} = \frac{p_2 v_2 - p_1 v_1}{j_2 - j_1} \quad (6)$$

In the present case air may be treated as a perfect gas. Therefore, substituting the equation of state for a perfect gas $pv = R_c T$ and letting $j = c_v T$, equation (6) may be modified as follows:

$$\frac{\Delta W_f}{\Delta j} = \frac{R_c T_2 - R_c T_1}{c_v T_2 - c_v T_1} = \frac{R_c}{c_v} = \frac{c_p - c_v}{c_v}$$

or

$$\frac{\Delta W_f}{\Delta j} = k - 1 \quad (7)$$

Equation (7) shows that for the compressible flow of air ($k = 1.4$) the change in flow work is only 40 percent as large as the change in internal energy. This coupling effect may be further illuminated by considering the total energy change given in equation (5a). Substituting equation (7) into equation (5a) and rearranging gives

$$\Delta W_f = \frac{k - 1}{k} \Delta E_k \quad (8)$$

Again substituting $k = 1.4$, it is seen that for air the change in flow work accounts for only 28.6 percent of the change in kinetic energy. In other words, the maximum possible value that C_{ER} can have when applied to the compressible flow of air is 28.6 percent.

A comparison of C_{ER} and C_{PR} can be made by considering their ratio. From their corresponding definitions,

$$\frac{C_{ER}}{C_{PR}} = \frac{\frac{p_2 v_2 - p_1 v_1}{v_1^2 / 2g_c}}{\frac{p_2 - p_1}{K_1 \rho v_1^2 / 2g_c}} = K_1 \frac{p_2 v_2 - p_1 v_1}{p_2 v_1 - p_1 v_1} \quad (9)$$

where K_1 is the compressibility correction factor which may be assumed to be equal to unity for the present purpose. Therefore, if it assumed that $K_1 = 1$ and the isentropic relationship

$$p_1 v_1^k = p_2 v_2^k$$

is used equation (9) may be rearranged to obtain the following relation:

$$\frac{C_{ER}}{C_{PR}} = \frac{\left(\frac{p_2}{p_1} \right)^{\frac{k-1}{k}} - 1}{\left(\frac{p_2}{p_1} \right) - 1} \quad (10)$$

From the plot of equation (10) given in figure 17, it can be seen that the maximum value of C_{ER}/C_{PR} is 28.6 percent.

The parameter C_{ER} was defined by Moore and Kline (ref. 4) for the purpose of overcoming the limitations imposed by equation (3). However, the foregoing discussion demonstrates that effective use of C_{ER} is limited to incompressible flow. It is therefore appropriate to suggest another means for overcoming the limitations inherent in equation (3). This is done by providing a more general definition of C_{PR} as follows:

$$C_{PR} = \frac{\frac{1}{A_2} \int_{A_2} p_2 dA_2 - \frac{1}{A_1} \int_{A_1} p_1 dA_1}{\frac{1}{A_1} \int_{A_1} q_1 dA_1} \quad (11)$$

From the momentum theorem for a fixed control volume (as given, e.g., in ref. 13, p. 16) it can readily be shown that equation (11) defines the pressure-recovery coefficient as the average increase in static pressure divided by the average entering impact pressure. Furthermore, equation (11) is applicable to both incompressible and compressible flows and to uniform and nonuniform velocity and pressure profiles at the entrance and exit sections of the diffuser.

The pressure-recovery coefficient used throughout the remainder of the report is that defined by equation (11). Several simplifications were made in developing a working expression for C_{PR} ; however, the resulting accuracy of the calculations is quite satisfactory as shown by table IV. (The details of this development are given in appendix A of ref. 1.)

PRESSURE EFFECTIVENESS

The definition of the pressure effectiveness η_p is given by the following equation:

$$\eta_p = \frac{C_{PR_{actual}}}{C_{PR_{ideal}}} \quad (12)$$

where $C_{PR_{ideal}}$ is the pressure-recovery coefficient that would be obtained for a frictionless, one-dimensional flow in the diffuser geometry in question.

Since it was entirely satisfactory to assume that the present diffuser flow was incompressible, a very simple expression for $C_{PR_{ideal}}$ was readily developed from the expression given by equation (3). The result is

$$C_{PR_{ideal}} = 1 - \frac{1}{(A_2/A_1)^2} \quad (13)$$

The working equation for η_p was obtained merely by substituting equations (11) and (13) into equation (12).

HEAD LOSS

Since the flows were very unsteady for many of the configurations and since the corresponding zones of stall were often random and chaotic, no attempt was made to measure the energy distributions in the diffuser. Consequently, an accurate evaluation of the losses in the vaned and unvaned units is not possible; however, a reasonable estimate of the relative losses can be made by assuming the flow to be both incompressible

and one-dimensional. The development of a suitable loss coefficient for incompressible, one-dimensional flow follows.

By definition

$$\bar{H}_L = \frac{\left(\frac{p_1}{\rho_1} + \frac{V_1^2}{2g_c}\right)w_1 - \left(\frac{p_2}{\rho_2} + \frac{V_2^2}{2g_c}\right)w_2}{\frac{V_1^2}{2g_c} w_1} \quad (14)$$

but since $w_1 = w_2$ (steady flow) and $\rho_1 = \rho_2$,

$$\bar{H}_L = \frac{(p_1 + q_1) - (p_2 + q_2)}{q_1} \quad (15)$$

Equation (15) demonstrates that for the simple flow under consideration, the head-loss coefficient reduces to the total-pressure-loss coefficient. Rearranging equation (15) gives

$$\bar{H}_L = \frac{q_1 - q_2}{q_1} - \frac{p_2 - p_1}{q_1} \quad (15a)$$

Using Bernoulli's equation, the definition of $C_{PR_{ideal}}$, and equation (3), it can readily be shown that equation (15a) is equivalent to the following equation:

$$\bar{H}_L = C_{PR_{ideal}} - C_{PR} \quad (16)$$

A comparison of the losses of the vaned and unvaned units, calculated using equation (16), is given subsequently. An interesting expression can be obtained by combining equations (12), (13), and (16). The result is as follows:

$$\bar{H}_L = \left[1 - \frac{1}{(A_2/A_1)^2}\right](1 - \eta_p) = C_{PR_{ideal}}(1 - \eta_p) \quad (17a)$$

For a given geometry, equation (17a) shows that the head-loss coefficient may be reduced by increasing η_p . This, of course, was known a priori; however, equation (17a) shows further that for constant values of η_p the head-loss coefficient increases as A_2/A_1 is increased. On first

thought this may seem unreasonable, but it can readily be explained. Equation (13) shows that $C_{PR_{ideal}}$ increases with A_2/A_1 , and equation (16) shows that \bar{H}_L is just the difference of two quantities C_{PR} and $C_{PR_{ideal}}$. When η_p is held constant then, by definition the ratio $C_{PR}/C_{PR_{ideal}}$ is constant. However, when two quantities having a fixed ratio are increased in value, the difference between the two quantities is increased. Thus, for constant values of η_p the head-loss coefficient is increased when A_2/A_1 is increased.

Division of equation (17a) by C_{PR} also yields an equation of significance, which is

$$\frac{\bar{H}_L}{C_{PR}} = \frac{H_L}{q_1} \frac{q_1}{p_2 - p_1} = \frac{H_L}{p_2 - p_1} = \frac{C_{PR_{ideal}}}{C_{PR}} (1 - \eta_p)$$

Since by definition

$$\eta_p = C_{PR}/C_{PR_{ideal}}$$

the following equation is obtained:

$$\frac{H_L}{p_2 - p_1} = \frac{1 - \eta_p}{\eta_p} \quad (17b)$$

where $H_L/(p_2 - p_1)$ is the head loss per unit actual pressure rise in the diffuser. Minimum head loss for a given pressure increase is therefore achieved when the value of the function $(1 - \eta_p)/\eta_p$ is a minimum. This occurs when η_p is a maximum since this is the same point at which $1 - \eta_p$ is a minimum.

It should also be noted that the loss coefficient \bar{H}_L in the form of equation (17a) or (17b) has a useful physical meaning even when the exit flow is far from one-dimensional. In particular, \bar{H}_L is the head loss of the diffuser (normalized on q_1) including both the loss due to dissipation and the excess of leaving kinetic energy above that which would occur for a one-dimensional exit velocity profile. If the kinetic energy leaving through the exit plane is a minimum, that is, if the exit flow is one-dimensional, then \bar{H}_L gives the purely dissipative loss. For other cases it charges the diffuser with both dissipation and excess of leaving loss above the minimum requisite for the given flow.

FLOW STEADINESS

It is difficult to give an adequate description of the flows without being somewhat subjective; therefore, in order to acquaint the reader with the terms that have been used, some brief definitions are given below. The ascending order of degree used for both steady and unsteady flow is illustrated as follows:

(1) A very steady flow is one in which there is no surging of the flow and for which it is quite difficult to discern any redistribution of the throat static pressure. At most, any individual static pressure might fluctuate approximately ± 1 percent of its mean value, and the period of fluctuation is 20 to 30 seconds or greater. In addition, the separation patterns remain fixed.

(2) A steady flow is similar to a very steady flow; however, noticeable throat-static-pressure redistributions occur with amplitudes on the order of ± 1 to ± 2 percent and with periods of approximately 15 to 20 seconds. Some noticeable shifting about of the zones of separation occurs although there is no rapid shifting back and forth.

(3) A fairly steady flow is one in which small pressure redistributions and minor flow surges occur. The amplitudes of the fluctuations of the individual pressures are approximately ± 2 to ± 4 percent. The fluctuations are caused in part by the redistribution of the static pressure and in part by the surging. The surge has an amplitude of approximately ± 1 to ± 2 percent; it is not violent and it has a period of approximately 20 to 30 seconds. Some random shifting about of the zones of separation can be observed.

(4) An unsteady flow is one in which the period of the fluctuations is of the order of 1 to 5 seconds and the amplitude is of the order of ± 5 to ± 10 percent. The fluctuations consist of both static-pressure redistributions and flow surges. The flow may surge up to as much as 5 percent and the period may be of the order of 5 seconds. Considerable shifting about of the zones of separation can be observed.

(5) A very unsteady flow is one in which the flow may pulsate with a periodic frequency of approximately 3 cps. If the flow doesn't pulsate, a rapid surging of the flow may occur with an erratic frequency of about $1/2$ to 1 cps and with an amplitude of ± 5 to ± 15 percent. The separations may shift rapidly about and/or whip in and out of the diffuser.

(6) A flow surge is characterized by random changes of the pressure recovery with corresponding changes in the flow rate (flow rate increasing with pressure recovery.) The rate of change may vary from very gradual to quite sudden, depending on the particular circumstance.

(7) A flow pulsation is characterized by a rapid periodic fluctuation of the pressure recovery with corresponding periodic variations in the zones of stall. A pulsation, unlike a surge, is further characterized by an audible beat.

TUFT MOVEMENTS

Interpretation

Flow visualization was obtained by wool tufts, approximately 1 inch long, placed throughout the diverging and parallel walls of the diffuser. In addition, a single tuft fastened to the end of a thin metal rod was used to explore the flow in regions away from the walls. The interpretations given the movement of each individual tuft are summarized as follows:

Movement and orientation of tuft	Type of flow	Notation
Tuft held firmly against wall, pointing downstream, no movement	Steady, undisturbed flow	None
Tuft held near wall, pointing downstream, occasional wiggling	Steady flow with occasional disturbance	None
Major part of the time tuft pointing downstream and wiggling; random "flickering" (tuft quickly points upstream and then downstream again) indicating a temporary and local separation	Intermittent transitory stall	I
Continual "whipping" of tuft in the upstream and downstream directions indicating rapid and chaotic occurrence and disappearance of separation	Local transitory stall	T
Major part of the time the tufts are continually whipping upstream and downstream; at random intervals the tufts are temporarily held in the upstream direction with their ends wiggling	Local transitory stall with intermittent fixed stall	TIF
Major part of the time the tufts are held in the upstream direction with their ends wiggling; temporary whipping of the tufts occurred at random intervals	Local fixed stall with intermittent transitory stall	FTT
Tufts held in the upstream direction with their ends wiggling; tufts are doubled back over the Scotch Tape used to attach them to the wall, and they are therefore held approximately 1/8 to 1/4 inch away from the surface	Local fixed stall	F

It is important to note that these interpretations and definitions describe the local flow in a small region under consideration; they do not necessarily describe the character of the overall separation. It may be recalled that there are four regimes of flow, each of which is characterized by a particular type of overall pattern. (See the section entitled "Introduction.") Only two of these regimes will be considered in the discussion given below, namely: (1) the regime of large transitory stalls in which the separation varies in position, size, and intensity with time (fig. 3(b)) and (2) the regime of fully developed stall in which the flow is relatively steady and in which the separation is nearly two-dimensional and firmly attached to one wall of the diffuser (fig. 3(c)). Thus, for example, the diffuser may be operating in a condition of fully developed stall, yet the separation in any particular region may consist only of local transitory stall. This will become more evident in the following discussion on the flow characteristics of the present unvaned diffuser with constant inlet conditions.

Effect of Tufts on Flow

Persh and Bailey (ref. 14) investigated the effect of the extent of surface roughness in a 23° conical diffuser. They found that the percent of surface roughened had no appreciable effect on the pressure recovery but that the presence of a small roughness strip just preceding the diffuser was sufficient to steady the flow. The combined effect of the preceding roughness strip and the roughened diffuser surface was to steady the flow even further. In the present diffuser approximately 2 to 5 percent of the surface area was affected by the wool tufts. The tufts may have produced a slight stabilizing effect on the flow, but this can be considered negligible because no difference in flow characteristics could be observed with or without the tufts. Therefore, since the tufts occupied only a small fraction of the surface and were not located any closer to the throat than 5 inches and since no difference in flow could be observed with or without the tufts, it can be concluded that the present diffuser surface was essentially equivalent to a smooth surface.

RESULTS AND DISCUSSION

The experimental results of the present investigation are presented in tabular form in tables VI and VII. Graphical representations are given in figures 18 to 36 and are discussed subsequently. The text has been arranged in the following general form: (a) The performance of the diffuser without vanes, (b) the performance of diffuser with vanes and the development of the design criteria, (c) the evaluation of the design criteria, and (d) conclusions.

The accuracy of the experimental results varied with the flow steadiness; therefore, uncertainties were estimated for both the most accurate and the least accurate results, and these are given in table IV along with the uncertainties of all the important measured variables. The method of Kline and McClintock (ref. 11) was used for estimating the uncertainties.

$$\begin{aligned} &\text{DIFFUSER WITHOUT VANES } (W_1 = 3.00 \text{ INCHES;} \\ &L/W_1 \cong 8.0; R_w \cong 2.4 \times 10^5) \end{aligned}$$

General Flow Characteristics

A series of tests was conducted in which all of the inlet conditions and L/W_1 were held approximately constant. The flow characteristics and the diffuser performance were recorded for $2\theta = 7.0^\circ, 14.0^\circ, 16.8^\circ, 21.0^\circ, 24.5^\circ, 28.0^\circ, 31.1^\circ, 35.0^\circ, 38.2^\circ$, and 42.0° . A description of the typical separation pattern that occurred for each angle is given in table VIII. In figure 18 the location of each test configuration and a brief description of the flow obtained for it has been superposed on a plot of the flow regimes obtained by Moore and Kline (ref. 4). A study of table VIII and figure 18 will show that the present results agree very well with the high-turbulence water-table results of Moore and Kline. The reader may wish to refer to these figures during the following brief descriptions of the vaneless diffuser flow characteristics.

At $2\theta = 7.0^\circ$ the flow was very steady. No separations could be observed at any location; however, very minor disturbances occurred at the downstream edges of the diverging walls.

At $2\theta = 14.0^\circ$ the diffuser setting was just above the high-turbulence line of appreciable stall. The flow was quite steady but intermittent transitory separation occurred in the downstream part of the diffuser. The overall separation varied in magnitude and intensity and shifted randomly from corner to corner. Simultaneously, slow moderate variations occurred in the throat static-pressure distribution.

At $2\theta = 16.8^\circ$ the flow was unsteady, but the fluctuations were not violent. Furthermore, a mild, faintly audible pulsation having a frequency of approximately 3 cps was observed. The overall separation shifted frequently from corner to corner while on the same diverging wall and occasionally shifted back and forth from one diverging wall to the other. Although the overall separation was present at all times, the local separation was of an intermittent transitory character. The throat static-pressure distribution was undergoing a continual change.

At $2\theta = 21.0^\circ$ the main overall separation, or stall, was firmly attached to the west wall and extended to within a few inches of the throat. This separation consisted of local transitory stall. Frequent zones of intermittent transitory stall occurred on the lower regions of the east wall. The main flow was quite unsteady, and very audible pulsations having a frequency of approximately 3 to 4 cps were observed. The pulsations were strong but not violent. It is to be noted that at $2\theta = 21.0^\circ$ and at each of the six remaining angles discussed below, a mirror image of the overall separation pattern was readily obtained by diverting the flow from the wall along which it was moving to the opposite wall. The flow was diverted by temporarily placing an obstruction or vane in its path.

At $2\theta = 24.5^\circ$ the flow was quite unsteady. There was a continual redistribution of the throat static pressure accompanied by random surging of the flow. Pulsations of the type observed for $2\theta = 21.0^\circ$ were not in evidence. The main overall separation was firmly attached to the east wall. It was nearly two-dimensional in form and extended to within a few inches of the throat; however, it consisted of local transitory stall with occasional small zones of temporary fixed stall. Occasional "flickers" of transitory stall occurred in the lower portion of the west wall.

At $2\theta = 28.0^\circ$ the diffuser setting was just above Moore and Kline's high-turbulence line bounding the three-dimensional, transitory stall regime from the two-dimensional, fully developed stall regime. The flow was relatively steady; the overall separation extended to within a few inches of the throat on the west wall and was very nearly two-dimensional in form. The main portion of the overall separation consisted of a local fixed stall with intermittent transitory stall. The side corners of the overall separation, formed by the diverging wall and the parallel walls, consisted primarily of local transitory stall. No separation was observed on the east wall. Slow and moderate variations occurred in the individual throat static pressures; however, the form of the static-pressure distribution remained essentially unchanged.

At $2\theta = 31.1^\circ$ the flow was fairly steady, and no separation occurred on the west wall. The overall separation was very nearly two-dimensional in form and extended to within a few inches of the throat. Overall, the flow was very similar to the flow at $2\theta = 28.0^\circ$. The only exceptions were that the local fixed stall had become more predominant and the corner regions of transitory stall had grown smaller.

At $2\theta = 35.0^\circ$ the flow was quite steady. The overall separation was essentially two-dimensional, extending to within approximately 1 inch of the throat on the west wall. It consisted primarily of local fixed stall; however, on the edges of the main separation there were a few local areas of transitory stall. No separation was observed on the east

wall. The tuft movements indicating the local stall were not so intense or violent as they were at $2\theta = 21.0^\circ$ and $2\theta = 28.0^\circ$. Only minor fluctuations of the throat static pressures occurred.

At $2\theta = 38.2^\circ$ the flow was steady, and the overall separation was essentially two-dimensional. The local separation was entirely fixed stall with the exception of the lower end of the diverging wall, which was fixed stall with intermittent transitory stall. Again, only minor variations occurred in the throat static pressure.

At $2\theta = 42.0^\circ$ the flow was very steady. The overall separation was essentially two-dimensional and consisted almost completely of local fixed stall. It extended to within approximately 1 inch of the throat on the west wall. No separation was observed on the east wall, and only minor fluctuations occurred in the throat static pressures.

The descriptions of the flow characteristics given above are somewhat subjective; however, it is believed that they illustrate the character of the different regimes of diffuser flow and the nature of the local separation that occurs in each regime. It is noted that when the diffuser operation first enters the fully developed stall regime, the overall separation consists primarily of local transitory stall. However, as the operating point shifts farther into the fully developed stall regime (say, at constant values of L/W), the character of the local separation gradually changes from predominantly transitory stall to predominantly fixed stall. The growth of the zone of local fixed stall is from the throat towards the exit and outward toward the side walls, as shown by the sketches in table VIII.

Diffuser performance.— A plot of the pressure-recovery coefficient C_{PR} and the pressure efficiency η_p obtained for the flows just described is given in figure 19, and a brief description of the flow corresponding to each test angle is given in figure 18. From a study of figures 18 and 19 many important characteristics of unmodified two-dimensional diffuser performance can be seen.

First, it can be seen that the maximum static-pressure recovery occurs near the line of appreciable stall defined experimentally by Moore and Kline (ref. 4). This result is in agreement with the preliminary air work done by Moore and Kline using the present diffuser. Further, the curve of maximum C_{PR} obtained from Reid's data (ref. 6), which has been superposed on figure 18, also shows that the maximum pressure recovery occurs near the point of appreciable stall. The slope of Reid's maximum C_{PR} curve is not the same as the slope of the line of appreciable stall obtained by Moore and Kline; however, when it is considered that Reid used a different diffuser with different

(although constant) inlet conditions, it can be concluded that the agreement between the two curves is both reasonable and significant.

Second, it can be seen that the static-pressure recovery begins to fall off rapidly as the included angle is increased beyond the point of maximum recovery, if both inlet conditions and L/W_1 are held constant. As the static-pressure recovery begins to decrease the flow becomes unsteady and large regions of three-dimensional transitory stall develop. When the included angle is increased further, so that the diffuser is operating well into the transition region between the transitory stall regime and the fully developed stall regime, the main separation attaches to one of the diverging walls and becomes somewhat two-dimensional in form. At this point, the local separation consists predominantly of transitory stall, the flow is very unsteady, the fluctuations are largest, and the pressure recovery is decreasing rapidly. As the angle is increased still further the flow approaches the regime of stable fully developed stall. Simultaneously, the local separation grows from a transitory stall to a fixed stall and the flow becomes increasingly steady. In addition, when the local separation becomes predominantly a fixed stall the pressure-recovery coefficient attains a minimum value. Finally, when the included angle becomes large enough, the flow becomes very steady and the fully developed stall consists almost entirely of local fixed stall.

Third, figure 18 shows that the line of appreciable stall does not vary excessively even though the inlet conditions vary considerably. This is illustrated by the curves in reference 4 which were obtained for two different levels of inlet turbulence. Furthermore, the occurrence of appreciable amounts of separation at angles slightly larger than the angle of maximum recovery, as observed in the present investigation and by others, suggests that the line of appreciable stall should approximately correspond to the line of maximum C_{PR} . As mentioned above, a plot of the line of maximum C_{PR} , from the data of Reid (ref. 6), is shown in figure 18. It can be seen that the line of appreciable stall for all of Moore and Kline's data and Reid's line of maximum C_{PR} do not differ from a mean value by more than ± 25 percent for all values of L/W_1 , and in most cases the difference is considerably less. Furthermore, it can be seen that the high-turbulence line of appreciable stall obtained by Moore and Kline represents an approximate mean value of the three curves. The implications of this are obvious; namely, this high-turbulence line of appreciable stall can be used to obtain an approximate value for the angle of maximum static-pressure recovery for any plane-wall, subsonic, two-dimensional diffuser for the range of L/W_1 that has been studied. In addition, since the maximum static-pressure recovery occurs near the point where an appreciable amount of transitory stall begins to develop, the high-turbulence line of appreciable stall obtained by Moore and Kline indicates the approximate value of the

included angle at which a significant amount of separation is produced. This latter idea will be shown subsequently to have an important application in the design of the vane clusters.

It should be noted at this point that the works of Reid (ref. 6) and Moore and Kline (ref. 4) and the present work have been conducted with relatively thin inlet boundary layers ($\delta^*/W_1 \approx 0.003 - 0.010$). For thicker and less favorable inlet boundary layers the actual line of appreciable stall probably lies at lower values of 2θ for a given value of L/W_1 than Moore and Kline's high-turbulence line of appreciable stall; consequently, a larger error in predicting 2θ for maximum recovery or appreciable separation would likely be incurred. Systematic studies of the effect on the line of appreciable stall of different inlet boundary-layer thicknesses and shapes is now under study in the current program, but data are not yet available; until data of this type are available, the high-turbulence curve obtained by Moore and Kline should be used with considerable caution.

The curve of pressure effectiveness η_p given in figure 19 illustrates the fact that the maximum value of η_p occurs at an appreciably smaller value of 2θ than does the maximum value of C_{PR} . (This phenomenon was also noted by Reid (ref. 6)). Using the definitions of η_p and $C_{PR_{ideal}}$ it can readily be shown that such a phenomenon must occur. For this purpose, consider a diffuser having W_1 , L/W_1 , and all inlet conditions held constant as the included angle is increased from 0° . At $2\theta = 0^\circ$ the diffuser is simply a pipe in which a loss in static pressure occurs; thus, $C_{PR} < 0$ and $\eta_p = -\infty$. At some small positive value of 2θ the momentum conversion will just offset the frictional static-pressure loss; therefore, both C_{PR} and η_p will be zero. As 2θ is increased further C_{PR} becomes positive and, for a time, increases faster than $C_{PR_{ideal}}$; however, as 2θ is increased still further the rate of increase of C_{PR} is reduced by the additional losses and by the production of a less uniform exit velocity profile. It can be seen from the definition of η_p that the logarithmic increase of η_p is equal to the difference of the logarithmic increases of C_{PR} and $C_{PR_{ideal}}$; that is,

$$\log_e \eta_p = \log_e C_{PR} - \log_e C_{PR_{ideal}}$$

To find the maximum value of η_p as a function of 2θ , the equation is differentiated and equated to zero. This yields

$$\frac{\partial}{\partial \theta} (\log_e \eta_p) = \frac{\partial}{\partial \theta} (\log_e C_{PR}) - \frac{\partial}{\partial \theta} (\log_e C_{PR_{ideal}}) = 0$$

or

$$\frac{1}{C_{PR}} \frac{\partial C_{PR}}{\partial \theta} = \frac{1}{C_{PR_{ideal}}} \frac{\partial C_{PR_{ideal}}}{\partial \theta} \quad (18)$$

Equation 18 shows that when the value of η_p is a maximum the fractional rate of increase with angle of C_{PR} and of $C_{PR_{ideal}}$ is identical. Further, since C_{PR} is positive and since by definition both $C_{PR_{ideal}}$ and $\frac{\partial C_{PR_{ideal}}}{\partial \theta}$ are positive, equation (18) shows that $\left(\frac{\partial C_{PR}}{\partial \theta} \right)_{\eta_{p,max}} > 0$. In

other words, the maximum value of C_{PR} cannot occur at the angle of maximum η_p . For angles greater than $2\theta_{\eta_{p,max}}$, the ideal pressure recovery increases proportionately faster than the actual pressure recovery and hence η_p decreases with further increase in 2θ . However, the actual pressure recovery will continue to rise with increase in angle until the added losses and increased rate of momentum efflux (brought about by the increase in angle) actually exceed the theoretical gain in recovery made possible by the increased angle.

The physical argument just noted regarding the relation between the losses and the recovery is easily proved mathematically from equation (16) as follows:

$$\bar{H}_L = C_{PR_{ideal}} - C_{PR}$$

Differentiating and equating $\frac{\partial C_{PR}}{\partial \theta}$ to zero yields

$$\frac{\partial \bar{H}_L}{\partial \theta} = \frac{\partial C_{PR_{ideal}}}{\partial \theta}$$

A discussion of the important effect of momentum efflux rate, as evidenced by the exit velocity profile, is given by Moore and Kline (ref. 3). They have shown that the optimum exit velocity profile is one-dimensional and that alteration in the profile has a very strong effect on both recovery and effectiveness. A more thorough discussion of the loss mechanisms and their relation to the optimum recovery and

effectiveness is given in reference 2. It is not repeated here since it depends on a prior discussion of the mechanism of transitory stall.

It is interesting to note that the optimum diffuser angle is not necessarily that for maximum effectiveness. In fact where pressure recovery and length are primary factors, as, for example, in aircraft, the maximum-pressure-recovery diffuser would be much more suitable than the maximum-effectiveness diffuser; the decision depends on the factors of concern in each case.

Most of the work in the present investigation has been done at total included angles greater than 21° . For this range of angles it can be seen from figure 19 that there is little difference between the curves of η_p and C_{PR} . This arises from the fact that the area ratios for the geometries under consideration yield values of $C_{PR_{ideal}}$ near unity. As a consequence of the similarity of C_{PR} and η_p in this region, the majority of the discussions to follow will be limited to considerations of C_{PR} only. Considerations of the envelope of η_p that can be obtained with properly designed vanes will be given subsequently.

$$\begin{aligned} \text{DIFFUSER WITH VANES } (L/W_1 \approx 8.0; W_1 = 3.00 \text{ INCHES;} \\ R_{W_1} \approx 2.4 \times 10^5) \end{aligned}$$

In the following discussions it should be remembered that a and α are defined by equations (1) and (2), respectively, unless it is specified otherwise. In addition, the longitudinal position of the clusters has been specified by the ratio b/a . This has been done in preference to using the length c because it is believed that the ratio b/a is more fundamental to the vaned diffuser flow.

Tests at $2\theta = 42.0^\circ$

Variations of n , f , and b/a .—For five values of vane length ($f = 3, 6, 9, 12$, and 15 inches), clusters were assembled using 1, 2, 3, 4, and 5 vanes. Tests were conducted with each cluster using, generally, four values of b/a . Families of curves of C_{PR} plotted against b/a are given for each value of f in figure 20. A discussion of the flow characteristics obtained for each configuration would be prohibitively long. Furthermore, it is believed that such detail is not desired since the results of the near-optimum configurations are of primary importance

in this investigation. Consequently, only a brief discussion of the results obtained at each value of f is given below.

It should be noted beforehand that three features are common to nearly all the curves shown in figure 20. These are as follows: (1) For b/a increasing from unity, each curve of C_{PR} either begins at a maximum value or attains a maximum value and then decreases; (2) as n is increased from 1 to 5 the maximum value of C_{PR} is increased; and (3) the value of b/a , at which the maximum value of C_{PR} occurs, increases as n is increased.

The family of C_{PR} curves for $f = 3.00$ inches is given in figure 20(a). The flow for all values of n at $b/a = 1.0$ was fairly steady, although minor slow and random fluctuations occurred in the throat pressures. The steadiest flow was obtained for $n = 4$. As b/a was increased (i.e., as the clusters were moved farther downstream) the fluctuations of the flow tended to increase; however, in all cases the fluctuations were relatively small and slow up to and somewhat beyond the point of maximum C_{PR} . The dashed portions of the curves indicate the region in which the fluctuations would probably be objectionable. Unlike the results of the other vane lengths, the pressure recovery for $n = 4$ was everywhere greater than the pressure recovery for $n = 5$.

The curves of C_{PR} for $f = 6.00$ inches are given in figure 20(b). They are similar to the curves for $f = 3.00$ inches; however, the corresponding values of C_{PR} are greater, and the maximum value of C_{PR} is obtained for $n = 5$. At $b/a = 1.0$ it was found that the flow for $n = 1$ was only fairly steady and that the flow for $n = 2$ was quite unsteady. For $n = 3$ and 4 the flow was steady and for $n = 5$ it was very steady. Again it was found that the flow fluctuations increased in frequency and the separation increased slightly in extent as b/a was increased; however, the fluctuations were minor and slow up to and somewhat beyond the point of maximum C_{PR} . The regions in which the flow fluctuations would probably be objectionable are again shown by the dashed portions of the curve.

The curves of C_{PR} for $f = 9.00$ inches are given in figure 20(c). These curves are similar to the curves for $f = 6.00$ inches; however, the maximum value of C_{PR} for $n = 5$ is appreciably greater than that for either $f = 3.00$ or 6.00 inches. A comparison of the curves in figures 20(a), 20(b), and 20(c) shows that the trend of the longer vanes for the larger values of n at values of b/a beyond the maximum value of C_{PR} is toward a greater rate of decrease of C_{PR} . At $b/a = 1.0$ the flow was fairly steady for $n = 1, 2$, and 3 and was very steady for $n = 4$ and 5. The flow was satisfactorily steady for all values of b/a

up to and somewhat beyond the maximum value of C_{PR} ; that is, the pressure fluctuations that occurred were slow and random and had amplitudes of approximately ± 2 to ± 4 percent of the mean value of their respective pressures. These fluctuations were primarily just redistributions of the throat pressures and not changes in the overall mean pressure.

The curves of C_{PR} for $f = 12.00$ inches are given in figure 20(d). It can be seen that, compared with $f = 9.00$ inches, an improvement in the maximum value of C_{PR} for $n = 3$ and 4 was obtained; however, no gain was obtained for $n = 5$. At $b/a = 1.0$ continual redistributions of the throat pressure and minor flow surges were obtained for $n = 1$ and 2 . For $n = 3$ the flow was fairly steady, and for $n = 4$ and 5 the flow was very steady. As b/a was increased up to and just beyond the maximum value of C_{PR} for $n = 3, 4$, and 5 the flow fluctuations increased in frequency and the separations became slightly stronger; however, the steadiness of the flow was, again, quite satisfactory. For $n = 1$ and 2 , the flow appeared to become somewhat steadier as b/a was increased. A new phenomenon occurred for the case of $n = 5$ and $b/a = 1.26$. As the diffuser flow was being increased from zero to the test value, a transitory stall developed in a corner of one of the outer vane passages. (The corner was formed by the diffuser diverging wall and parallel wall.) While the stall existed, small flow pulsations occurred and the pressure recovery was quite poor. On one occasion the stall "washed out" of its own accord, and on others it was easily removed by creating additional turbulence in the entrance flow. (Rapid hand waving back and forth in front of the stall zone was sufficient to cause it to wash out.) After the stall was removed the flow was quite steady and, as can be seen from figure 20(d), the pressure recovery was very good.

The curves of C_{PR} for $f = 15.00$ inches are given in figure 20(e). The curves for $n = 2, 3$, and 4 are quite similar to the previous curves obtained for the other values of f ; however, the maximum values of C_{PR} are somewhat greater. In other respects they are essentially the same and need no further discussion. The curves for $n = 1$ and particularly for $n = 5$ are quite different. For the case of $n = 1$ and $b/a = 1.0$ the flow would occur in two different patterns, one in which the overall separation was asymmetric, or three-dimensional, and the other in which the overall separation was symmetric and nearly two-dimensional. It can be seen that a considerable difference in C_{PR} was obtained for the two different patterns. The symmetric separation, with the smaller value of C_{PR} , was the preferred pattern (the flow would select this pattern more frequently than the other). For the case of $n = 5$ and $b/a = 1.23$ an instability phenomenon was discovered. The flow would exist for a time in one of two different patterns; however, neither pattern was stable. The pattern (A) for which the largest value of C_{PR} was obtained was

steadier than the pattern (B) for which the smaller value of C_{PR} was obtained (see fig. 20(e) for the locations of (A) and (B)). However, in pattern (A) the flow was subject to an almost continual redistribution of the throat static pressure and to occasional sudden surges or pulsations. If the flow was disturbed, for example, by a slight blockage of the entrance flow, the flow would shift to pattern (B). Unlike pattern (A), the separation in pattern (B) was quite extensive and asymmetric. In fact, in one corner of one of the outer vane passages there was a continual flow which actually came up through the outer channel and went back down through the adjacent channel. The flow "spilled" over approximately 2 to 3 inches of the outer vane leading edge. While in pattern (B), the flow was quite unsteady and was subject to frequent surges. On one occasion the flow shifted back to pattern (A); however, pattern (B) was preferred.

A comparison of the approximate size and location of the zones of separation that occurred in the diffuser, with 2θ set at 42.0° , is shown in figure 21. Figure 21(a) illustrates the separation that occurred in the unvaned diffuser. This has been described previously. Figure 21(b) illustrates the type of separation, or stall, that occurred with the vanes installed. Note that the major part of the separation is found on the parallel walls and not on the diverging walls in the vaned unit. It was found that the vane holding mechanisms (the dowels and hooks used to suspend the vanes) were partly responsible for the side-wall separation. In a test which will be discussed later, it is shown that an appreciable improvement in C_{PR} can be obtained, in some instances, by improving the holding mechanisms.

Determination of optimum value of f .— The maximum value of C_{PR} , for which the flow is at least fairly steady, has been determined from each of the curves in figure 20. From these data, curves of maximum C_{PR} have been plotted in figure 22 using n as the parameter. In addition, values of L/W_1 obtained from Moore and Kline's high-turbulence line of appreciable stall (line aa in fig. 3) have been superposed on each corresponding curve. Note that f/a and α for the vane clusters are equivalent, respectively, to L/W_1 and 2θ for a diffuser. From figure 22 it can be seen that $(f/a)_{as}$ falls near the knee on the flat upper portion of each curve in every case. This is both fortunate and very significant. It may be recalled that the line of appreciable stall indicates the approximate included angle at which appreciable separation is developed in a plane-walled, two-dimensional diffuser. Thus, it would be anticipated that when this situation occurred in the vane channels further increases of f/a for fixed values of α would result in increased zones of separation and hence would yield little or no further increase in the diffuser pressure recovery. This is in complete accord with the present experimental observations as shown in figure 22.

Further explorations made with the "tuft probe" did, in fact, reveal that increases of vane length for constant values of α and a resulted in increased zones of separation in the ends of the vane channels and occurrences of minor separations at the trailing edges of several of the vanes. Thus, at least for the case of $2\theta = 42.0^\circ$, the high-turbulence line of appreciable stall (ref. 4) can be used to determine the optimum value of f simply by making $f/a = (f/a)_{as}$ for the corresponding value of α .

Determination of optimum value of n .— A comparison of the maximum values of C_{PR} obtained for each value of n can be made from the curves in figure 22. However, it is more illuminating if these values are plotted against the vane angle α where $\alpha = 2\theta/(n + 1)$. This has been done in figure 23. The resulting curve shows that at least a near-maximum value of C_{PR} has been obtained. It shows, further, that the addition of another vane ($n = 6$ and $\alpha = 6^\circ$) would probably result in a small decrease of C_{PR} . Therefore, it can be concluded that the value of n for which $\alpha = 7.0^\circ$ is at least very near the optimum value for the case of $2\theta = 42.0^\circ$.

Effect of variation of α_o/α .— At the outset of the present investigation it was suspected that the diffuser performance might be optimized by making small adjustments in α . In order to investigate this possibility, tests were conducted for several values of α with $n = 5$, $f = 15$ inches, $f/a = 30$, and $b/a = 1.01$. The results of these tests are shown by the curve of C_{PR} plotted against α_o/α given in figure 24. It can be seen that the maximum value of C_{PR} occurred at or very near $\alpha_o/\alpha = 1$. In other words, the equal-angle arrangement defined by equation (3) is shown to yield the best performance. It must be remembered that there are other possible ways in which to adjust the angle settings of the vanes; that is, it may be that unequal adjustments of the individual values of α in a given cluster will yield an improvement in C_{PR} . Adjustments of this type were precluded by the restrictions imposed on the vane cluster geometries. However, in view of the good pressure recovery that can be obtained with the present cluster geometry, it is not likely that a large increase in C_{PR} can be obtained by such additional adjustments.

Determination of optimum value of a .— Tests were conducted using two additional values of a for $f = 15$ inches and $\alpha = 7.0^\circ$. Denoting a of equation (1) by a_1 , these values were as follows: $a < a_1$ and $a > a_1$. Since a was not the same in all of these tests, the values of pressure-recovery coefficient shown in figure 25 have been plotted against $(4a + 2b)/W_1$ instead of against b/a . For a given value of $(4a + 2b)/W_1$ the cluster has the same value of c regardless of the value of a . It

is interesting to note that with $a > a_1$ the resulting value of C_{PR} was considerably less than that obtained with $a = a_1$, except for one test point. Furthermore, the flow was not so steady with $a > a_1$. For $a < a_1$, the resulting flow steadiness and C_{PR} were comparable to those obtained for $a = a_1$; however, in the useful range of $(4a + 2b)/W_1$, the pressure recovery for $a = a_1$ was slightly greater. (The flows were fairly steady, or better, only for the region $[(4a + 2b)/W_1] < 1.065$.) It can be concluded from these results that the most suitable value of a is a_1 for $2\theta = 42.0^\circ$.

Effect of vane end clearance.- Since in a practical design the vanes would probably be constructed without end clearance, a brief investigation was made of the flow in the regions of the ends of the vanes. It was found that the flow on the parallel walls went diagonally downstream from the inner vane channels towards the outer vane channels. Tests were consequently conducted using a near-optimum cluster geometry for the following situations: (1) The cluster placed against one of the diffuser side walls, thus fixing all the end clearance at the opposite end; (2) the cluster centered between the side walls (the usual procedure); and (3) the clearance at both ends of each individual vane sealed with drafting tape. The results of these tests, along with the cluster geometry and orientation, are presented in table IX. The difference between the pressure-recovery coefficients obtained for the unsealed noncentered cluster and the unsealed centered cluster indicates that there is a significant effect due to the asymmetric positioning of the cluster. When the cluster was placed against the diffuser side wall, the separation pattern was asymmetric with respect to a plane parallel to, and midway between, the side walls. Nearly all the separation was located on the end-clearance side. When the cluster was centered, the separation was symmetrical and similar to that illustrated in figure 21(b). The flow was steadier when the cluster was centered; however, it was satisfactorily steady even when the cluster wasn't centered.

When the ends were sealed with tape, the resulting flow was essentially the same as that for the centered unsealed cluster. Of course, the flow pattern on the side walls in the region of the cluster was different because the crossflow was prevented; however, no appreciable difference in the side-wall exit flow could be observed. The pressure-recovery coefficient obtained for the centered unsealed cluster is shown, in table IX, to be slightly greater than the pressure-recovery coefficient obtained for the sealed cluster. Since the difference obtained is within the uncertainty interval of C_{PR} , no significant trend was established; however, it can be concluded in the case of the optimum clusters at $2\theta = 42.0^\circ$ that when the clusters are centered the end clearance causes no significant effect on the diffuser performance.

Tests at $2\theta = 28.0^\circ$

With 2θ set at 28.0° tests were conducted which were comparable to those described above for $2\theta = 42.0^\circ$. The same values of f were used, but n was limited to 3 with the exception of one cluster for which $n = 4$.

Variations of f , n , and b/a .— The results obtained are shown by the families of pressure-recovery curves given in figure 26. The general characteristics of these curves are similar to the corresponding curves presented for $2\theta = 42.0^\circ$.

For $f = 3.00$ inches the curves of C_{PR} are given in figure 26(a). It is interesting to note that, although very considerable improvements in C_{PR} were obtained, the flow steadiness was unsatisfactory for nearly all the configurations with $f = 3.00$ inches. For $n = 3$, with b/a equal to approximately 1.2, two values of C_{PR} were obtained, one for each of the two flow patterns that occurred. The transition which occurred in shifting from one pattern to the other was not violent, but the large difference in C_{PR} nevertheless illustrates the unsatisfactory character of the flow. Two patterns occurred for some of the other test configurations in the regions shown by the dashed curves; however, no additional data were recorded for these patterns.

The results obtained for $f = 6.00$ inches are given in figure 26(b). It can be seen that, overall, the flows were steadier than those obtained for $f = 3.00$ inches. The character of the unsteady flows had changed; that is, they did not shift back and forth between different patterns. Instead, they fluctuated about a given pattern. With $n = 1$ and 3 for $b/a = 1.21$ and 1.52, respectively, audible pulsations occurred having a frequency of approximately 3 cps.

For $f = 9.00$ inches (fig. 26(c)) the flows obtained with $n = 1$ and 2 were not much steadier than the corresponding flows for $f = 6$ inches. Audible pulsations occurred for all the tests with $n = 1$ and for $n = 2$ when $b/a = 1.38$. The flows obtained with $n = 3$ at $b/a = 1.00$ and 1.16 were very steady; however, the separations in the flow at $b/a = 1.16$ were stronger and more extensive than those at $b/a = 1.00$. The flow at $b/a = 1.35$ and $n = 3$ was critical and would occasionally break down into a pulsating flow for short periods of time. For $b/a = 1.48$ and $n = 3$ the flow was very unsteady, and an extensive asymmetric corner stall developed in which the separation zone extended up to the region of the vane leading edges. A continuous overflow from the outer channel into the adjacent channel occurred along several inches of the corresponding outer vane leading edge.

Four curves of C_{PR} are presented for $f = 12.00$ inches in figure 26(d). Again, for $n = 1$ the flow was unsteady for all values of b/a . With $n = 2$ the flow was just fairly steady. With $n = 3$ the flow was very steady for a value of b/a less than that at maximum C_{PR} : at $b/a = 1.28$ the flow had become critical and at $b/a = 1.42$ it was quite unsteady. The flow obtained for $n = 4$ exhibited somewhat different characteristics; it was very steady over a range of b/a from zero to approximately 1.4. As b/a was increased further, the fluctuations developed in size and frequency until, at $b/a = 1.64$, the flow was only fairly steady. Two values of C_{PR} are shown at $b/a = 1.64$. The lower value was obtained in bringing the flow up to speed. The initial flow was unsteady and had large regions of asymmetric separation. It appeared to be "stable," but in the course of 10 to 15 minutes it shifted, by stages, to the fairly steady flow for which the larger value of C_{PR} was obtained. This latter pattern was stable.

The results obtained for $f = 15.00$ inches (fig. 26(e)) were practically the same as those obtained for $f = 12.00$ inches. The only significant exception was that the values of C_{PR} for $n = 3$ and $f = 15.00$ inches were slightly less than the corresponding values for $f = 12.00$ inches. The flow steadiness and the zones of separation were essentially the same in all respects.

In summary of the above flows at $2\theta = 28.0^\circ$, it may be said that the characteristics of the flows which were suitable for practical application were similar to those obtained for $2\theta = 42.0^\circ$. The flows were the steadiest for $b/a = 1.0$. As b/a was increased up to its maximum useful value the fluctuations increased in size and frequency. In addition, the zones of separation increased in size and intensity. As before, useful flows were considered to be those which were at least fairly steady. Figure 21(b) again illustrates the separation patterns which occurred when the diffuser had an efficient vane design, for example, using $f = 12.00$ inches, $n = 3$, and $b/a = 1.2$.

It was considerably more difficult to obtain a steady flow for $2\theta = 28.0^\circ$ than for $2\theta = 42.0^\circ$. This is illustrated by the fact that at $2\theta = 28.0^\circ$ all of the flows for $n = 1$ and several of the flows for $n = 2$ were unsatisfactory for practical application. This is probably due to the fact that the unvaned diffuser flow at $2\theta = 28.0^\circ$ is just out of the regime of large transitory stall (figs. 18 and 19).

Determination of optimum value of f .— The maximum value of C_{PR} that can be obtained for each value of f and n was determined from figure 26. These values of C_{PR} were plotted against f/a using n as the parameter (fig. 27). The value of f/a corresponding to the

high-turbulence line of appreciable stall obtained by Moore and Kline is shown by the solid symbol point on each curve. It can be seen that $(f/a)_{as}$ again falls approximately on the high side of the knee of each curve; however, in the case of $n = 3$ a maximum value of C_{PR} was obtained just before $f/a = (f/a)_{as}$. Explorations with tuft probe revealed that the zones of separation in the vane channels increased when f/a was increased with α held constant. When the flows were at least fairly steady, the separation patterns that occurred were similar to the pattern illustrated in figure 21(b). For the case of $n = 3$, $f = 15.00$ inches, and $b/a = 1.2$, additional stalls were observed in the region of the trailing edges on the inner surfaces of several of the vanes. These results are in very good agreement with the results obtained for $2\theta = 42.0^\circ$; the only significant difference is that somewhat unsteady flows were obtained with $n = 1$ and 2 for $2\theta = 28.0^\circ$. It is believed, however, that this difference does not detract from the significance of the concept of using the line of appreciable stall for determining the optimum value of f .

Determination of optimum value of n .— The maximum value of C_{PR} obtained for each value of n , with $f = 12.00$ inches, has been plotted against α in figure 28. It is interesting to note the rapid decrease of C_{PR} that occurred when n was increased from 3 to 4. This phenomenon strengthens the assumption made previously regarding the addition of another vane in the comparable tests at $2\theta = 42.0^\circ$.

Figure 28 shows that, for $2\theta = 28.0^\circ$, the most suitable value of n is that which makes $\alpha = 7.0^\circ$. Since this same conclusion was reached for $2\theta = 42.0^\circ$, it is reasonable to conclude that, for the range of 2θ investigated, when 2θ is a multiple of 7.0° then the optimum value of n is that which makes $\alpha = 7.0^\circ$. Additional considerations regarding diffusers in which 2θ is not an exact multiple of 7.0° will be presented subsequently.

Effect of variations of α_o/α .— Tests were conducted which were comparable to those discussed previously for $2\theta = 42.0^\circ$. For the present case two values of b/a were used with $f = 12.00$ inches and $n = 3$. The results for $b/a = 1.04$, which correspond to the configurations tested at $2\theta = 42.0^\circ$, are shown in figure 29. Unlike the former results, it can be seen that the ratio of α_o/α is not critical. Furthermore, the maximum value of C_{PR} occurs at a value of α_o/α slightly greater than 1.0. The results which were obtained for $b/a = 1.20$ are also shown in figure 29. At this position, however, the angle adjustment was critical, and the maximum value of C_{PR} occurred at $\alpha_o/\alpha = 1.0$. The latter results are in agreement with the results obtained for $2\theta = 42.0^\circ$.

The results of the vane-angle adjustment tests obtained thus far lead to the conclusion that the equal-angle arrangement is the most suitable when the diffuser total included angle is a multiple of 7° . This is justified on the basis of the simplicity afforded by the equal-angle arrangement and also by the fact that the maximum value of C_{PR} occurs at or very near $\alpha_o/\alpha = 1.0$.

Determination of optimum value of a .— Tests were made using three values of a with $n = 3.0$, $f = 12.00$ inches, and $\alpha = 7.0^\circ$. These values were (1) $a = a_1$ (where a_1 is determined by equation (1)), (2) $a > a_1$, and (3) $a < a_1$. From the resulting curves shown in figure 30 it can be seen that little difference in C_{PR} was obtained over the useful range of $(2a + 2b)/W_1$, regardless of whether a is greater or less than a_1 . Overall, the flow was slightly steadier and the maximum value of C_{PR} was slightly larger when $a = a_1$. Considering the desirability of a simple criterion, and on the basis of the results thus far presented, it can be concluded that the most suitable value of a is a_1 .

Effect of vane end clearance.— End-clearance tests were conducted which were identical to those described for $2\theta = 42.0^\circ$. The results, along with the cluster geometry and orientation, are presented in table IX(b). The difference obtained between any two values of C_{PR} is less than the uncertainty interval for C_{PR} . Further, the flow steadiness for each configuration was essentially the same. Consequently, it can be concluded that, for the optimum clusters at $2\theta = 28.0^\circ$ and 42.00° , the end clearance has no significant effect on the diffuser performance. It is noted that the effect of cluster end clearance has been evaluated only for odd values of n , and since the holder mechanism is different for even values of n , it cannot be said at this point that the end-clearance effect is negligible for even values of n . Further considerations for even values of n are given subsequently.

Determination of optimum value of b/a ($2\theta = 28.0^\circ$ and 42.0°).— There are at least two considerations involved in obtaining a good diffuser performance. One is the production of a smooth flow and the other is the attainment of a large pressure recovery. With these ideas in mind a study was made of the curves given in figures 20 and 26. It was found that a steady flow was reasonably insured and a near-maximum value of C_{PR} was obtained when b/a was set equal to 1.2. Conservative design for good recovery with assurance of steady flow might well be a compromise value of b/a in the neighborhood of 1.1 since the curves of C_{PR} plotted against b/a for optimum values of n are quite flat.

These considerations of b/a are completely empirical and are limited to the near-optimum cluster configurations.

Summary of Results for $2\theta = 28.0^\circ$ and 42.0°

The vane design criteria that has been thus far developed can be summarized as follows:

- (1) An equal-angle cluster should be used where $\alpha = \frac{2\theta}{n+1}$.
- (2) The number of vanes n should be selected so that $\alpha = 7.0^\circ$.
- (3) The vane spacing a should be determined from the relation $a = \frac{W_1}{n+1}$.
- (4) The vane length f should be selected so that $f/a = (f/a)_{as}$, where $(f/a)_{as}$ is obtained from Moore and Kline's high-turbulence line of appreciable stall (ref. 4) at the corresponding value of α .
- (5) The cluster should be positioned so that $b/a = 1.2$.

When α satisfies the definition given in item (1) then item (2) is not applicable unless 2θ is a multiple of 7.0° . Considerations for 2θ when it is not a multiple of 7.0° are given below.

Items (3), (4), and (5) do not directly involve 2θ . For the range of 2θ investigated, it is believed that they are applicable for all values of 2θ regardless of whether 2θ is a multiple of 7.0° . No additional testing was done to investigate explicitly the suitability of items (3), (4), and (5). However, the excellence of the pressure recoveries that were obtained in later tests leaves little doubt of the adequacy of these criteria.

Investigations at Other Angles

Determination of optimum value of n for any value of 2θ .— This part of the experimental investigation was designed on the basis of the following hypothesis. For any angle 2θ , n should be selected so that the difference between the resulting value of α and 7.0° is a minimum. (It is to be understood that α is defined by equation (2).) The curve of α which yields the minimum difference between α and 7.0° is plotted

against 2θ in figure 31. There are four values of 2θ , in the range between 14.0° and 42.0° , at which $\alpha_n - 7 = 7 - \alpha_{n+1}$. These values are $2\theta = 16.8^\circ$, 24.0° , 31.1° , and 38.2° . Tests were conducted at values of $2\theta = 16.8^\circ$, 24.5° ,¹ 31.1° , and 38.2° . Two values of n were used for each of these tests, namely, n and $n + 1$ for which α was, respectively, greater than and less than 7.0° . In addition, tests were conducted at $2\theta = 21.0^\circ$ with $n = 1, 2$, and 3 .

In all these tests, the values of α , a , and b/a were determined from items (1), (3), and (5) given in the preceding summary. It was not possible to use the exact values of f specified by item (4) because only five vane lengths were available. However, with the exception of $2\theta = 16.8^\circ$, the actual values of f were sufficiently close to the specified values to assure performance consistent with the design criteria. Fortunately, the performance obtained at $2\theta = 16.8^\circ$ also appears compatible with the design criteria.

It was intended that the curves of C_{PR} plotted against 2θ , obtained for each value of n , would be extrapolated to determine their points of intersection and thereby locate the value of 2θ at which $C_{PR_n} = C_{PR_{n+1}}$. The combined curves of C_{PR} would determine an envelope of maximum C_{PR} . The criterion for the determination of n at any value of 2θ would then simply be a matter of selecting that value of n corresponding to the point in question on the envelope.

Before considering the results of the above tests, it should be noted that a series of tests was conducted at $2\theta = 14.0^\circ$. Several values of b/a were studied for each value of f with $n = 1.0$. It was found that the maximum value of C_{PR} obtained with the vanes was identical to the value of C_{PR} obtained without the vanes.

The results of all the above tests are presented in figure 32. It can be seen that the curves of C_{PR} obtained when n was even fall below the envelope of C_{PR} described by the curves obtained when n was odd. This was not altogether surprising because it had been suspected that the vane holding mechanism for odd values of n was more favorable than the mechanism for even values of n . It is shown in figure 10 that a dummy vane end was required when the value of n was even but not when the value of n was odd. It is believed that the

¹ $2\theta = 24.5^\circ$ was used in place of $2\theta = 24.0^\circ$ because the diffuser was inadvertently set at the former value. Since $2\theta = 24.5^\circ$ would accomplish the desired objectives, it was felt unjustified to spend the additional time required to readjust the diffuser.

additional disturbance of the flow caused by the dummy vane end is responsible for the anomaly shown in figure 32. This belief was substantially verified in a later test at $2\theta = 31.1^\circ$ in which the vane holding mechanism for even values of n was modified. The pressure-recovery coefficient obtained for this test is indicated in figure 32. A more detailed discussion of the modified holder mechanism is given below.

The envelope of C_{PR} defined by the curves for odd values of n can be used to determine the desired values of n for any given 2θ . However, it is probable that the vane ends would be attached directly to the diffuser walls in an actual application where no requirement for adjustment existed. At any rate, the actual mechanism would undoubtedly be more streamlined than the dummy vane end used in the present investigation. Therefore, it is more realistic to estimate the probable value of C_{PR} which would be obtained with streamlined holders for $n = 2$ and 4. Such an estimate is shown by the dashed curves in figure 32.

Modification of vane holder, $2\theta = 31.1^\circ$.— A photograph of the assembled cluster and the modified holder mechanism is shown in figure 10(c). With the exception of the holder mechanism, the cluster was identical to the four-vane cluster in the tests described in the preceding section.

The modified holder mechanism consisted simply of four steel dowels inserted into four small teardrop-shaped receptacles. Each receptacle was soldered to its respective cluster assembly dowel. No provisions were made to adjust the position of the holders relative to the cluster. The cluster was positioned at $b/a = 1.15$ instead of at $b/a = 1.2$ in order to reduce the overall size of the receptacles required. If the cluster had been positioned at $b/a = 1.2$, then the axis of the supporting dowels would have intersected with the axis of the cluster assembly dowels. At $b/a = 1.15$ the supporting dowels passed under the cluster assembly dowels; consequently, receptacles of small cross section could be employed. As mentioned previously, the pressure-recovery coefficient increased markedly with the modified hangers. The test point is shown in figure 32.

An additional test was made in which the end clearance of the cluster was sealed with drafting tape. In contrast to the results of the previous tests of this character, a significant difference in C_{PR} was found to occur. The values of C_{PR} obtained are as follows: With no tape, $C_{PR} = 0.706$; with tape, $C_{PR} = 0.735$. The flows were steady in both instances, but if a choice were to be made it would be in favor of the taped or zero-end-clearance flow. It is not fully understood why such a difference occurred when the modified holders were used. It has been shown previously that no such effect occurred when the values of n were

odd. However, for odd values of n the center vane serves as part of the holder mechanism and as a result there are few obstructions in the flow. It is possible for odd values of n that most of the disturbances which are caused by the holders are damped and confined immediately by the presence of the center vane. Consequently, the addition of tape over the end clearance serves little purpose. In contrast, for even values of n there is no center vane to affect any control of the disturbance created by the holding mechanism; that is, the disturbances may propagate downstream much more readily. Thus, it may be that when the end clearances are sealed for even values of n the holder disturbances are confined to the center channel and consequently an increase in C_{PR} results. This explanation is plausible; however, it is only conjectural.

The significance of the present overall results is not lessened by the fact that the holder mechanism and the end clearance for even values of n reduced the actual value of C_{PR} below what it was possible to obtain. In other words, the relative effects for even values of n could still be determined and this was the more important matter. The only instance in which the reduction in C_{PR} was detrimental was in the general determination of the optimum value of n . However, since the order of magnitude of these effects has been determined (see the test points for the modified holder given in fig. 32), it is believed quite reasonable to estimate the probable value of C_{PR} for even values of n . The results thus obtained are very plausible and any deviations of C_{PR} from the estimated curves should be quite small.

Effect of variation of α_0/α at $2\theta = 24.5^\circ$.— Two curves of C_{PR} plotted against α_0/α are given in figure 33, one for $n = 2$ and one for $n = 3$. The cluster geometry and position corresponding to both values of n were as follows: $f = 15$ inches, $a = W_1/(n + 1)$, and $b/a = 1.2$. At $2\theta = 24.5^\circ$, $\alpha = 8.0^\circ$ with $n = 2$ and $\alpha = 6.0^\circ$ with $n = 3$. With these configurations, it was possible to study the effects of adjustment in α when total divergence angle was not near a multiple of 7° .

The curves in figure 33 show that the value of α_0/α is not critical for either value of n over the range of α investigated. The maximum value of C_{PR} for each value of n appears to occur at values of α_0/α slightly less than 1.0; however, the difference between the maximum value of C_{PR} and the value at $\alpha_0/\alpha = 1.0$ is insignificant. From this evidence and from the results that have been presented previously, it can be concluded that the equal-angle arrangement is the most satisfactory over the range of 2θ which has been investigated.

DESIGN CRITERIA

Finally, a summary can be made of the complete design criteria which has been developed in the present investigation. It is to be recalled that the vane cluster geometries are restricted as follows: (1) The vanes are of equal length f ; (2) the vanes are uniformly spaced with respect to each other; (3) the value of α is equal for all adjacent vanes; (4) the leading edges of the vanes are tangent to a plane perpendicular to the geometric axis of the diffuser; and (5) the cluster is symmetrically disposed with respect to the diffuser. The vanes in question are simple thin flat plates which have well-rounded leading edges and smoothly faired trailing edges.

The design criteria have been developed under the condition of a relatively thin and favorable turbulent inlet boundary layer. It is reasonable to assume that results, comparable to the present results may be obtained with δ^*/W_1 several times larger than the present value of approximately 0.003. However, the effect of the inlet boundary layer on the performance of a well-vaned diffuser is not known and awaits further study. Until such information is available, it is to be understood that the following statements concerning the diffuser performance and flow characteristics can be applied with assurance only to diffusers having "thin" turbulent inlet boundary layers.

An excellent pressure recovery and a reasonably smooth flow can be obtained with a two-dimensional, wide-angle, plane-wall, subsonic diffuser when the previously described vane clusters are installed in accordance with the design criteria given below. For $L/W_1 \cong 8$, the smallest value of 2θ for which vanes are helpful is approximately 14.5° . The vaned-diffuser performance has not been studied for values of 2θ significantly larger than 42.0° because of geometric limitations of the apparatus. The criteria are:

- (1) The angle α should be determined from the equation

$$\alpha = \frac{2\theta}{n + 1}$$

- (2) The proper value of n , for any given value of 2θ , may be determined from the envelope of C_{PR} shown in figure 32. (The estimated portions of the curve for $n = 2$ and $n = 4$ should be used in preference to the actual curves obtained from this investigation.) When 2θ is a multiple of 7.0° then n should be selected so that $\alpha = 7.0^\circ$.

(3) The vane spacing a should be determined from the equation

$$a = \frac{W_1}{n + 1}$$

(4) The vane length f should be selected so that $f/a = (f/a)_{as}$. The value of $(f/a)_{as}$, corresponding to α determined by item (1), should be obtained from the high-turbulence line of appreciable stall obtained by Moore and Kline (ref. 4). This curve is shown as line aa in figure 4.

(5) For optimum recovery, the cluster should be positioned so that $b/a = 1.2$; where smooth flow is more important a lower value of b/a in the range of $10 < b/a < 1.2$ should be used.

Performance Obtainable at $2\theta = 28.0^\circ$ Over Range of L/W_1

It was beyond the feasible scope of the present investigation to map out completely the performance of the vaned-diffuser configurations. However, in order to evaluate typical performance capabilities of a well-vaned diffuser over the usual range of practice in terms of length ratio as well as divergence angle, tests were conducted with the following values of L/W_1 : 4.17, 6.25, 10.4, 12.5, 15.6, and 18.8. Values of n , α , a , and b/a were selected in accordance with the design criteria. Again, it was not possible to use the exact required values of f because only five vane lengths were available. The actual values of f employed are given in the following table for the conditions $2\theta = 28.0^\circ$, $n = 3$, $\alpha = 7.0^\circ$, and $(f/a)_{as} = 19.3$:

W_1 , in.	a , in.	f , in.		L , in.
		Required	Used	
6.00	1.50	28.9	15.0	25.0
4.00	1.00	19.3	15.0	25.0
2.40	.60	11.6	12.0	25.0
2.00	.50	9.65	9.0	25.0
1.60	.40	7.72	9.0	25.0
1.33	.33	6.44	6.0	25.0

With the exception of $W_1 = 6.00$ and 4.00 inches, the actual values of f were in reasonable agreement with the required values. It is interesting to note that when $W_1 = 6.00$ inches the required value of f is greater than the length of the diffuser. Obviously, in such a case the vanes should not extend beyond the diffuser exit plane. Configurations of this type are commonly known as Oswatitsch diffusers. (An Oswatitsch diffuser is a wide-angle diffuser divided into a number of 7° passages all running the full length of the diffuser.)

The curves of C_{PR} obtained with and without the vanes are given in figure 34. Two values of throat-width Reynolds number were used, and it can be seen that this produced a very large effect on the recovery of the unvaned unit but essentially no effect on the recovery of the vaned unit.

The nature of the difference between the two curves of unvaned-diffuser performance shown in figure 34 is quite inexplicable. Previous results have shown that an increase in turbulence level tends to forestall the onset of fully developed separation as the angle is increased at a constant value of L/W_1 . Figure 18 shows that at $2\theta = 28.0^\circ$ an increase of turbulence level should produce a similar phenomenon as L/W_1 is increased at a constant value of 2θ . Since it is shown in figure 14 that an increase in Reynolds number corresponds to an increase in turbulence level, it would seem logical that the higher Reynolds number curve in figure 34 should have the break at the higher value of L/W_1 . Actually, the converse occurs. The cause of this phenomenon was not explored further because the phenomenon itself does not detract from the desired objective. In fact, the difference between the two vaneless-diffuser-performance curves helps to illustrate the beneficial effects of the vanes. In other words, without the vanes the performance of the given geometries was quite dependent upon the inlet conditions. However, when the diffuser was vaned in accordance with the above design criteria, a good performance was obtained which was essentially independent of the inlet conditions, and good recovery and smooth flow were obtained for each geometry tested.

It has been mentioned that the actual values of f for $L/W_1 = 4.00$ and 6.00 were considerably less than the values specified by the design criteria. Figure 34 shows that the resulting effect on C_{PR} was not large at $L/W_1 = 6.0$. For this case f was only approximately 22 percent smaller than the value specified by item (4) in the preceding section. However, the effect at $L/W_1 = 4.0$ was appreciable. For this case the design criteria called for an Oswatitsch diffuser, but the longest vane available was too short by approximately 32 percent. The agreement that is shown in figure 34 between the extrapolated portion of the vaned-diffuser C_{PR} curve and the predicted behavior of the appropriate Oswatitsch diffuser is felt to be particularly encouraging. In order to predict the performance of the Oswatitsch diffuser, a unit was visualized which was divided over its full length into four vane channels. Each individual vane channel then had a 7.0° total divergence angle and a value of f/a which was four times the value of the diffuser L/W_1 . From this geometry the vane-channel area ratio R was calculated, and the corresponding value of C_{PR} was obtained from the data of Reid (ref. 6).

In all the vaned-diffuser configurations the resulting flows were at least fairly steady. On the other hand, the flows obtained for several of the vaneless configurations were definitely unsteady. The separation patterns obtained for all the vaned configurations were very much like the pattern illustrated in figure 21(b).

Summary of Performance Obtainable Using Present

Vane Design Criteria

Recovery, effectiveness, and head loss.—Curves of C_{PR} , $C_{PR_{ideal}}$, η_p , and \bar{H}_L are given in figure 35. In figure 35(a) smooth curves of C_{PR} and η_p have been drawn for the vaned-diffuser results; the curve of C_{PR} was obtained by taking a mean of the odd values of n and the estimated even values of n from the curves given in figure 32. (This method is believed to be valid for the reasons given previously.) The curves of η_p and \bar{H}_L were calculated from the curves of C_{PR} and $C_{PR_{ideal}}$ shown in figure 35.

Figure 35 clearly illustrates the good performance that can be obtained by using the vaned-diffuser configurations specified by the present design criteria. For a value of L/W_1 of approximately 8.0, a nearly twofold improvement in C_{PR} can be obtained at an included angle of 42.0° . (It is probable that comparable results can be obtained for much larger angles.) More importantly, for any value of 2θ from 14.0° to at least 42.0° , a value of C_{PR} may be obtained which is nearly equal to the maximum value of C_{PR} obtainable with a vaneless diffuser set at its optimum-pressure-recovery angle. In other words, using vanes, it is possible to design two-dimensional, wide-angle diffusers which will perform nearly as well as, if not better than, the former two-dimensional optimum-pressure-recovery vaneless diffusers. The excellence of the pressure recoveries obtained at a constant angle ($2\theta = 28.0^\circ$) with variable values of L/W_1 also suggest strongly that satisfactory pressure recoveries can be obtained for any combination of 2θ and L/W_1 over the range of the parameters investigated. Furthermore, it is relatively certain that satisfactorily steady flows will also be obtained for all configurations using the design criteria developed.

The curve of $C_{PR_{vaned}}$ shown in figure 35(b) (for $2\theta = 28.0^\circ$) decreases slowly as L/W_1 is increased beyond approximately 6.0. For other values of 2θ it is probable that the maximum value of C_{PR} will

occur at $L/W_1 > 6.0$ for $2\theta < 28.0^\circ$ and at $L/W_1 < 6.0$ for $2\theta > 28.0^\circ$. However, it must be remembered that when $L/W_1 = 0$ then $C_{PR} = 0$. Therefore, the maximum value of C_{PR} for any value of 2θ probably cannot occur at a value of L/W_1 much less than 5.0.

As previously noted the curves of \bar{H}_L given in figure 35 include not only the head loss due to dissipation but also the excess leaving kinetic energy above that required for a one-dimensional exit flow. Nevertheless, as a basis for comparison these curves are very significant. They show that for included angles greater than about 23.0° , the head loss incurred with the vaneless configurations is about 2 to $2\frac{1}{2}$ times as large as the head loss incurred with the vaned configurations.

Effect of inlet conditions.— Figure 35(b) illustrates another desirable feature of a vaned diffuser, which is, in contrast to the corresponding vaneless units, that they are much less sensitive to changes in inlet conditions. This is shown by the fact that, for identical geometries and two flow rates, the curves of C_{PR} obtained with the unvaned units for each flow rate were completely different. On the other hand, no appreciable difference in C_{PR} was obtained with the vaned units using the same flow rates and the same range of geometry. The relative insensitiveness of the vaned units was further demonstrated in the course of the testing. When a large-scale turbulence was created in the entrance flow (e.g., by rapid hand waving back and forth in the entrance region), large areas of separation in the diffuser could be either diminished in extent or completely washed out in the case of unvaned or poorly vaned units; this was accompanied by a surge in the flow indicating that a larger pressure recovery was obtained. When the creation of the additional disturbance was stopped, the flow would revert to its former pattern. In contrast, when the same kind of turbulence was created in the entrance region of the well-vaned configurations, very little change occurred; at most, the throat manometers would show a slight decrease in throat pressure (indicating a slight increase in C_{PR}), but no change in flow pattern could be discerned.

Effect of wall disturbances.— It should be noted in respect to these designs, that care must be exercised to insure that large disruptions of the boundary layer are not inadvertently created. The effect of such disruptions, even though they may appear minor to the eye, can be quite serious. This is well illustrated by the tests of the various hanger systems described previously; however, even greater effects than those described earlier were observed with the first set of modified hangers that were tried. This first modified hanger system consisted of thin flat plates which were soldered to the ends of the vanes. These plates served the dual purpose of holding the cluster together and of simultaneously sealing

the end clearances. The plates were supported in the diffuser with small flatheaded screws which extended from the plates through the pressure tap fittings in the diffuser side walls. The cluster configurations conformed to the design criteria, but it was found impossible to obtain either a good pressure recovery or a smooth flow at any value of b/a . On the other hand, when the streamlined holders (described previously) were used with this same cluster configuration, both very good pressure recovery and flow steadiness were obtained.

In such designs the important thing seems to be that the boundary layer should not be disrupted across the entire wall surface. If disruption is unavoidable it should be limited to dimensions which are small normal to the flow. This then allows the small stall created to be filled in downstream by the crosswise mixing of the flow. This effect can be rationalized in terms of the behavior discussed in reference 2.

Exit velocity profile.— The diffuser exit velocity profile is very useful in qualitatively evaluating the diffuser performance, and it is also often of importance to the performance of downstream components. It has been shown by Moore and Kline (ref. 3) that the ideal exit velocity profile is a one-dimensional profile. However, a one-dimensional profile does not necessarily, by itself, guarantee high performance since frictional effects also reduce recovery. For example, a study of the use of screens in diffusers has been made by Schubauer and Spangenberg (ref. 15). They found that almost any desired degree of one-dimensionality of the exit flow could be attained simply by adding a sufficient number of screens, but the total-pressure loss from friction due to the screens more than offset the gain realized by the more nearly one-dimensional exit profile.

The dimensionless velocity contours given in figure 36 show that large improvements in the exit velocity profile can be obtained with well-designed vanes. The normalizing velocity for these contours is the corresponding ideal one-dimensional velocity that would have been obtained at the same diffuser flow rate. The zones of separation are shown by crosshatching.

At $2\theta = 16.8^\circ$ the addition of one vane did not appreciably reduce the maximum exit velocity; however, it did have the effect of "flattening out" the flow so that a much smaller portion attained the maximum velocity. Also, for the vaned flow the total area of the separated zones was somewhat smaller and the separation occurred only in the corners.

At $2\theta = 24.5^\circ$, 31.1° , and 42.0° , the character of the exit flow was completely altered by the addition of the vanes. This effect is particularly noticeable for $2\theta = 31.1^\circ$ and 42.0° . It can be seen that the separation was not only markedly reduced in extent, but it was also

almost completely confined to the side walls of the diffuser. Furthermore, the maximum exit velocities were reduced by a factor of approximately 2.0. It is not surprising that large improvements in C_{PR} result when properly designed vanes are used.

As the results of the present tests were accumulated, the recoveries found were so large in comparison with the values found for the unvaned diffuser, that it was believed that large further improvements were not likely. A careful examination of figures 36 to 39 shows, however, that this is not altogether true. It is of course true that if the recovery is increased from, say, 20 percent or even 40 percent up to 75 percent, then a further gain of the same magnitude is not even theoretically possible. However, it is also true that significant further improvements are theoretically feasible, and this is substantiated by the fact that appreciable areas of stall still do exist in the exit of the vaned diffusers at high angles. Suggestions for possible means of further improvement are given later.

Inlet Mach number.— The present investigation has been limited to values of inlet Mach number low enough so that the flow is essentially incompressible. Consequently, it is logical to question the applicability of the present vane design criteria to flows in which appreciable compressibility effects occur. Fortunately, some investigations have been conducted in which the diffuser inlet Mach number has been varied from very low values up to values where choking conditions occur. In general, it has been found that no appreciable change in performance occurs as a result of the higher flow rate until some part of the diffuser begins to operate at sonic conditions. In particular, Young and Green (ref. 16) found this to be true for a two-dimensional diffuser in which they installed splitter vanes. Their performance curves were quite flat up to inlet Mach numbers of approximately 0.6 to 0.7. At values of Mach number much greater than 0.7 their diffuser losses increased at a very high rate. The results of the other available investigations are very similar to those of Young and Green. On the basis of these results, it is reasonable to suppose that the present design criteria are applicable to high-speed flows as long as sonic conditions do not prevail anywhere in the diffuser; however, this conclusion should be verified experimentally. It is noted that for higher Mach numbers particular attention must be paid the leading edges of the vanes as well as the curved portions of the throat. Because of the corresponding local flow accelerations, it is likely that sonic conditions will be obtained at these locations before they occur elsewhere in the diffuser. In this connection the use of $b/a > 1$, that is, of a value of $c > 0$, should be of definite assistance in achieving good performance at inlet Mach numbers approaching unity. Since for $c > 0$ some flow deceleration occurs before the commencement of the vanes, the likelihood of occurrence of local sonic flow and shock waves near the leading edges of the vanes is much reduced.

It is recognized that thin vanes of the type used in this investigation are susceptible to aerodynamic flutter in high-speed flows. In fact, some flutter difficulties were experienced in the present preliminary testing. Flutter first occurred using a single 9-inch vane. This was readily stopped by installing small-diameter bracing rods which held the vane in the center 1 inch or so downstream of the leading edge. Flutter was again encountered at the trailing edge of the 12- and 15-inch vanes for the single-vane installation. This flutter was readily stopped by passing a 1/16-inch-diameter steel rod through the center of the vane 1/2 inch upstream of the trailing edge and through both diverging walls of the diffuser. The wire was grasped firmly at the vane and the walls by small set screws. No difficulty was experienced with the multiple vane clusters because the six cluster assembly dowels produced a sufficiently rigid vane assembly. It is believed that the vanes can be adequately braced for any practical application; however, care should be exercised to insure that the braces are not near the walls they parallel and that they are small and well streamlined. It is possible that a poorly designed brace could produce an excessive disruption of the boundary layer and thus precipitate large regions of separation; this would nullify much of the effect of the vanes.

Design Considerations

The foregoing discussions have indicated that the use of vanes for production of wide-angle diffusers of high performance is now well established for the case of low-speed flows in a two-dimensional geometry. With these results in mind, it is well to discuss briefly the problems that can be foreseen in adapting them to practical designs. There are several important considerations.

First, are the designs critical in respect to the use of vane clusters requiring careful tolerance of manufacture? Since no special manufacturing methods or measuring techniques were used in obtaining the present results, the answer to this question is definitely no. It is not anticipated that special problems of this sort will normally arise.

Second, how critical are the various optimums presented in the design criteria that have been developed? The answer to this question is given by the curves discussed previously. Examination of these curves shows that the optimums are quite flat in regard to vane length and placement and also (at least near the maximum points) in regard to the ratio of individual passage angles. The curves of recovery as a function of individual passage angle, figures 23 and 28, however, are relatively sharp although the peaks are flat enough to insure reasonable tolerances. Also, as noted previously, the value of b/a should not exceed 1.20 since in some cases unstable flows may then ensue. In fact, for smooth flows, a value less than 1.20 may well be a better compromise.

Unstable flows may also be encountered when the vane is made longer than that specified by the design criteria. Thus, considerable latitude is available to the designer provided two rules are held in mind: (1) The individual passage angles should be varied as little as possible from optimum, and (2) the optimum value of vane length and of b/a should not be exceeded.

Third, the question concerning extension of the favorable results found in the present investigation to other geometries and other inlet conditions naturally arises. Since the design method built up in this work is founded essentially on empirical observations of the flow and since only a qualitative theory of the nature of vane action is available (see ref. 2), this question cannot yet be answered with certitude. Further experimental investigations for other geometries and other inlet conditions are being pursued, but this does not solve current design problems; therefore, the following remarks are made.

It is believed that vaned systems should give good performance for other geometries, but no design procedure can yet be given. Judgment in applying the results of Moore and Kline (refs. 3 and 4) and the other available diffuser data is therefore the only present recourse.

The results found in this work will probably hold good without major alteration up to inlet Mach numbers where shocks or choking first occur in the unit.

The effect of variation in inlet free-stream turbulence on vaned units does not seem to be critical. The effect of variation in inlet boundary-layer thickness is unknown, but it is relatively safe to assume that more conservative designs must be used where thick inlet boundary layers occur. The amount of conservatism needed is still a matter for judgment.

The effect of skewed inlet velocity profiles on vaned systems should be slight unless the skewing is very large and of such a nature that large stalls are produced on the leading edges of one or more vanes. The usual corrective actions for such an occurrence can, of course, be taken.

Possibilities for Further Improvement

Additional vane adjustments.- In the present investigation it was necessary to limit the degrees of freedom of the vaned-diffuser geometries in order to obtain a feasible test program. However, now that specific criteria have been developed with which large improvements in performance can be obtained, it is useful to consider additional vane-cluster refinements. As mentioned previously, one such refinement would

be to adjust the divergence angles between adjacent vanes in a symmetrical but nonuniform manner, that is, to make the divergence angles of the outer channels smaller than the adjacent channels and so on. Two other possibilities are (1) using vanes of different lengths in the same cluster, and (2) placing the leading edges of the vanes in a given cluster at different axial locations. These adjustments are only speculative and await further study. However, it is believed that further refinements in the vane geometry do not hold as much promise as the combined use of the present cluster geometries and suitable vortex generators or other boundary-layer control devices.

Vortex generators.- The combination of the works of Moore and Kline and others and the mechanisms discussed in reference 2 suggest that additional improvements in performance can be obtained by superposition of vortex generators or turbulence promoters with the present vaned diffuser geometries. Moore and Kline (ref. 3) clearly illustrated the important effect of turbulence level in one water-table test in which they completely eliminated a fully developed two-dimensional stall by placing small-diameter rods in the upstream flow near the diffuser inlet. Initially, the stall extended to within a few inches of the diffuser throat, but as the rods were successively inserted (normal to the parallel wall) across the entering flow stream, the point of inception of the fully developed stall progressed downstream step by step until it was finally washed from the diffuser. When the rods were removed, the diffuser again developed a fully developed stall.

Valentine and Carroll (ref. 17) and Wood (ref. 18) investigated various types of vortex generators placed just upstream of the throat in, respectively, conical and annular diffusers. It was found that considerable improvements could be obtained in both flow steadiness and static-pressure rise. The results presented in references 17 and 18 cannot readily be compared with those of the present investigation because of differences in inlet flow conditions and geometry. However, the ratio of the performance increase to the performance of the unmodified units and the amount of extension of divergence angle are both much larger in the present work than those obtained in these studies. Nevertheless, the results of Valentine and Carroll and of Wood illustrate the possibilities of vortex generators. It is not likely, however, that vortex generators placed upstream of the throat will be as effective in vaned units as similar vortex generators placed at discrete locations in the diffuser. The reason for this has been discussed previously in the section entitled "Effect of Inlet Conditions."

Several tests were conducted in the present investigation in which a pair of $1\frac{1}{8}$ -inch-diameter rods were placed in the entrance flow. The rods were perpendicular to the parallel side walls and were symmetrically located 1 inch above the outer extremity of each of the entrance lips of

the diverging walls. The Reynolds number of each rod, based on the rod diameter, was approximately 4,500. The objective of these tests was to create an increase in turbulence level in the flow adjacent to the diverging walls. The vaned-diffuser geometry used is given in table IX. (These are the same configurations used in the end-clearance tests.) The results are given as follows:

2θ , deg	End-clearance condition	C_{PR}	
		With rods	Without rods
28.0	Open ends	0.771	0.764
28.0	Taped ends	.767	.763
42.0	Open ends	.726	.716
42.0	Taped ends	.720	.711

The improvements obtained in C_{PR} by the addition of the rods are relatively small. At $2\theta = 28.0^\circ$ the increase is of the order of the uncertainty in C_{PR} , but the trend in all the tests is consistent and in agreement with the changes in the flow patterns that were observed. In other words, when the rods were added the resulting flows were steadier in every case and showed a slight reduction of the overall extent of separation. No account was taken of the drag of the rods which, of course, would reduce the overall gain in C_{PR} . However, these tests were conducted primarily to demonstrate further the effect of changes in the inlet turbulence level. An evaluation of more properly oriented vortex generators awaits further study.

COMPARISON WITH WORK OF MOORE AND KLINE

The present work was an extension of the work of Moore and Kline (refs. 3 and 4), and essentially complete agreement has been obtained on all but one point. This exception is in the preliminary work (ref. 4) conducted with the air apparatus used in this investigation. In the report of this work Moore and Kline present curves of C_{PR} plotted against 2θ at constant values of L/W_1 for the vaneless diffuser. These curves are quite different in character (at high values of 2θ) from the curve shown in figure 19 of the present report. Instead of a continuous curve, Moore and Kline obtained curves in which C_{PR} decreased suddenly at a particular value of 2θ . For further increases in 2θ , the curve then continued in a smooth fashion emanating from the low value of C_{PR} . The reason that such a difference occurred between

their results and the present results is attributed to the fact that a different experimental technique was used. Because of the lack of other means of flow control at that time, Moore and Kline held the fan speed constant and then increased 2θ . At a given value of 2θ , which was dependent upon the flow rate, the flow would breakdown resulting in both reduced pressure recoveries and reduced flow rates. However, it has been shown that a change in flow rate produces a change in inlet turbulence. It is believed that this change in turbulence level and the coupled effect of the fan-diffuser combination are responsible for the difference in results that has been obtained. It should be recalled that in the present work a constant value of flow rate was forced on the diffuser for each curve, regardless of the fan speed. When operating at constant flow rate, the inlet conditions were held constant and, consequently, the smooth curve shown in figure 19 was obtained.

SUMMARY OF RESULTS

An investigation of the use of flat vanes in two-dimensional subsonic diffusers was conducted. The results of this work taken in conjunction with the results of some of the preceding work, all of which have been obtained using a thin turbulent inlet boundary layer and nearly constant inlet velocity profile, are summarized as follows:

1. Water-table results indicate that four regimes of flow are obtained in a simple plane-wall two-dimensional diffuser as the included angle is varied, with the ratio of wall length to throat width, the flow rate, and all inlet conditions held constant. Increasing the divergence angle from 0° causes these regimes to appear in the following order: (1) A regime of well-behaved apparently unseparated flow, (2) a regime of large transitory stall in which the separation varies in size, intensity, and location with time, (3) a regime of essentially two-dimensional, relatively steady, fully developed stall in which the flow follows along one wall with little or no expansion occurring, and (4) a regime of jet flow in which the flow separates from both diverging walls and proceeds through the diffuser in a fashion similar to that of a free jet. The boundaries between these regimes are not unique functions of included angle but depend strongly on at least the ratio of wall length to throat width and turbulence level. The boundary between regimes (1) and (2) is called the line of appreciable stall.

2. Results on the air apparatus indicate the following behavior as the included angle of a vaneless two-dimensional diffuser is increased, with the ratio of wall length to throat width, flow rate, and all inlet conditions held constant: (1) The pressure effectiveness attains a

maximum value at an angle appreciably smaller than the angle of maximum pressure recovery; (2) the pressure recovery becomes a maximum at or near the line of appreciable stall; (3) at an angle slightly greater than the angle of maximum recovery the flow becomes very unsteady, large transitory stalls develop, and the pressure recovery decreases very rapidly; (4) when the angle is increased sufficiently the flow is again relatively steady, a fully-developed stall occurs, and the pressure recovery is near a minimum. Jet flow was not obtained because of geometric limitations of the apparatus. (With the ratio of wall length to throat width set at approximately 8.0, maximum pressure effectiveness was obtained at approximately 8.5° , maximum pressure recovery, and shortly thereafter the beginning of unsteady flow, was obtained at approximately 14.0° , relatively steady flow with fully-developed stall was obtained at approximately 31.0° , and continuing steady flow with low pressure recovery was obtained up to 42.0° .)

3. With the use of the vane design criteria developed, the following very good diffuser performance is possible over the investigated range of length ratio and included angle: (1) From about 14.0° to 42.0° a pressure recovery may be obtained which is very nearly equal to, and in some instances greater than, the maximum value obtainable in a vaneless unit set at optimum pressure-recovery angle; (2) a satisfactorily steady flow can be obtained at angles up to 42.0° ; (3) the flow is much less sensitive to variations in inlet conditions than the corresponding vaneless diffuser; and (4) a significant reduction in head loss, which amounts to about a 2.5-fold reduction in some instances, may be obtained.

4. The performance of the diffuser with optimum vane configurations has not been completely mapped out, but tests made with variable included angle at constant length ratio and with variable length ratio at constant included angle strongly suggest that good diffuser performance can be obtained for any combination of these parameters over the ranges investigated.

5. Studies of the available literature indicate that good diffuser performance can probably be obtained in vaned units for high-speed flow as long as sonic conditions do not prevail anywhere in the diffuser.

6. Specific criteria for the design of the optimum vane configurations developed are presented. The salient features of these configurations are: (1) The vanes are relatively short and are located in the vicinity of the throat; (2) the vanes are symmetrically arranged; (3) the number of vanes is chosen so that the individual-vane-passage divergence angles are approximately 7.0° ; and (4) the length of the vanes is chosen so that the operation of each individual vane passage is at or near the line of appreciable stall obtained in the high-turbulence water-table work.

7. Manufacturing and positioning of the vanes are not critical, but care must be exercised to avoid disruption of the boundary layer. Where disruptions are unavoidable, the disrupting device should be removed as far as possible from the wall that it parallels, it should be streamlined, and it should be made with the smallest feasible dimensions normal to flow.

8. Greatly improved diffuser flows result with the use of the vane configurations developed. At large angles (30° and larger) the pressure-recovery coefficient can be increased from about 0.38 in the unvaned unit to about 0.70 in the vaned unit. The areas of separation can be greatly reduced and the exit velocity profiles can be very appreciably flattened. (A twofold reduction in maximum efflux velocity is readily possible.) Significant additional improvements appear to be feasible by the superposition of these optimum vane configurations with suitably designed vortex generators placed at discrete locations throughout the diffuser.

Stanford University,
Stanford, Calif., May 2, 1957.

REFERENCES

1. Cochran, D. L.: The Use of Short Flat Vanes As a Means for Producing Efficient Wide-Angle Two-Dimensional Subsonic Diffusers. Ph. D. Thesis, Stanford Univ., Apr. 1957.
2. Kline, Stephen J.: On the Nature of Stall. Rep. MD-4, Contract AF 49(638)-207 and 295, Air Force Office Sci. Res., ARDC, and Dept. Mech. Eng., Stanford Univ., June 1958.
3. Moore, C. A., and Kline, S. J.: Investigation of Airfoils, Plates, Grids and Rods for Boundary Layer Control in Subsonic Diffusers. Contract NAW-6317, NACA and Stanford Univ., Aug. 16, 1954.
4. Moore, C. A., and Kline, S. J.: Some Effects of Vanes and of Turbulence on Two-Dimensional Wide-Angle Subsonic Diffusers. NACA TN 4080, 1958.
5. Patterson, G. N.: Modern Diffuser Design. Aircraft Engineering, vol. X, no. 115, Sept. 1938, pp. 267-273.
6. Reid, Elliott G.: Performance Characteristics of Plane-Wall Two-Dimensional Diffusers. NACA TN 2888, 1953.
7. Vedernikoff, A. N.: An Experimental Investigation of the Flow of Air in a Flat Broadening Channel. NACA TM 1059, 1944.
8. Tults, Harold: Flow Expansion and Pressure Recovery in Fluids. Proc. Am. Soc. Civil Eng., vol. 80, no. 567, Dec. 1954, pp. 1-26.
9. Jones, J. B., and Binder, R. C.: Boundary Layer Flow in the Corners of a Diffuser. Res. Ser. No. 115, vol. XXXVI, no. 2, Purdue Eng. Exp. Station, Mar. 1952.
10. Kalinske, A. A.: Conversion of Kinetic Energy to Potential Energy in Flow Expansion. Trans. Am. Soc. Civil Eng., vol. III, 1946, pp. 355-390.
11. Kline, S. J., and McClintock, F. A.: Describing Uncertainties in Single-Sample Experiments. Mech. Eng., vol. 75, no. 1, Jan. 1953, pp. 3-8.

12. Little, B. H., Jr., and Wilbur, Stafford W.: Performance and Boundary-Layer Data From 12° and 23° Conical Diffusers of Area Ratio 2.0 at Mach Numbers up to Choking and Reynolds Numbers up to 7.5×10^6 . NACA Rep. 1201, 1954. (Supersedes NACA RM L9H10 by Copp and Klevath, RM L9K10 by Persh, and RM L50C02a by Little and Wilbur.)
13. Shapiro, Ascher H.: The Dynamics and Thermodynamics of Compressible Fluid Flow. Vol. I. The Ronald Press Co., c.1953, p. 16.
14. Persh, Jerome, and Bailey, Bruce M.: Effect of Surface Roughness Over the Downstream Region of a 23° Conical Diffuser. NACA TN 3066, 1954.
15. Schubauer, G. B., and Spangenberg, W. G.: Effect of Screens in Wide-Angle Diffusers. NACA Rep. 949, 1949.
16. Young, A. D., and Green, G. L.: Tests of High-Speed Flow in Diffusers of Rectangular Cross-section. R. & M. No. 2201, British A.R.C., 1944.
17. Valentine, E. Floyd, and Carroll, Raymond B.: Effects of Some Primary Variables of Rectangular Vortex Generators on the Static-Pressure Rise Through a Short Diffuser. NACA RM L52B13, 1952.
18. Wood, Charles C.: Preliminary Investigations of the Rectangular Vortex Generators on the Performance of a Short 1.9:1 Straight-Wall Annular Diffuser. NACA RM L51G09, 1951.

TABLE I

LONGITUDINAL POSITIONS OF ALUMINUM WALL PLUGS

Holes numbered from curved end of plate	Distance from trailing edge of aluminum plate measured along inner surface of aluminum plate, in. (a)
1	26.000
2	25.667
3	25.333
4	25.000
5	24.667
6	24.333
7	24.000
8	23.000
9	22.000
10	21.000
11	20.000
12	19.000
13	18.000
14	17.000
15	15.000
16	13.000
17	11.000
18	9.000
19	7.000
20	5.000
21	3.000
22	1.000

^aTolerances on dimensions are ± 0.010 inch.

TABLE II

LONGITUDINAL POSITIONS OF ALUMINUM
WALL PLUGS IN PLEXIGLAS SIDES

Hole number	Distance from lower edge of plate, in. (a)
1	23.375
2	22.625
3	21.875
4	20.875
5	19.875
6	18.875
7	17.875
8	16.875
9	15.875
10	14.875
11	13.875
12	12.875
13	11.875
14	10.875
15	9.875
16	8.875
17	7.875
18	6.875
19	5.875
20	4.875
21	3.875
22	2.875
23	1.875
24	.875

^aTolerances on dimensions are ± 0.010 inch.

TABLE III

FLOW CONDITIONS FOR DISCHARGE DUCT CALIBRATIONS

Number	Condition upstream of diffuser throat	Fan speed, rpm	Mass flow rate, lb/sec	Fan speed Flow rate
1	Unobstructed	650	3.39	192
2	Unobstructed	1,060	5.79	183
3	Unobstructed	1,610	8.85	182
4	^a One-half area symmetrically blocked	1,600	6.42	250
5	^a One-half area asymmetrically blocked	1,600	4.30	372

^aThe entrance flow area was blocked by placing strips approximately 2 inches wide across the lips of the diffuser diverging walls.

TABLE IV

ACCURACY OF DATA

[Uncertainties given in this table have been estimated on the basis of 20:1 odds using the method of Kline and McClintock (ref. 11); uncertainties are presented in terms of either an uncertainty interval or a percent uncertainty depending upon which is more appropriate for the quantity under consideration]

(a) Uncertainties in variables

	Uncertainty
Minimum space between adjacent vanes, a , in.	0.01
Minimum space between diverging wall and adjacent vane, b , in.	0.01
Distance from throat to vane leading edge, c , in.	1/16
Vane length, f , in.	1/32
Distance between diffuser parallel walls, G , in.	1/32
Length of diffuser diverging wall, L , in.	1/8
Barometric pressure, p_a , in. Hg	0.05
Wet bulk temperature, T_{wb} , $^{\circ}\text{F}$	3.0
Ambient air temperature, T_a , $^{\circ}\text{F}$	3.0
Diffuser throat width, W_1 , in.	0.01
Diffuser exit width, W_2 , in.	1/32
Divergence angle between adjacent vanes, α , deg	0.25
Diffuser total divergence angle, 2θ , deg	0.25
Air viscosity, μ , percent	2.0

(b) Uncertainties in results

	Uncertainty	
	Best case	Worst case
Ambient air density, ρ_a , percent	0.8	0.8
Throat-wall-pressure depression (average of six readings), $p_a - p_{w1}$, percent	0.2	3.9
Average inlet air density, ρ_{1av} , percent	0.8	1.0
Weight flow rate, w , percent	1.7	2.9
Inlet Reynolds number, R_{w1} , percent	2.6	3.5
Average inlet dynamic head, q_{1av} , percent	3.5	5.8
Exit pressure depression (average of four readings) $p_a - p_2$, percent	1.4	11.0
Pressure-recovery coefficient, C_{PR} , percent	1.2	9.2
Diffuser area ratio, A_2/A_1 , percent	0.4	0.4
Ideal pressure-recovery coefficient, $C_{PR_{ideal}}$, percent	0.03	0.03
Pressure effectiveness, η_p , percent	1.2	9.2

TABLE V

DIFFUSER AND VANE GEOMETRIES

2 θ , deg	L/W ₁ (approximate)	Maximum number of vanes in given cluster	Lengths of vanes tested, in.	R _{W1} (approximate)
Phase I (approximately constant value of L/W ₁)				
42.0	8.0	5	3, 6, 9, 12, 15	2.4 $\times 10^5$
28.0	8.0	4	3, 6, 9, 12, 15	2.4
14.0	8.0	1	3, 6, 9, 12, 15	2.4
16.8	8.0	2	15	2.4
21.0	8.0	3	15	2.4
24.5	8.0	3	15	2.4
31.1	8.0	4	15	2.4
38.2	8.0	5	12, 15	2.4
31.1	8.0	4	15	2.4
Phase II (constant included angle)				
28.0	18	3	6	1.6
28.0	15	3	9	1.6
28.0	12	3	9	1.6, 2.4
28.0	10	3	12	1.6, 2.4
28.0	6	3	15	1.6, 2.4
28.0	4	3	15	1.6, 2.4

TABLE VI

PERFORMANCE OF DIFFUSER WITHOUT VANES

2θ , deg	W_1 , in.	L/W_1	A_2/A_1	q , lb/sq ft	R_{W1}	C_{PR}	η_p
7.00	3.00	8.09	1.99	30.4	2.49×10^5	0.662	0.885
14.00	3.00	8.17	2.96	29.5	2.45	.765	.864
14.00	3.00	8.17	2.96	29.8	2.42	.745	.842
16.80	3.00	8.21	3.40	30.9	2.47	.731	.800
21.00	3.00	8.26	3.94	29.4	2.40	.625	.668
21.00	3.00	8.26	3.94	29.0	2.35	.641	.685
24.50	3.00	8.30	4.43	29.6	2.37	.567	.598
28.00	3.00	8.35	4.94	29.0	2.39	.437	.455
28.00	3.00	8.35	4.94	48.0	3.06	.432	.451
28.00	1.33	18.81	9.87	65.0	1.55	.485	.489
28.00	1.60	15.66	8.36	47.8	1.59	.461	.467
28.00	2.00	12.52	6.91	31.2	1.61	.555	.566
28.00	2.00	12.52	6.91	57.1	2.17	.458	.467
28.00	2.40	10.44	5.91	22.3	1.66	.611	.628
28.00	2.40	10.44	5.91	50.7	2.49	.455	.468
28.00	4.00	6.26	3.95	7.61	1.61	.579	.619
28.00	4.00	6.26	3.95	16.4	2.36	.549	.586
28.00	6.00	4.18	2.97	3.33	1.59	.533	.601
28.00	6.00	4.18	2.97	7.47	2.39	.544	.613
31.10	3.00	8.38	5.44	30.5	2.44	.374	.387
35.00	3.00	8.43	5.94	29.7	2.48	.387	.398
38.20	3.00	8.47	6.46	30.4	2.43	.375	.383
42.00	3.00	8.52	6.88	31.0	2.46	.394	.402
42.00	3.00	8.52	6.88	30.9	2.46	.362	.369
42.00	3.00	8.52	6.88	30.0	2.44	.391	.399

TABLE VII

PERFORMANCE OF DIFFUSER WITH VANES

(a) $2\theta = 28.0^\circ$; $L/W_1 = 8.35$; $W_1 = 3.00$ inches;

$$A_2/A_1 = 4.92; a = \frac{W_1}{n+1}; \alpha = \frac{2\theta}{n+1}$$

f, in.	n	a, in.	α , deg	c, in.	f/a	b/a	R_{W1}	q_1 , lb/sq ft	C_{PR}	η_p
3.00	1	1.50	14.00	0.28	2.00	1.00	2.37×10^5	29.0	0.558	0.582
3.00	1	1.50	14.00	1.22	2.00	1.06	2.35	28.3	.570	.594
3.00	1	1.50	14.00	1.67	2.00	1.12	2.36	28.8	.574	.598
3.00	1	1.50	14.00	2.47	2.00	1.25	2.24	25.8	.498	.519
3.00	2	1.00	9.33	.94	3.00	1.00	2.36	28.2	.618	.644
3.00	2	1.00	9.33	1.30	3.00	1.07	2.33	27.7	.623	.694
3.00	2	1.00	9.33	1.72	3.00	1.16	2.41	29.5	.682	.711
3.00	2	1.00	9.33	2.34	3.00	1.31	2.48	31.2	.687	.717
3.00	2	1.00	9.33	2.65	3.00	1.38	2.42	29.8	.651	.679
3.00	3	.75	7.00	1.16	4.00	1.00	2.43	30.1	.703	.733
3.00	3	.75	7.00	1.47	4.00	1.09	2.40	29.5	.708	.738
3.00	3	.75	7.00	1.47	4.00	^a 1.09	2.22	25.2	^a .596	.621
3.00	3	.75	7.00	1.84	4.00	1.19	2.41	29.7	.727	.758
3.00	3	.75	7.00	2.16	4.00	1.30	2.44	30.4	.731	.762
3.00	3	.75	7.00	2.64	4.00	1.46	2.47	31.4	.720	.751
6.00	1	1.50	14.00	.59	4.00	1.00	2.37	29.6	.640	.668
6.00	1	1.50	14.00	1.37	4.00	1.08	2.43	30.9	.649	.676
6.00	1	1.50	14.00	1.75	4.00	1.14	2.39	30.0	.623	.650
6.00	1	1.50	14.00	2.19	4.00	1.21	2.43	31.1	.605	.631

^aTwo distinct patterns were obtained at this setting.

TABLE VII.- Continued

PERFORMANCE OF DIFFUSER WITH VANES

(a) $2\theta = 28.0^\circ$; $L/W_1 = 8.35$; $W_1 = 3.00$ inches; $A_2/A_1 = 4.92$;

$$a = \frac{W_1}{n+1}; \alpha = \frac{2\theta}{n+1} - \text{Continued}$$

f, in.	n	a, in.	α , deg	c, in.	f/a	b/a	R_{W1}	q_1 , lb/sq ft	C_{PR}	η_p
6.00	2	1.00	9.33	0.94	6.00	1.00	2.40×10^5	29.3	0.702	0.732
6.00	2	1.00	9.33	1.41	6.00	1.10	2.43	30.1	.720	.750
6.00	2	1.00	9.33	2.09	6.00	1.26	2.41	29.6	.719	.749
6.00	2	1.00	9.33	2.59	6.00	1.37	2.41	29.6	.659	.687
6.00	3	.75	7.00	1.19	8.00	1.00	2.38	29.6	.729	.760
6.00	3	.75	7.00	1.66	8.00	1.15	2.38	29.6	.736	.767
6.00	3	.75	7.00	2.25	8.00	1.33	2.37	30.3	.751	.783
6.00	3	.75	7.00	2.87	8.00	1.52	2.40	31.0	.613	.639
9.00	1	1.50	14.00	.62	6.00	1.00	2.39	29.6	.665	.693
9.00	1	1.50	14.00	1.34	6.00	1.08	2.40	29.8	.648	.674
9.00	1	1.50	14.00	1.89	6.00	1.16	2.45	31.0	.651	.679
9.00	1	1.50	14.00	2.37	6.00	1.23	2.40	29.8	.500	.521
9.00	2	1.00	9.33	1.03	9.00	1.02	2.31	28.5	.721	.752
9.00	2	1.00	9.33	1.56	9.00	1.13	2.39	30.1	.732	.763
9.00	2	1.00	9.33	2.09	9.00	1.26	2.36	29.5	.737	.768
9.00	2	1.00	9.33	2.59	9.00	1.37	2.39	30.2	.716	.747
9.00	3	.75	7.00	1.16	12.00	1.00	2.40	29.3	.738	.769
9.00	3	.75	7.00	1.70	12.00	1.16	2.40	29.5	.751	.783
9.00	3	.75	7.00	2.30	12.00	1.35	2.41	29.9	.768	.801
9.00	3	.75	7.00	2.75	12.00	1.48	2.38	28.9	.589	.614
12.00	1	1.50	14.00	.66	8.00	1.00	2.38	30.0	.683	.712
12.00	1	1.50	14.00	1.31	8.00	1.08	2.37	29.9	.665	.693
12.00	1	1.50	14.00	1.91	8.00	1.16	2.36	29.8	.647	.675
12.00	1	1.50	14.00	2.28	8.00	1.22	2.40	30.7	.626	.653
12.00	2	1.00	9.33	.98	12.00	1.00	2.41	29.7	.697	.727
12.00	2	1.00	9.33	1.39	12.00	1.09	2.39	29.3	.716	.746

TABLE VII.- Continued

PERFORMANCE OF DIFFUSER WITH VANES

(a) $2\theta = 28.0^\circ$; $L/W_1 = 8.35$; $W_1 = 3.00$ inches; $A_2/A_1 = 4.92$;

$$a = \frac{W_1}{n+1}; \alpha = \frac{2\theta}{n+1} - \text{Concluded}$$

f, in.	n	a, in.	α , deg	c, in.	f/a	b/a	R_{W1}	q_1 , lb/sq ft	C_{PR}	η_p
12.00	2	1.00	9.33	1.97	12.00	1.21	2.41×10^5	29.6	0.745	0.777
12.00	2	1.00	9.33	2.41	12.00	1.32	2.41	29.6	.728	.759
12.00	3	.75	7.00	1.23	16.00	1.01	2.37	29.6	.750	.782
12.00	3	.75	7.00	1.69	16.00	1.15	2.37	29.6	.766	.799
12.00	3	.75	7.00	2.09	16.00	1.28	2.47	32.4	.775	.808
12.00	3	.75	7.00	2.59	16.00	1.42	2.43	31.1	.625	.651
12.00	4	.60	5.60	1.42	20.00	1.00	2.43	30.5	.639	.666
12.00	4	.60	5.60	1.98	20.00	1.22	2.39	29.5	.688	.717
12.00	4	.60	5.60	2.39	20.00	1.38	2.37	29.1	.699	.729
12.00	4	.60	5.60	3.03	20.00	1.64	2.41	30.2	.743	.775
12.00	4	.60	5.60	3.03	20.00	^a 1.64	2.41	30.0	^a .548	.572
15.00	1	1.50	14.00	.62	10.00	.99	2.42	30.3	.686	.715
15.00	1	1.50	14.00	1.30	10.00	1.07	2.43	30.6	.676	.705
15.00	1	1.50	14.00	2.09	10.00	1.19	2.45	31.1	.659	.687
15.00	2	1.00	9.33	1.03	15.00	1.02	2.34	29.2	.703	.733
15.00	2	1.00	9.33	1.47	15.00	1.10	2.37	29.9	.718	.748
15.00	2	1.00	9.33	1.97	15.00	1.22	2.40	30.6	.753	.785
15.00	2	1.00	9.33	2.48	15.00	1.34	2.36	29.7	.746	.778
15.00	3	.75	7.00	1.22	20.00	1.00	2.41	29.6	.742	.774
15.00	3	.75	7.00	1.65	20.00	1.14	2.42	30.1	.757	.790
15.00	3	.75	7.00	2.27	20.00	1.33	2.42	30.1	.774	.807
15.00	3	.75	7.00	2.77	20.00	1.49	2.45	30.8	.598	.624

^aTwo distinct patterns were obtained at this setting.

TABLE VII.- Continued

PERFORMANCE OF DIFFUSER WITH VANES

(b) $2\theta = 28.0^\circ$; $W_1 = 3.00$ inches; $L/W_1 = 8.35$;

$A_2/A_1 = 4.92$; $a = \frac{W_1}{n+1} = 0.75$ inch; $n = 3$;

$f = 12.0$ inches; α variable

c , in.	b/a	α , deg	α_0/α	R_{W_1}	q_1 , lb/sq ft	C_{PR}	η_p
1.25	1.04	14.00	0.00	2.43×10^5	31.5	0.223	0.232
1.25	1.04	9.33	.50	2.41	30.1	.718	.749
1.25	1.04	8.40	.67	2.42	30.2	.728	.759
1.25	1.04	7.50	.87	2.38	29.4	.743	.775
1.25	1.04	7.00	1.00	2.38	29.5	.742	.774
1.25	1.04	6.50	1.25	2.39	29.6	.745	.776
1.25	1.04	4.67	2.00	2.39	29.6	.723	.754
1.91	1.20	6.00	1.33	2.38	29.3	.602	.627
1.91	1.20	6.50	1.15	2.40	29.7	.763	.795
1.91	1.20	7.00	1.00	2.35	29.4	.763	.795
1.91	1.20	7.50	.87	2.39	30.0	.768	.800
1.91	1.20	8.00	.75	2.37	29.5	.754	.786

TABLE VII.- Continued

PERFORMANCE OF DIFFUSER WITH VANES

(c) $2\theta = 28.0^\circ$; $W_1 = 3.00$ inches; $L/W_1 = 8.35$; $A_2/A_1 = 4.92$; $f = 12.0$ inches; $n = 3$; $\alpha = \frac{2\theta}{n+1} = 7.00^\circ$; a variable

c, in.	a, in.	b, in.	$\frac{2a+2b}{W_1}$	R_{W_1}	q_1 , lb/sq ft	C_{PR}	η_p
0.62	0.70	0.69	0.93	2.41×10^5	30.6	0.711	0.741
1.05	.70	.77	.98	2.51	33.4	.751	.783
1.50	.70	.86	1.04	2.42	30.2	.754	.786
1.94	.70	.96	1.11	2.41	29.9	.765	.797
2.41	.70	1.08	1.19	2.43	30.6	.752	.784
1.05	.80	.67	.91	2.41	29.9	.746	.778
1.53	.80	.76	.98	2.41	29.8	.757	.790
1.95	.80	.87	1.05	2.41	30.1	.763	.796
2.35	.80	.96	1.11	2.41	30.4	.638	.665

TABLE VII.- Continued

PERFORMANCE OF DIFFUSER WITH VANES

(d) $2\theta = 42.0^\circ$; $W_1 = 3.00$ inches; $L/W_1 = 8.52$;

$$A_2/A_1 = 6.88; a = \frac{W_1}{n+1}; \alpha = \frac{2\theta}{n+1}$$

f, in.	n	a, in.	α , deg	c, in.	f/a	b/a	R_{W_1}	q_1 , lb/sq ft	C_{PR}	η_p
3.00	1	1.50	21.00	0.68	2.00	1.00	2.44×10^5	30.3	0.448	0.457
3.00	2	1.00	14.00	.95	3.00	1.00	2.41	29.9	.538	.550
3.00	2	1.00	14.00	1.17	3.00	1.09	2.42	30.7	.523	.534
3.00	2	1.00	14.00	1.67	3.00	1.17	2.34	28.7	.464	.474
3.00	2	1.00	14.00	2.78	3.00	1.55	2.40	30.0	.395	.403
3.00	3	.75	10.50	1.12	4.00	1.00	2.39	29.9	.578	.590
3.00	3	.75	10.50	1.44	4.00	1.12	2.39	30.0	.583	.595
3.00	3	.75	10.50	1.80	4.00	1.28	2.35	29.1	.529	.540
3.00	3	.75	10.50	2.77	4.00	1.71	2.33	29.0	.388	.396
3.00	4	.60	8.40	1.27	5.00	1.00	2.42	30.2	.640	.653
3.00	4	.60	8.40	1.39	5.00	1.07	2.40	29.8	.641	.654
3.00	4	.60	8.40	1.73	5.00	1.23	2.40	29.8	.661	.674
3.00	4	.60	8.40	2.62	5.00	1.75	2.40	29.7	.517	.528
3.00	5	.50	7.00	1.44	6.00	1.00	2.37	28.9	.627	.640
3.00	5	.50	7.00	1.62	6.00	1.09	2.40	29.6	.639	.652
3.00	5	.50	7.00	2.00	6.00	1.34	2.39	29.4	.587	.599
3.00	5	.50	7.00	2.62	6.00	1.84	2.37	29.0	.430	.439
6.00	1	1.50	21.00	.66	4.00	1.00	2.43	30.2	.458	.468
6.00	2	1.00	14.00	.89	6.00	1.00	2.43	31.1	.619	.632
6.00	2	1.00	14.00	1.41	6.00	1.11	2.31	28.1	.589	.602
6.00	2	1.00	14.00	1.74	6.00	1.20	2.37	29.7	.574	.586
6.00	2	1.00	14.00	2.61	6.00	1.49	2.38	29.9	.447	.456
6.00	3	.75	10.50	1.14	8.00	1.00	2.43	29.8	.662	.676
6.00	3	.75	10.50	1.39	8.00	1.09	2.49	31.2	.680	.694
6.00	3	.75	10.50	1.80	8.00	1.24	2.40	29.3	.630	.643
6.00	3	.75	10.50	2.61	8.00	1.61	2.41	29.7	.550	.562

TABLE VII.- Continued

PERFORMANCE OF DIFFUSER WITH VANES

(d) $2\theta = 42.0^\circ$; $W_1 = 3.00$ inches; $L/W_1 = 8.52$; $A_2/A_1 = 6.88$;

$$a = \frac{W_1}{n+1}; \alpha = \frac{2\theta}{n+1} - \text{Continued}$$

f, in.	n	a, in.	α , deg	c, in.	f/a	b/a	R_{W_1}	q_1 , lb/sq ft	C_{PR}	η_p
6.00	4	0.60	8.40	1.25	10.00	1.00	2.42×10^5	29.9	0.649	0.663
6.00	4	.60	8.40	1.42	10.00	1.06	2.40	29.5	.662	.675
6.00	4	.60	8.40	1.80	10.00	1.25	2.41	29.7	.680	.694
6.00	4	.60	8.40	2.36	10.00	1.58	2.46	30.9	.578	.590
6.00	5	.50	7.00	1.50	12.00	1.00	2.39	29.6	.643	.657
6.00	5	.50	7.00	1.69	12.00	1.10	2.37	29.3	.665	.678
6.00	5	.50	7.00	1.94	12.00	1.28	2.38	29.5	.684	.698
6.00	5	.50	7.00	2.50	12.00	1.68	2.39	29.6	.484	.494
9.00	1	1.50	21.00	.67	6.00	1.00	2.37	29.5	.462	.471
9.00	1	1.50	21.00	1.25	6.00	1.07	2.39	30.1	.437	.446
9.00	1	1.50	21.00	1.81	6.00	1.17	2.39	30.0	.413	.422
9.00	1	1.50	21.00	2.62	6.00	1.35	2.39	29.9	.387	.395
9.00	2	1.00	14.00	1.00	9.00	1.00	2.39	29.3	.591	.604
9.00	2	1.00	14.00	1.41	9.00	1.09	2.45	29.6	.611	.624
9.00	2	1.00	14.00	1.81	9.00	1.21	2.38	29.0	.571	.583
9.00	2	1.00	14.00	2.52	9.00	1.44	2.40	29.5	.501	.512
9.00	3	.75	10.50	1.17	12.00	1.00	2.30	29.1	.667	.682
9.00	3	.75	10.50	1.34	12.00	1.06	2.32	29.4	.670	.684
9.00	3	.75	10.50	2.06	12.00	1.37	2.29	28.7	.641	.655
9.00	3	.75	10.50	2.58	12.00	1.60	2.35	30.2	.582	.595
9.00	4	.60	8.40	1.28	15.00	1.00	2.31	30.1	.658	.672
9.00	4	.60	8.40	1.17	15.00	1.13	2.27	29.3	.670	.684
9.00	4	.60	8.40	2.05	15.00	1.36	2.33	30.7	.676	.691
9.00	4	.60	8.40	2.37	15.00	1.59	2.29	29.7	.450	.460
9.00	5	.50	7.00	1.47	18.00	1.00	2.26	29.1	.657	.671
9.00	5	.50	7.00	1.69	18.00	1.14	2.29	29.9	.685	.700
9.00	5	.50	7.00	1.92	18.00	1.30	2.29	29.8	.702	.717
9.00	5	.50	7.00	2.59	18.00	1.73	2.27	29.3	.480	.491

TABLE VII.- Continued

PERFORMANCE OF DIFFUSER WITH VANES

(d) $2\theta = 42.0^\circ$; $W_1 = 3.00$ inches; $L/W_1 = 8.52$; $A_2/A_1 = 6.88$;

$$a = \frac{W_1}{n+1}; \alpha = \frac{2\theta}{n+1} - \text{Continued}$$

f, in.	n	a, in.	α , deg	c, in.	f/a	b/a	R_{W1}	q_1 , lb/sq ft	C_{PR}	η_p
12.00	1	1.50	21.00	0.72	8.00	1.00	2.40×10^5	29.8	0.435	0.444
12.00	1	1.50	21.00	1.36	8.00	1.09	2.37	29.2	.456	.465
12.00	1	1.50	21.00	1.94	8.00	1.20	2.45	31.1	.437	.447
12.00	2	1.00	14.00	.97	12.00	1.01	2.31	29.5	.688	.621
12.00	2	1.00	14.00	1.20	12.00	1.06	2.32	29.6	.605	.619
12.00	2	1.00	14.00	1.72	12.00	1.20	2.34	30.0	.602	.615
12.00	2	1.00	14.00	2.28	12.00	1.38	2.32	29.6	.550	.562
12.00	3	.75	10.50	1.16	16.00	1.00	2.36	29.6	.680	.695
12.00	3	.75	10.50	1.44	16.00	1.09	2.36	29.5	.681	.696
12.00	3	.75	10.50	1.67	16.00	1.18	2.37	29.8	.686	.700
12.00	3	.75	10.50	2.23	16.00	1.44	2.41	30.7	.642	.656
12.00	4	.60	8.40	1.27	20.00	.99	2.40	29.6	.652	.666
12.00	4	.60	8.40	1.45	20.00	1.06	2.39	29.3	.672	.686
12.00	4	.60	8.40	1.81	20.00	1.24	2.38	29.1	.689	.704
12.00	4	.60	8.40	2.28	20.00	1.51	2.40	29.8	.587	.600
12.00	5	.50	7.00	1.50	24.00	1.01	2.37	29.2	.673	.688
12.00	5	.50	7.00	1.64	24.00	1.10	2.39	29.7	.690	.705
12.00	5	.50	7.00	1.89	24.00	1.26	2.38	29.4	.704	.720
12.00	5	.50	7.00	2.36	24.00	1.58	2.41	30.3	.520	.531
15.00	1	1.50	21.00	.72	10.00	1.00	2.41	29.7	.431	.440
15.00	1	1.50	21.00	.72	10.00	1.00	2.47	31.2	.482	.493
15.00	1	1.50	21.00	.94	10.00	1.03	2.43	30.2	.473	.483
15.00	1	1.50	21.00	.47	10.00	1.11	2.41	29.7	.449	.459
15.00	2	1.00	14.00	1.00	15.00	1.01	2.36	28.9	.605	.618
15.00	2	1.00	14.00	1.27	15.00	1.08	2.36	28.9	.618	.631
15.00	2	1.00	14.00	1.55	15.00	1.15	2.39	29.6	.623	.636
15.00	2	1.00	14.00	1.75	15.00	1.21	2.39	29.6	.610	.624

TABLE VII.- Continued

PERFORMANCE OF DIFFUSER WITH VANES

(d) $2\theta = 42.0^\circ$; $W_1 = 3.00$ inches; $L/W_1 = 8.52$; $A_2/A_1 = 6.88$;

$$a = \frac{W_1}{n+1}; \alpha = \frac{2\theta}{n+1} - \text{Concluded}$$

f, in.	n	a, in.	α , deg	c, in.	f/a	b/a	R_{W1}	q_1 , lb/sq ft	C_{PR}	η_p
15.00	3	0.75	10.40	1.14	20.00	1.00	2.35×10^5	29.1	0.678	0.693
15.00	3	.75	10.40	1.39	20.00	1.08	2.36	29.9	.692	.707
15.00	3	.75	10.40	1.75	20.00	1.22	2.35	29.5	.693	.708
15.00	3	.75	10.40	2.20	20.00	1.42	2.36	29.9	.635	.648
15.00	4	.60	8.40	1.33	25.00	1.00	2.38	29.5	.659	.673
15.00	4	.60	8.40	1.48	25.00	1.12	2.39	29.7	.678	.693
15.00	4	.60	8.40	1.81	25.00	1.26	2.40	30.1	.698	.713
15.00	4	.60	8.40	2.28	25.00	1.53	2.37	29.2	.559	.571
15.00	5	.50	7.00	1.52	30.00	1.00	2.35	29.3	.677	.692
15.00	5	.50	7.00	1.73	30.00	1.14	2.36	29.7	.699	.714
15.00	5	.50	7.00	2.06	30.00	1.36	2.37	29.9	.533	.545
15.00	5	.50	7.00	2.37	30.00	1.56	2.36	29.5	.507	.517
15.00	5	.50	7.00	2.05	30.00	1.34	2.37	29.3	.519	.530
15.00	5	.50	7.00	2.05	30.00	1.23	2.39	29.7	.711	.726
15.00	5	.50	7.00	2.05	30.00	1.23	2.45	31.2	.598	.610

TABLE VII.- Continued

PERFORMANCE OF DIFFUSER WITH VANES

(e) $2\theta = 42.0^\circ$; $W_1 = 3.00$ inches; $L/W_1 = 8.52$;

$A_2/A_1 = 6.88$; $a = \frac{W_1}{n+1} = 0.50$ inch; $n = 5$;

$f = 15.0$ inches; α variable

c , in.	b/a	α , deg	α_o/α	R_{W_1}	q_1 , lb/sq ft	C_{PR}	η_p
1.52	1.01	10.50	0.00	2.47×10^5	31.5	0.267	0.273
1.52	1.01	8.40	.50	2.39	29.5	.652	.666
1.52	1.01	8.00	.62	2.38	30.3	.667	.681
1.52	1.01	7.50	.80	2.40	29.9	.682	.697
1.52	1.01	6.50	1.23	2.39	29.8	.679	.694
1.52	1.01	6.00	1.50	2.35	29.2	.579	.591

TABLE VII.- Continued

PERFORMANCE OF DIFFUSER WITH VANES

(f) $2\theta = 42.0^\circ$; $W_1 = 3.00$ inches; $L/W_1 = 8.52$; $A_2/A_1 = 6.88$; $f = 15.0$ inches; $n = 5$; $\alpha = \frac{2\theta}{n+1} = 7.00^\circ$; a variable

c , in.	a , in.	b , in.	$\frac{4a + 2b}{W_1}$	R_{W_1}	q_1 , lb/sq ft	C_{PR}	η_p
1.48	0.533	0.431	1.00	2.37×10^5	29.5	0.594	0.607
1.83	.533	.533	1.07	2.37	29.4	.513	.524
1.37	.533	.480	1.03	2.42	30.8	.584	.596
1.94	.533	.574	1.09	2.42	30.2	.593	.544
1.80	.533	.527	1.06	2.41	30.1	.514	.525
1.66	.533	.473	1.03	2.72	38.2	.692	.706
1.66	.533	.473	1.03	2.47	31.7	.597	.609
1.66	.533	.473	1.03	2.39	29.5	.537	.548
1.22	.475	.772	1.14	2.42	30.5	.575	.587
.87	.475	.667	1.08	2.38	29.6	.717	.732
.68	.475	.609	1.04	2.59	28.6	.676	.690
.48	.475	.545	.99	2.46	30.5	.668	.682
.27	.475	.475	.95	2.43	29.7	.632	.646

TABLE VII.- Continued

PERFORMANCE OF DIFFUSER WITH VANES

(g) Tests to determine envelope of C_{PR} ; $W_1 = 3.00$ inches;

$$a = \frac{W_1}{n + 1}; \quad b/a = 1.20$$

2θ , deg	L/W_1	n	f , in.	c , in.	α , deg	α_o/α	R_{W_1}	q_1 , lb/sq ft	C_{PR}	η_p
16.8	8.21	1	15.00	0.72	8.40	----	2.44×10^5	30.2	0.766	0.838
16.8	8.21	2	15.00	1.48	5.60	1.00	2.43	30.0	.745	.815
21.0	8.26	2	15.00	2.19	7.00	1.00	2.40	30.3	.741	.798
24.5	8.30	2	15.00	1.02	10.50	.64	2.40	30.3	.734	.773
24.5	8.30	2	15.00	1.02	8.75	.87	2.39	29.5	.751	.791
24.5	8.30	2	15.00	1.02	8.00	1.00	2.40	29.7	.755	.795
24.5	8.30	2	15.00	1.02	7.00	1.21	2.40	29.8	.748	.788
24.5	8.30	2	15.00	1.02	6.50	1.35	2.39	30.1	.756	.796
24.5	8.30	3	15.00	1.94	7.00	.71	2.37	29.7	.751	.791
24.5	8.30	3	15.00	1.94	6.50	.85	2.37	29.6	.759	.800
24.5	8.30	3	15.00	1.94	6.00	1.00	2.37	29.6	.761	.801
24.5	8.30	3	15.00	1.94	5.60	1.14	2.38	29.2	.752	.792
24.5	8.30	3	15.00	1.94	4.67	1.57	2.38	29.4	.761	.801
24.5	8.30	3	15.00	1.94	7.50	.60	2.39	29.4	.739	.778
31.1	8.38	4	15.00	1.81	6.25	.99	2.37	29.7	.680	.703
31.1	8.38	3	15.00	1.75	7.77	1.00	2.43	31.3	.739	.764
38.2	8.47	5	15.00	1.84	6.33	1.00	2.48	31.7	.584	.596
38.2	8.47	5	12.00	1.84	6.33	1.00	2.39	30.3	.695	.712
38.2	8.47	4	12.00	1.72	7.60	1.00	2.34	29.2	.674	.690

TABLE VII.- Concluded

PERFORMANCE OF DIFFUSER WITH VANES

(h) Tests with vanes selected by design criteria; $2\theta = 28.0^\circ$;

$$a = \frac{W_1}{n+1}; \alpha = \frac{2\theta}{n+1} = 7.00; b/a = 1.20; n = 3$$

W_1 , in.	L/W_1	c , in.	a , in.	f , in.	f/a	R_{W_1}	q_1 , lb/sq ft	C_{PR}	η_p
1.33	18.81	1.45	0.33	6.00	18.00	1.61×10^5	69.7	0.721	0.728
1.60	15.66	1.53	.40	9.00	22.50	1.58	47.6	.707	.717
2.00	12.52	1.56	.50	9.00	18.00	1.53	28.3	.706	.721
2.00	12.52	1.56	.50	9.00	18.00	2.36	68.0	.724	.739
2.40	10.44	1.73	.60	12.00	20.00	2.35	46.6	.745	.766
2.40	10.44	1.73	.60	12.00	20.00	1.60	21.5	.738	.759
3.00	8.35	1.57	.75	12.00	16.00	1.60	13.3	.763	.795
4.00	6.26	2.14	1.00	15.00	15.00	2.42	16.8	.753	.804
4.00	6.26	2.14	1.00	15.00	15.00	1.62	7.53	.753	.804
6.00	4.18	2.64	1.50	15.00	10.00	2.38	7.16	.697	.786
6.00	4.18	2.64	1.50	15.00	10.00	1.62	3.34	.677	.763

TABLE VIII

SEPARATION PATTERNS

[Each pair of squares represents diverging walls viewed looking out from inside diffuser; I = Intermittent transitory stall; T = Transitory stall; TIF = Transitory stall with intermittent fixed stalls; FIT = Fixed stall with intermittent transitory stall; F = Stable fixed stall. For vaneless diffuser: $W_1 = 3.00$ inches; $L/W_1 \approx 8.0$; $R_{W_1} \approx 2.4 \times 10^5$]

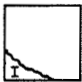

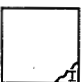
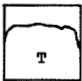
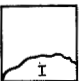
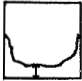

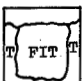

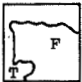
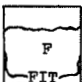
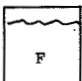
2θ, deg	Flow	West wall	East wall
7.0	Very steady	Unstalled	Unstalled
14.0	Quite steady		Unstalled
16.8	Unsteady; faintly audible oscillations, not violent		
21.0	Very steady strong pulsations; frequency, 3 to 4 cps		
24.5	Quite unsteady; intense and violent transitory stall		
28.0	Fairly steady		No separation; occasional disturbances
31.1	Fairly steady	No separation; occasional separation on lower end	
35.0	Quite steady		No separation; very minor disturbances
38.2	Steady		No separation; very minor disturbances
42.0	Very steady		No separation; very minor disturbances

TABLE IX

EFFECT OF VANE END CLEARANCE

(a) $2\theta = 42.0^\circ$; $L/W_1 \approx 8.0$; $R_{W_1} \approx 2.4 \times 10^5$; $f = 15$;
 $\alpha = 7.0^\circ$; $n = 5$; $a = 0.475$ inch; $b/a = 1.4$ (for
 these configurations $\left(a = 0.475 < \frac{W_1}{n+1}\right)$ the flows
 were all fairly steady even though $b/a > 1.2$)

Description	C_{PR}
Cluster against north wall, all clearance at south wall	0.692
Cluster centered	.716
Cluster centered, both ends taped	.711

(b) $2\theta = 28.0^\circ$; $L/W_1 \approx 8.0$; $R_{W_1} \approx 2.4 \times 10^5$; $f = 12$ inches;
 $\alpha = 7.0^\circ$; $n = 3$; $a = 0.750$; $b/a = 1.2$

Description	C_{PR}
Cluster against north wall, all clearance at south wall	0.766
Cluster centered	.764
Cluster centered, both ends taped	.763

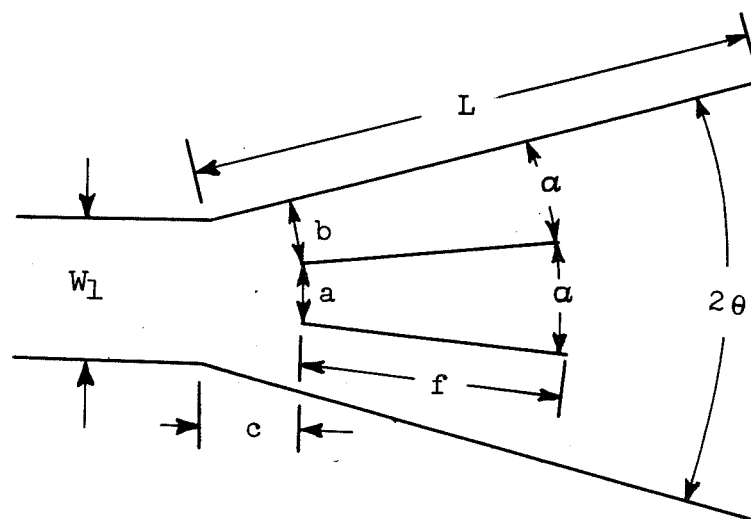
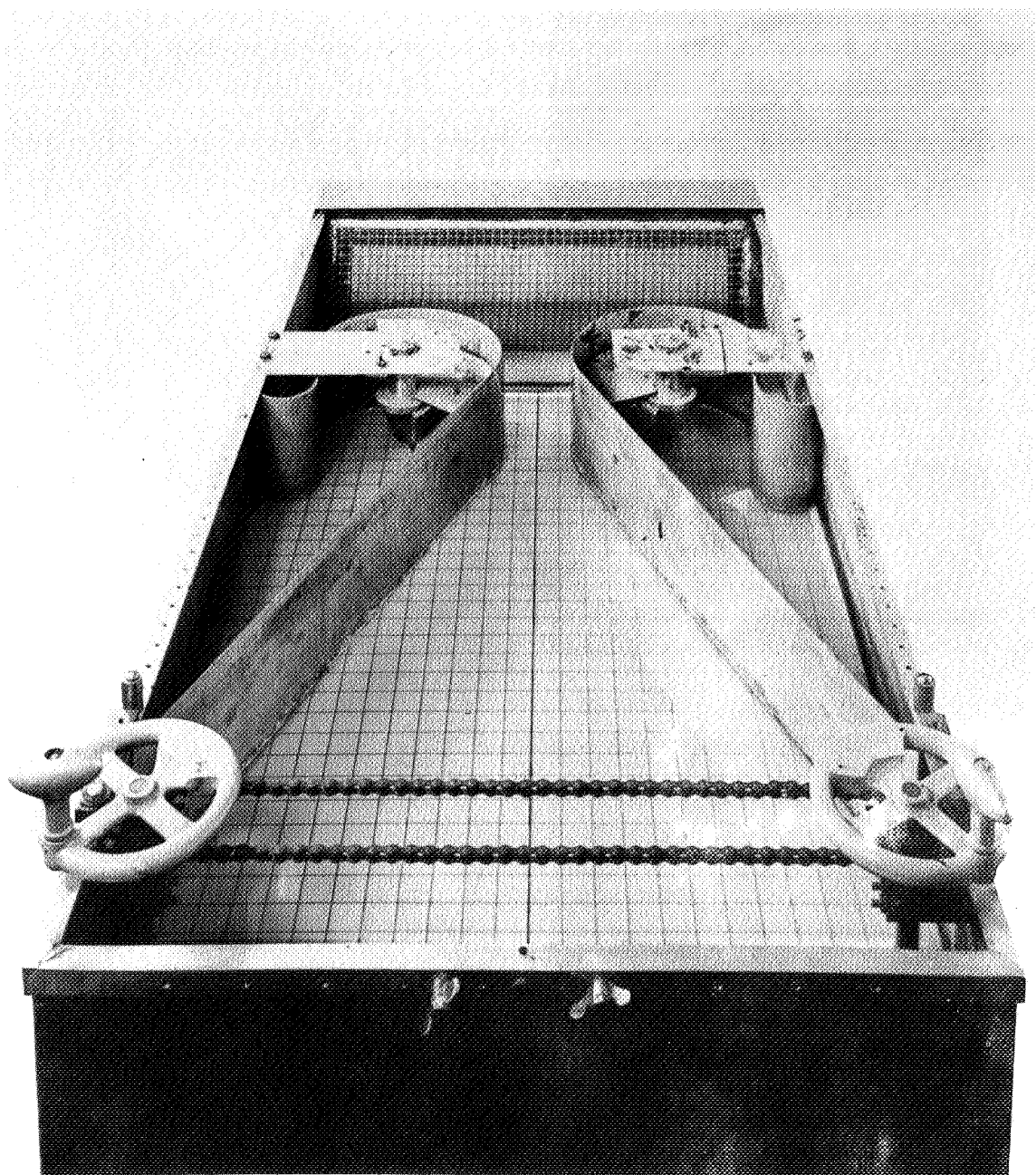
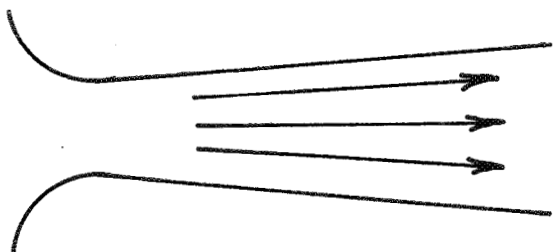
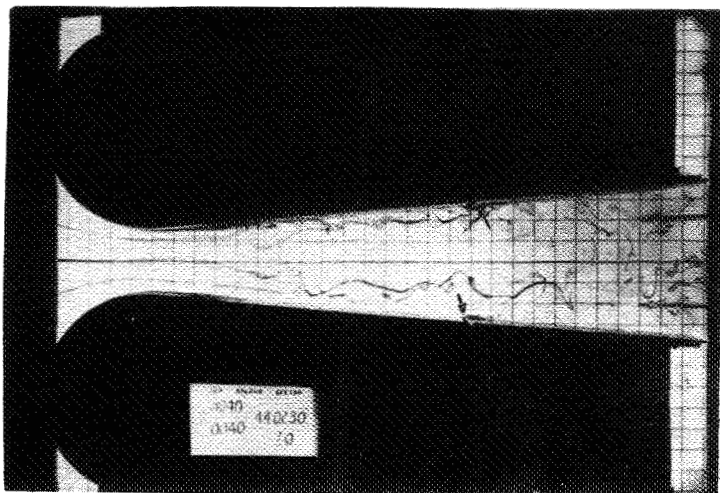


Figure 1.- Typical vane installation.

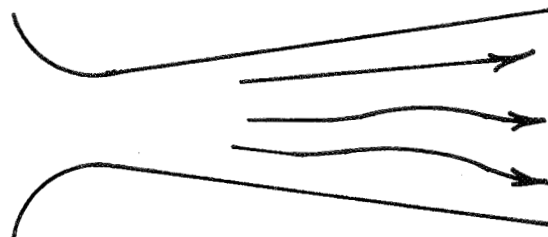
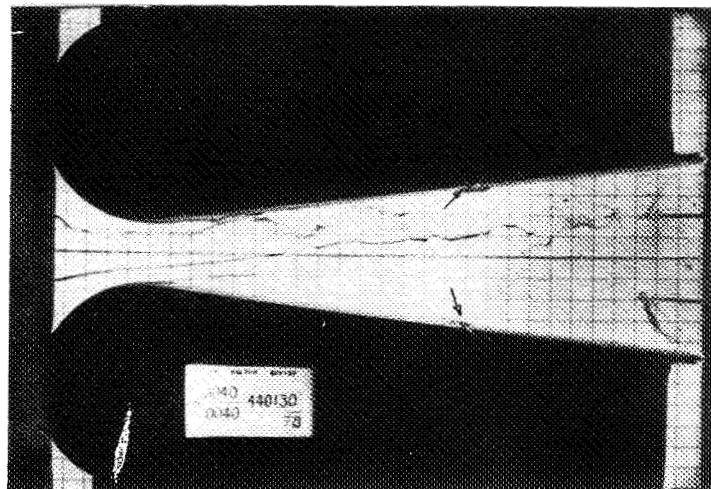


L-58-2660

Figure 2.- Water table used in work of Moore and Kline (refs. 3 and 4).

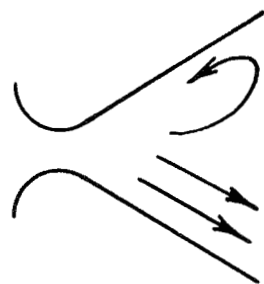
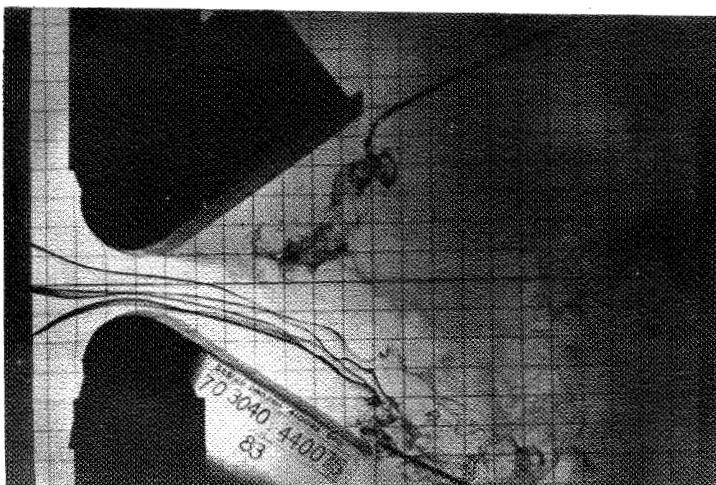


(a) $2\theta = 10^\circ$. $L/W_1 = 8.2$.
No apparent stalls.

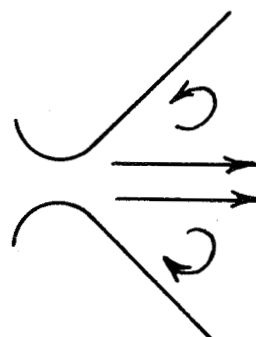
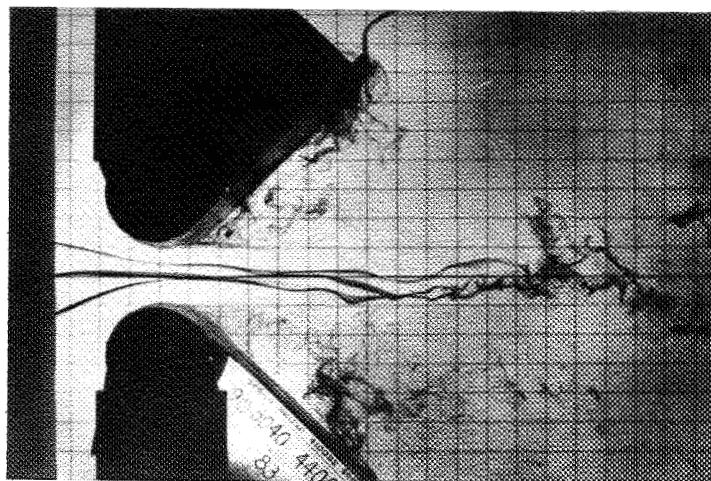


(b) $2\theta = 15^\circ$. $L/W_1 = 8.23$.
Transitory stall.

Figure 3.- Typical dye trace photographs. Inlet flow conditions, wall length, and throat width are held constant. Photographs are from reference 4.



(c) $2\theta = 70^\circ$. $L/W_1 \approx 8.30$.
Fully developed stall.



(d) $2\theta = 90^\circ$. $L/W_1 \approx 8.30$.
Jet flow.

Figure 3.- Concluded.

- aa Line of appreciable stall
 bb Transition between transitory and two-dimensional flow
 cc Transition from two dimensional to jet flow
 dd Transition from jet to two-dimensional flow
 -- Low turbulence — High turbulence

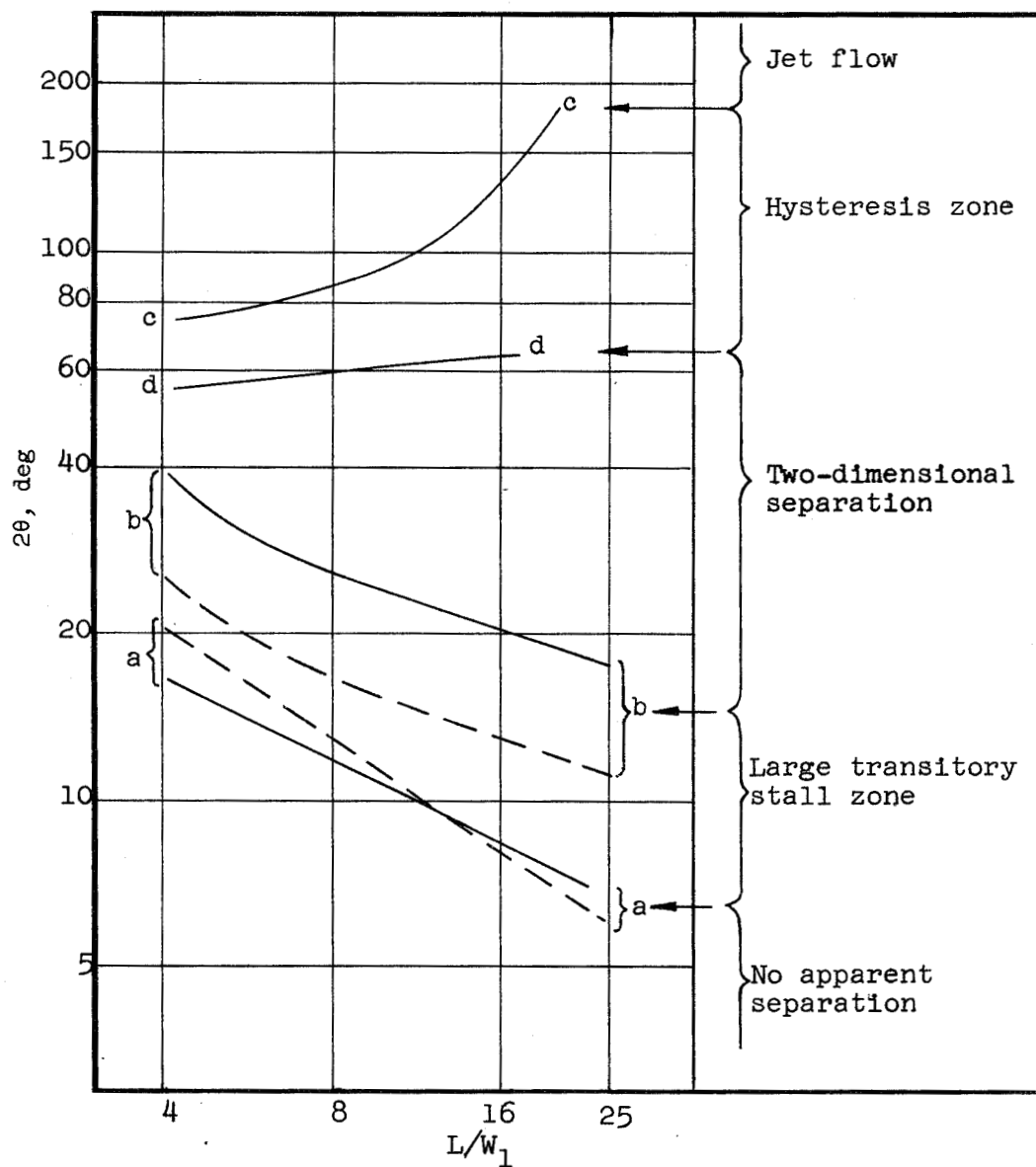
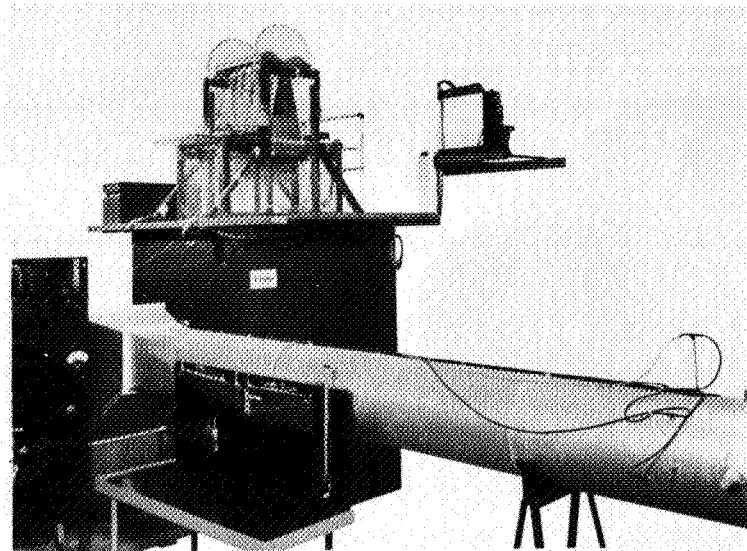
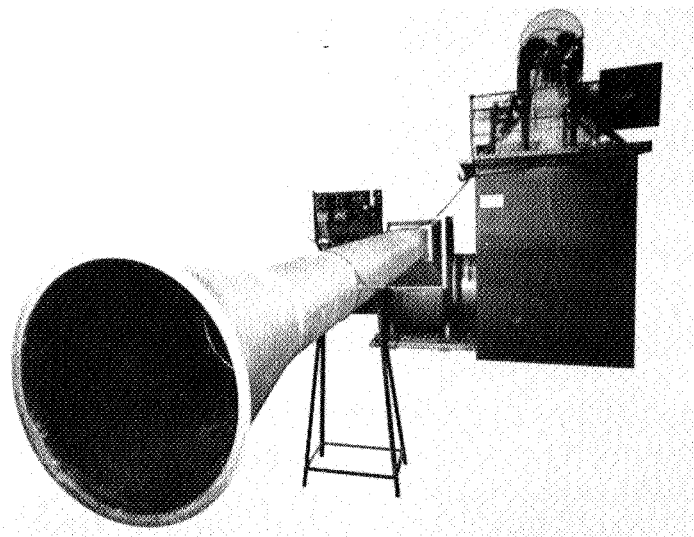


Figure 4.- Regimes of diffuser flow (ref. 4).



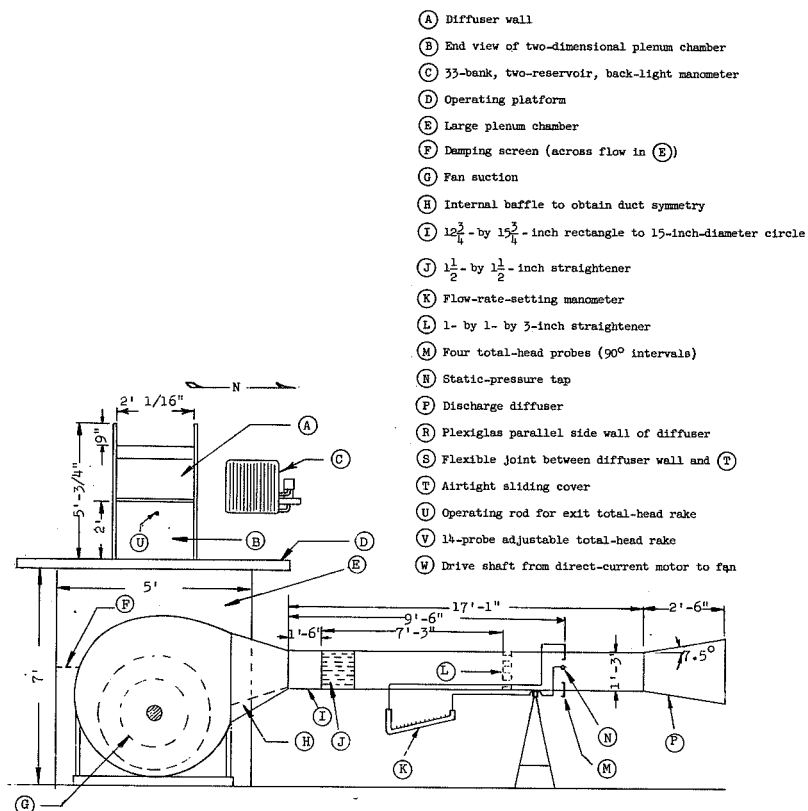
(a) Southwest view (guard rail removed).



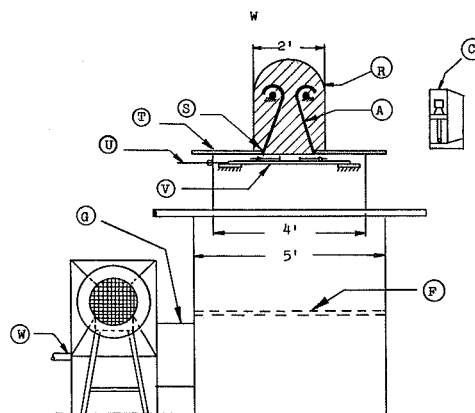
(b) Southeast view (guard rail removed).

L-58-2661

Figure 5.- General views of apparatus.

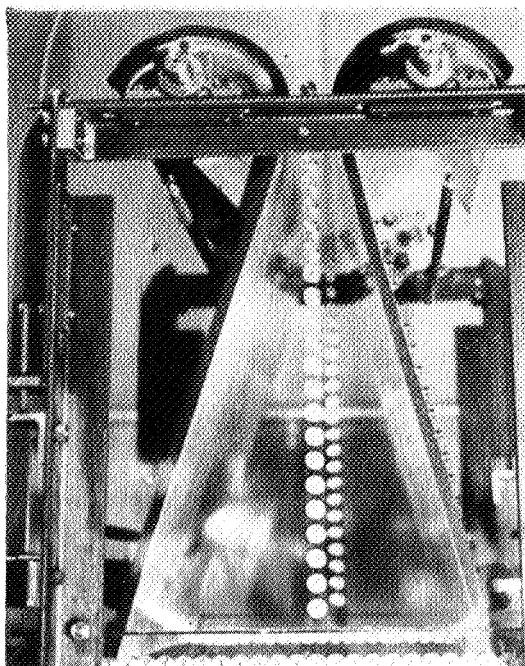


(a) Side view.

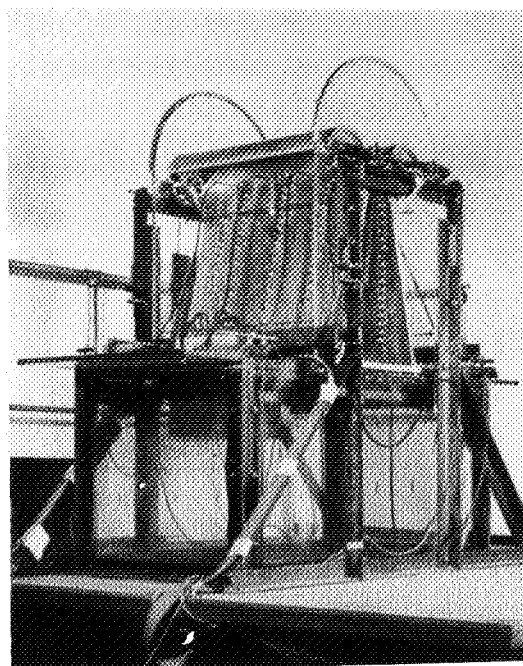


(b) End view.

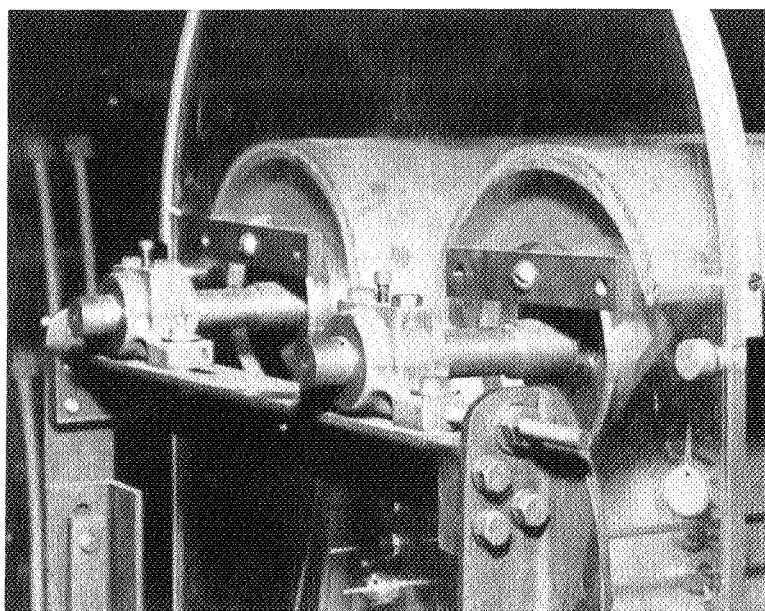
Figure 6.- Schematic view of test apparatus.



(a) North side.



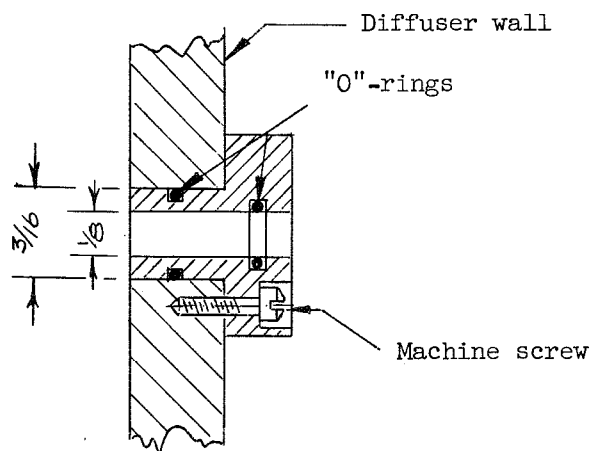
(b) Southwest oblique view showing general arrangement.



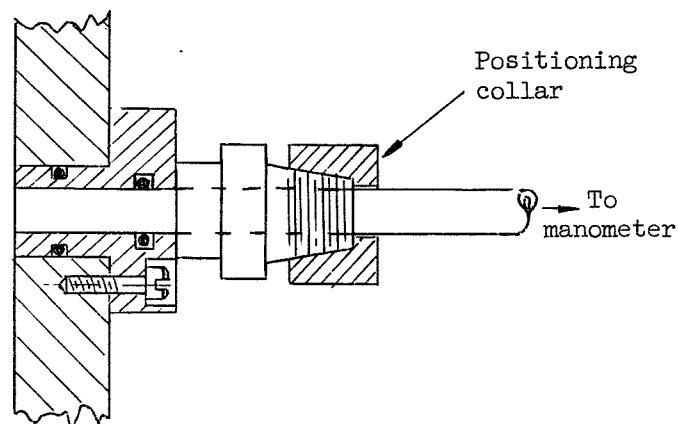
(c) Pillow block and shaft detail.

L-58-2662

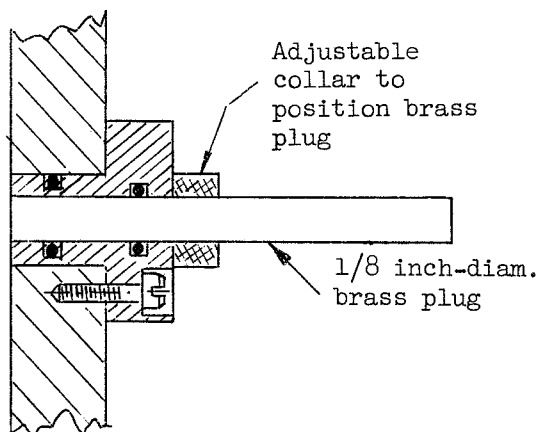
Figure 7.- Close-up views of apparatus.



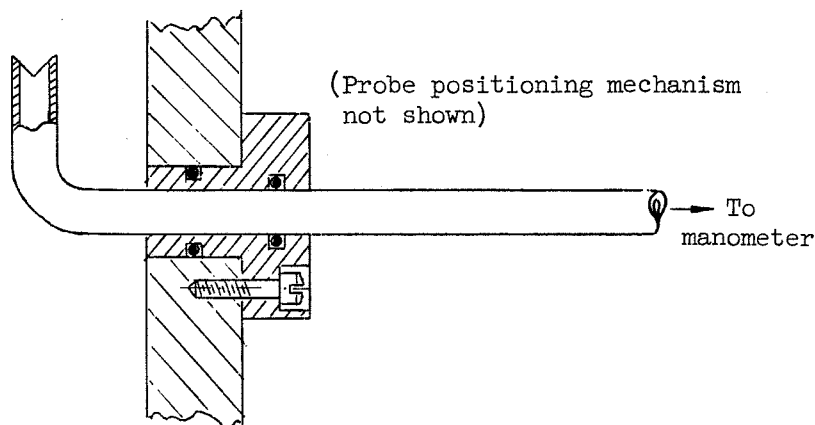
(a) Fitting open to surroundings.



(c) Fitting used as static-pressure tap.

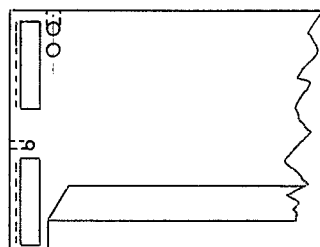


(b) Closed with brass plug (normal condition).

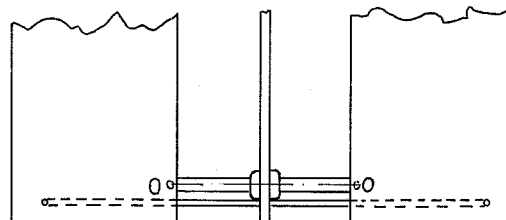


(d) Fitting used for probe access.

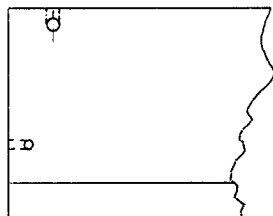
Figure 8.- Aluminum pressure tap fittings.



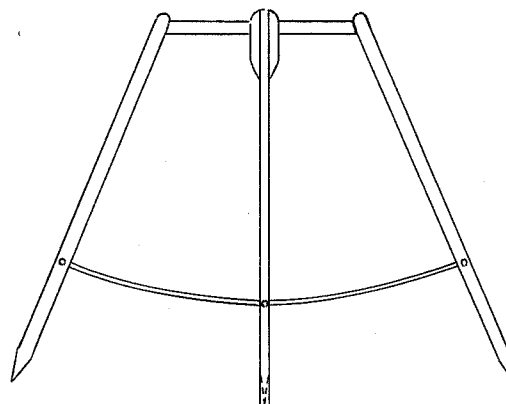
(a) Three-inch center vane end detail.



(c) Top view of typical 3-inch odd-number vane assembly.

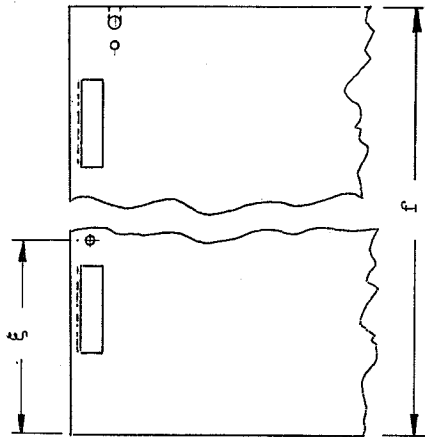


(b) Three-inch side vane end detail.

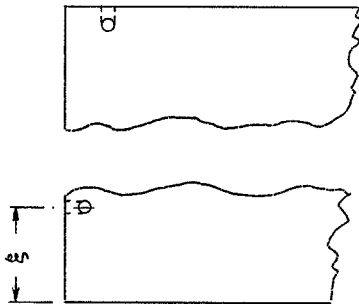


(d) End view of typical 3-inch three-vane assembly.

Figure 9.- Typical vane assemblies.

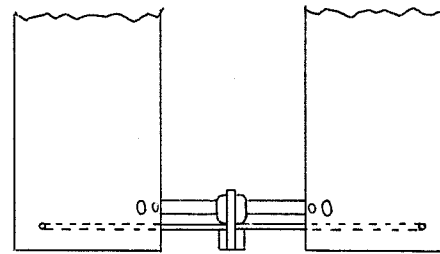


(e) Long center vane end detail



(f) Long side vane end detail.

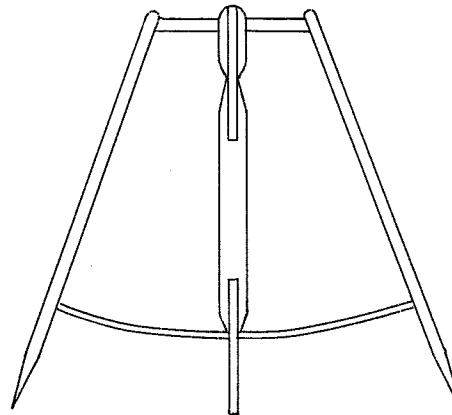
f, in.	ξ, in.
6	$2\frac{7}{16}$
9	$1\frac{9}{16}$
12	$2\frac{9}{16}$
15	$4\frac{9}{16}$



(g) Top view of typical assembly of long even-numbered vanes.

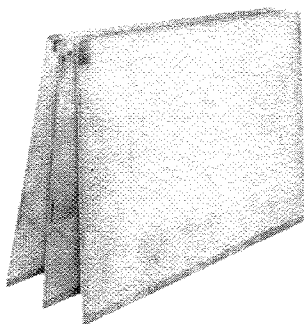


(i) Dummy end for vane assembly.

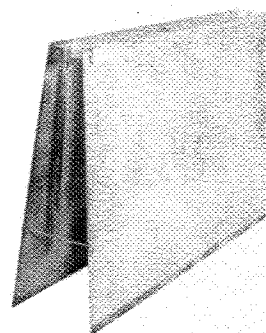


(h) End view of typical assembly of long even-numbered vanes.

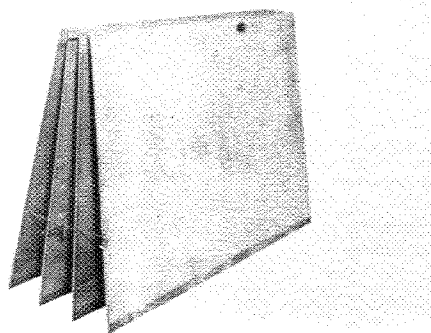
Figure 9.- Concluded.



(a) Assembly of odd-numbered long vanes.



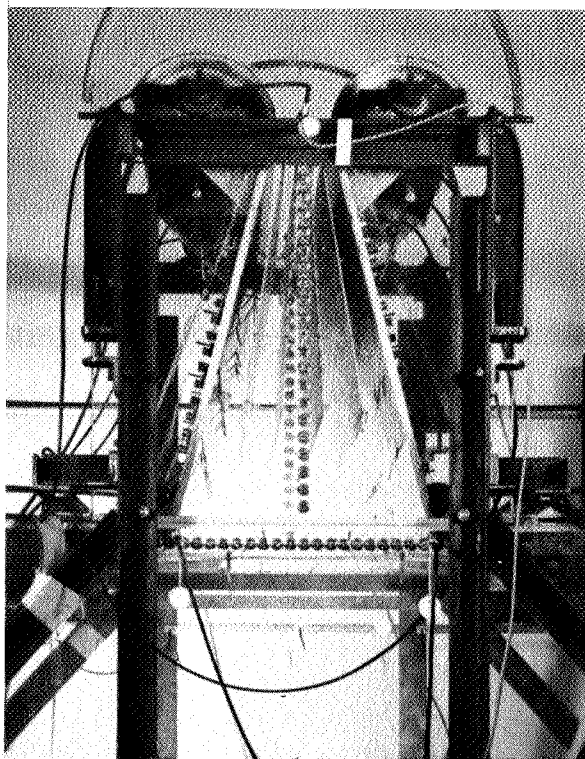
(b) Assembly of even-numbered long vanes.



(c) Even-numbered vane assembly with modified holder mechanism.

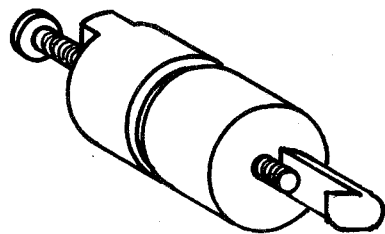
L-58-2663

Figure 10.- Typical vane-cluster assemblies.

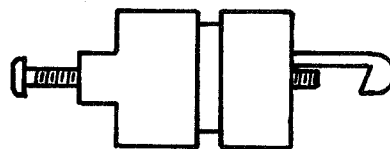


L-58-2664

(a) End view showing five 12-inch vanes installed in diffuser.



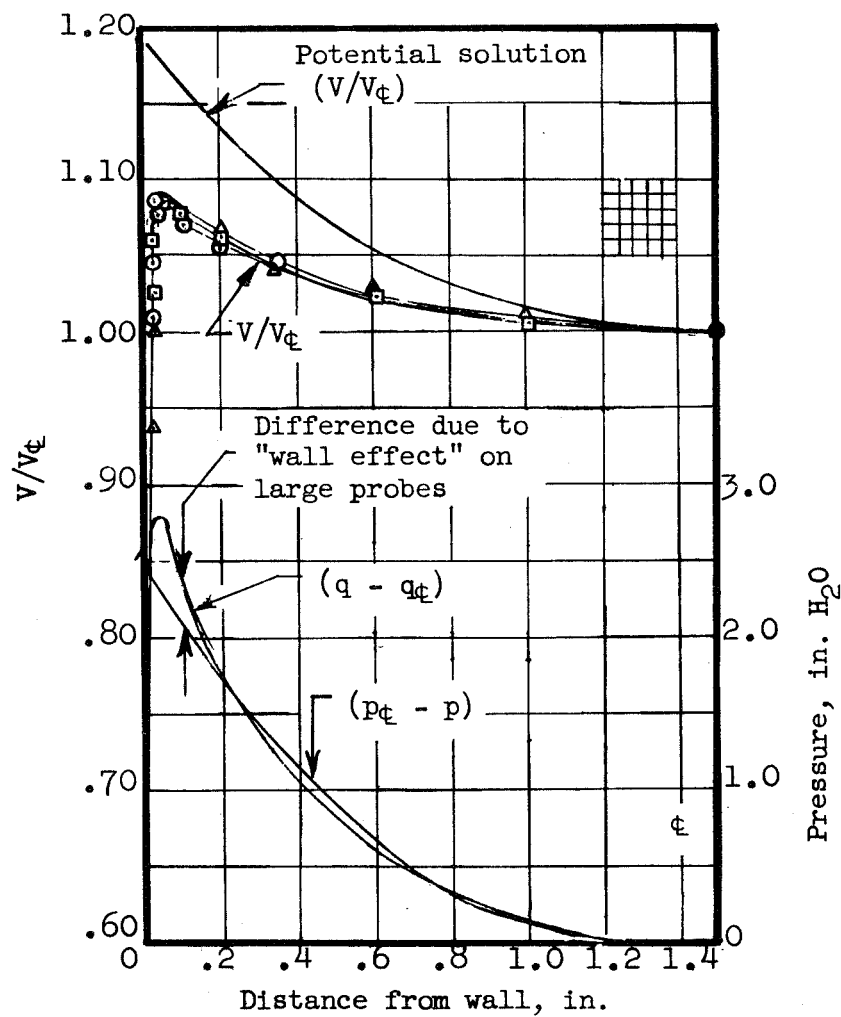
Oblique View



Top View

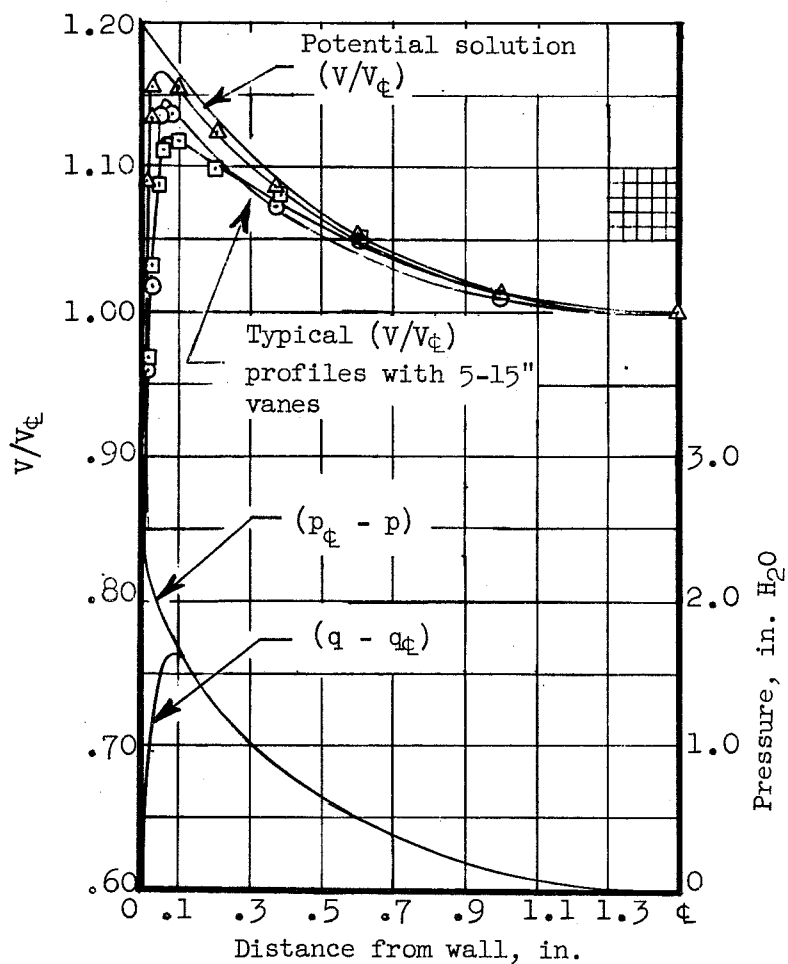
(b) Vane-cluster supporting hooks.

Figure 11.- Typical vane installation.

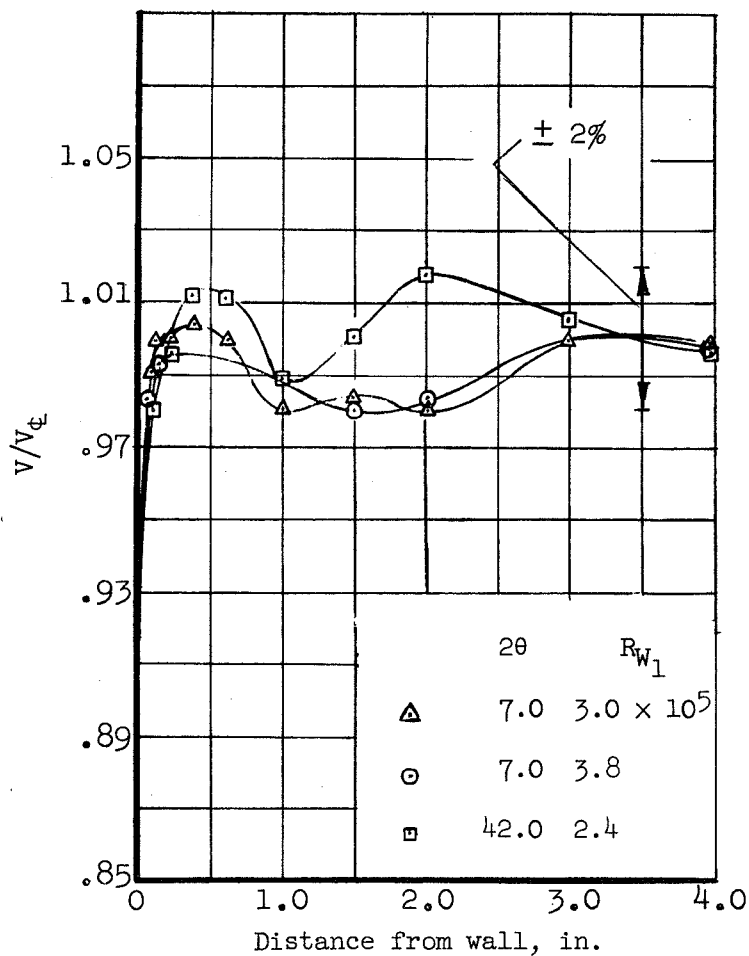


(a) Vertical planes parallel to diffuser side walls;
 $2\theta = 7.0^\circ$.

Figure 12.- Inlet velocity and pressure profiles. $W_1 = 3.00$ inches;
 for constant total head, $q - q_\phi = p - p_\phi$.

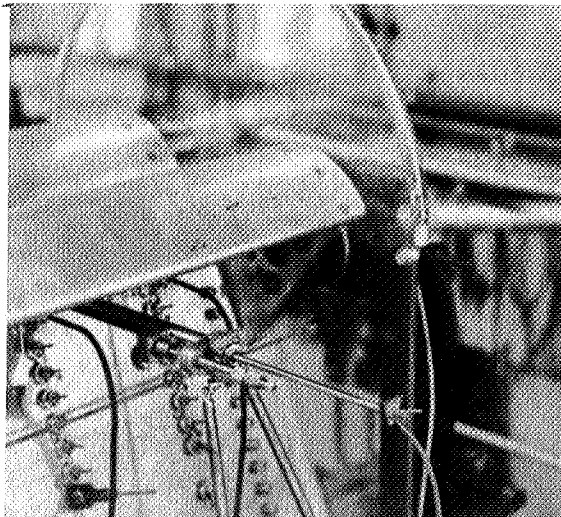


(b) Vertical planes parallel to diffuser side walls; $2\theta = 42.0^\circ$.



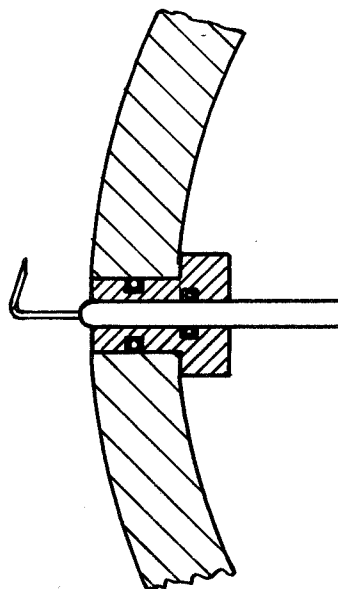
(c) Vertical center plane perpendicular to diffuser side walls.

Figure 12.- Concluded.



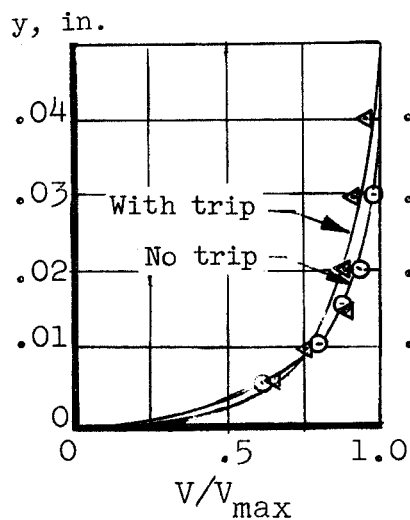
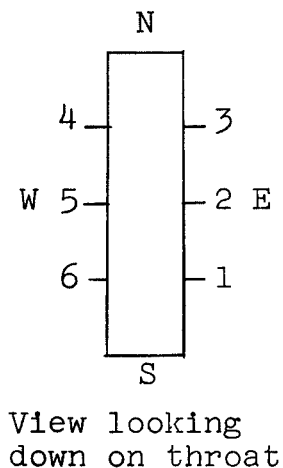
L-58-2665

(a) Boundary-layer traverse mechanism installed in the diffuser.

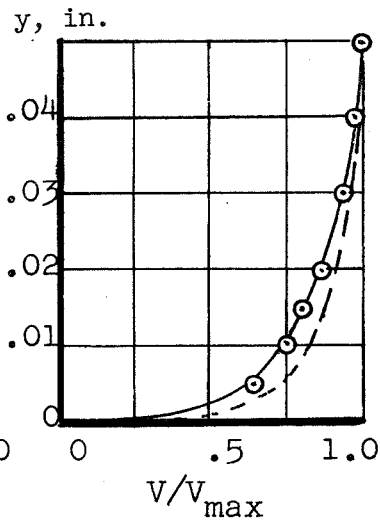


(b) Schematic diagram of boundary-layer probe.

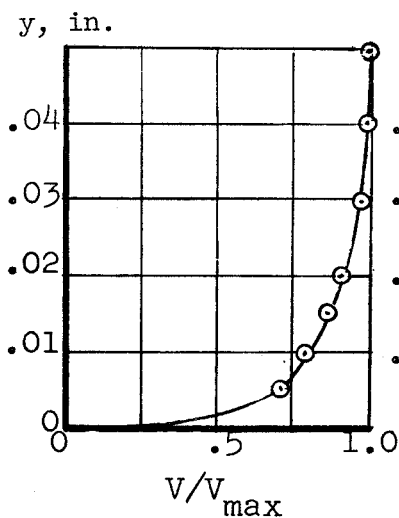
Figure 13.- Boundary-layer traverse.



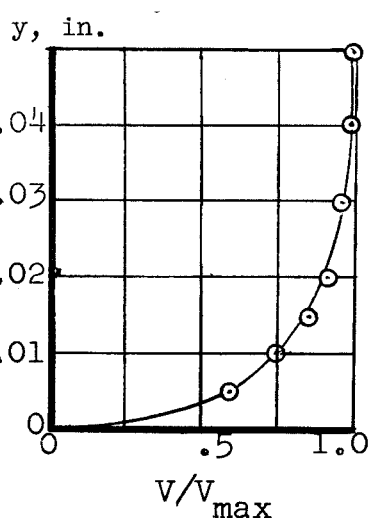
(a) Location W-5. With no trip;
 $2\theta = 7.0^\circ$; $\delta^* = 0.0064$ in.;
 $\delta^{**} = 0.0036$ in., and $H = 1.78$;
 with trip, $\delta^* = 0.0082$ in.,
 $\delta^{**} = 0.0053$ in., and $H = 1.55$.



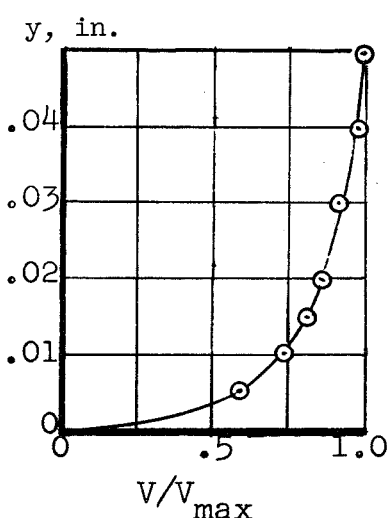
(b) Location E-2. With trip; $2\theta = 7.0^\circ$;
 $\delta^* = 0.0079$ in.; $\delta^{**} = 0.0051$ in.;
 $H = 1.55$. Dashed line indicates
 $1/7$ law.



(c) Location W-4. With trip; $2\theta = 7.0^\circ$;
 $\delta^* = 0.0058$ in.; $\delta^{**} = 0.0039$ in.;
 $H = 1.49$.

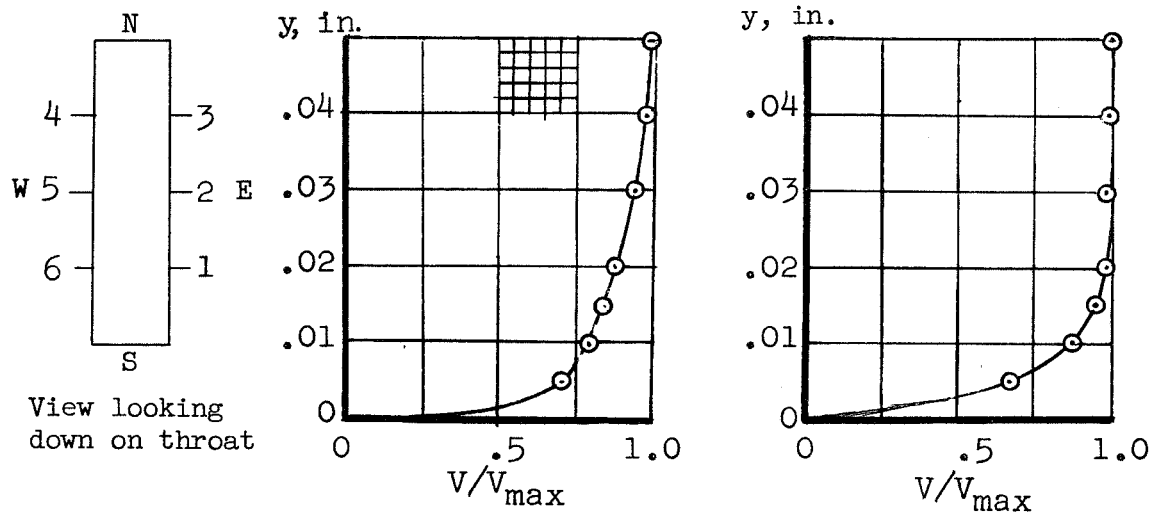


(d) Location E-3. With trip; $2\theta = 7.0^\circ$;
 $\delta^* = 0.0074$ in.; $\delta^{**} = 0.0043$ in.;
 $H = 1.72$.



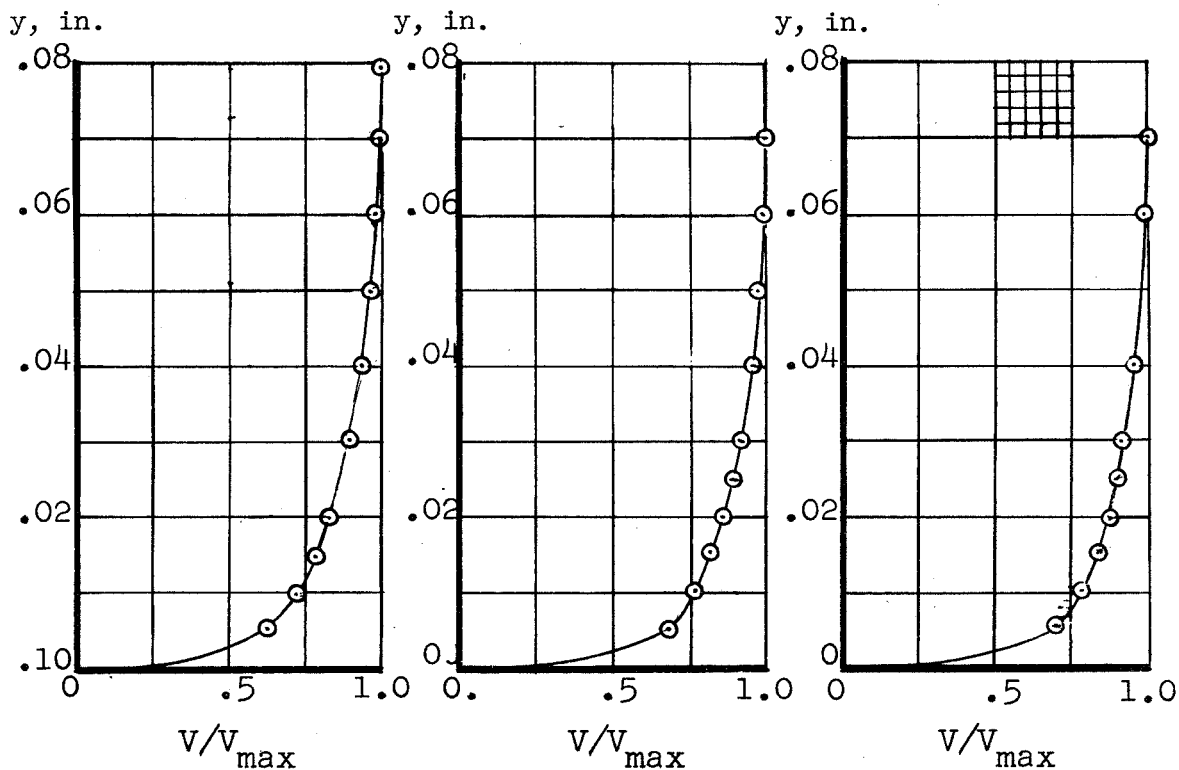
(e) Location W-6. With trip; $2\theta = 7.0^\circ$;
 $\delta^* = 0.0086$ in.; $\delta^{**} = 0.0054$ in.;
 $H = 1.59$.

Figure 14.- Inlet boundary-layer profiles. $W_1 = 3.00$ inches;
 $L/W_1 \approx 8.0$; $R_{W_1} \approx 2.4 \times 10^5$.



(f) Location E-1. With trip; $2\theta = 7.0^\circ$;
 $\delta^* = 0.0067$ in.; $\delta^{**} = 0.0047$ in.;
 $H = 1.43$.

(g) Location S. No trip; $2\theta = 7.0^\circ$;
 $\delta^* = 0.0046$ in.; $\delta^{**} = 0.0026$ in.;
 $H = 1.77$.



(h) Location W-4. With trip;
 $2\theta = 42.0^\circ$; $\delta^* = 0.0099$ in.;
 $\delta^{**} = 0.0069$ in.; $H = 1.44$.

(i) Location W-5. With trip;
 $2\theta = 42.0^\circ$; $\delta^* = 0.0083$ in.;
 $\delta^{**} = 0.0057$ in.; $H = 1.46$.

(j) Location W-6. With trip;
 $2\theta = 42.0^\circ$; $\delta^* = 0.0082$ in.;
 $\delta^{**} = 0.0055$ in.; $H = 1.49$.

Figure 14.- Concluded.

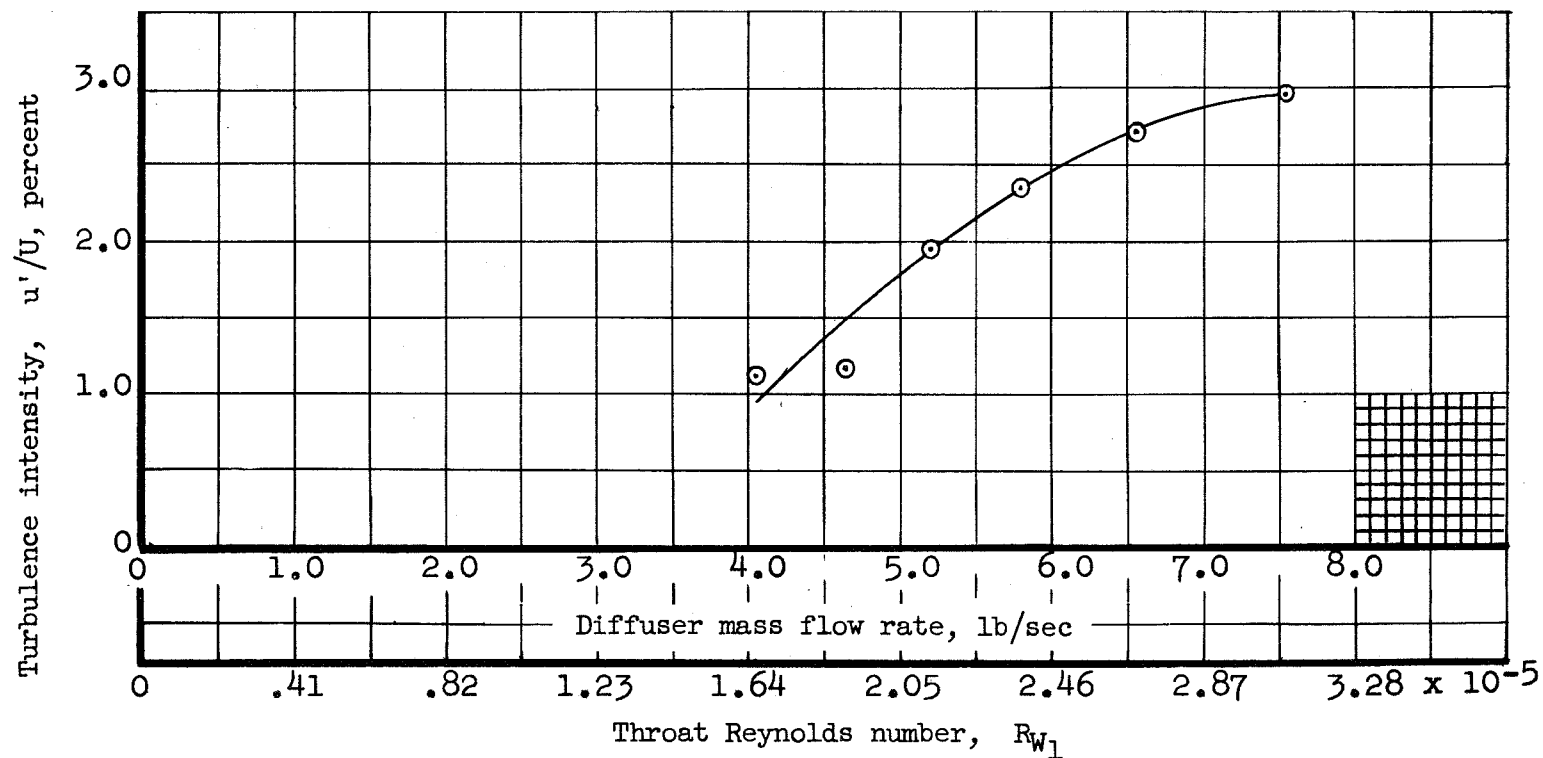


Figure 15.- Turbulence intensity plotted against flow rate. $2\theta = 7.0^\circ$; $W_1 = 3.00$ inches; $L/W_1 \approx 8.0$; intensity measured in center of throat; hot wire normal to both flow and parallel walls.

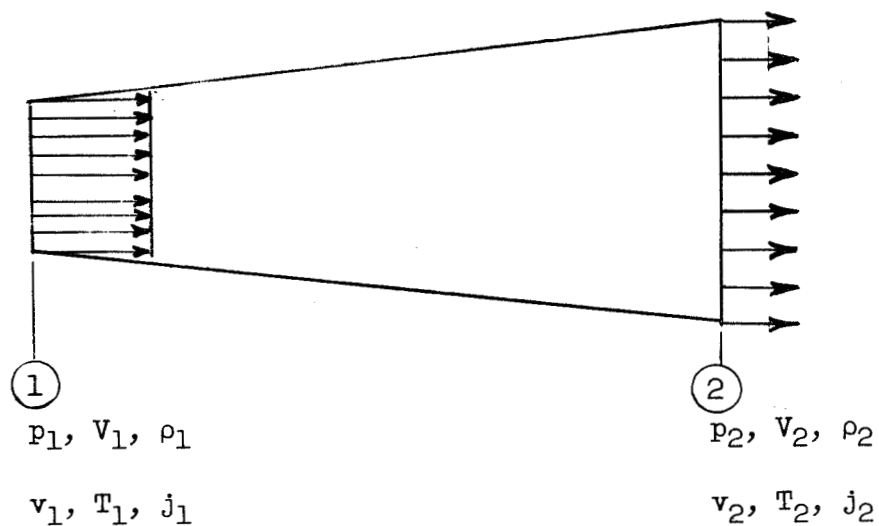
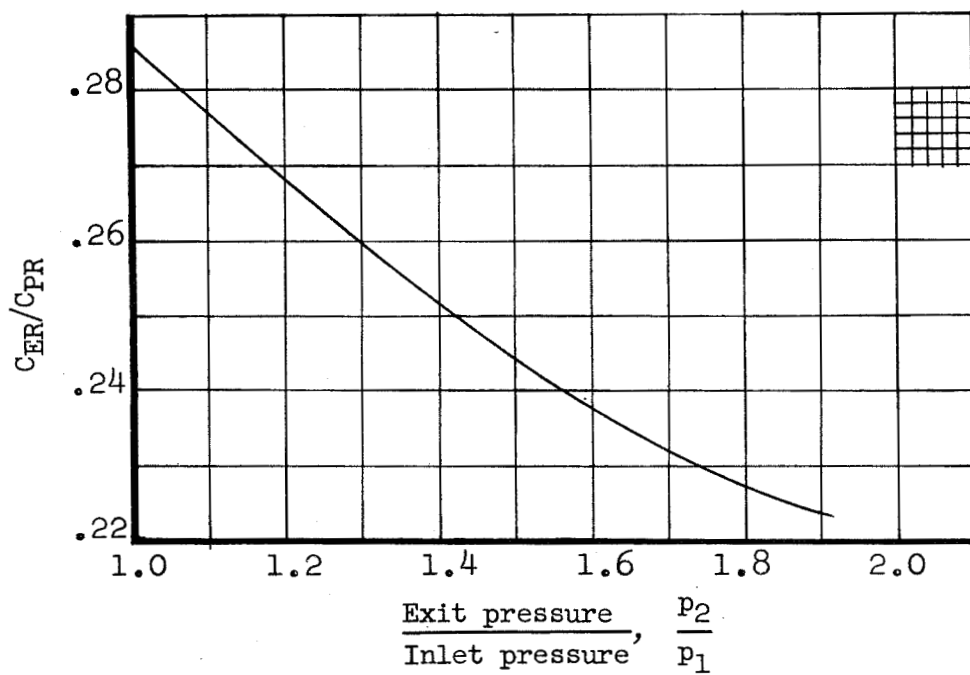


Figure 16.- Ideal one-dimensional flow.

Figure 17.- Ratio of C_{ER} to C_{PR} for one-dimensional adiabatic flow of air.

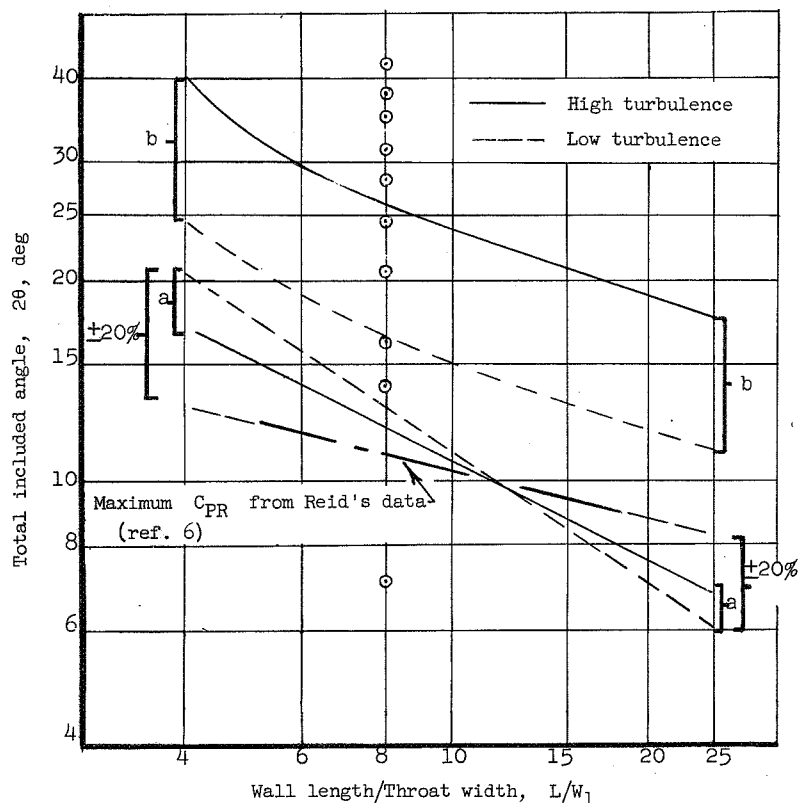


Figure 18.- Comparison of present diffuser performance and flow regime data of reference 4. aa indicates line of appreciable stall; bb indicates transition between two-dimensional and three-dimensional separation.

2θ , deg	Flow condition	Local stall condition
42.0	Very steady	Two-dimensional; fixed
38.2	Steady	
35.0	Quite steady; essentially two-dimensional	Mostly fixed
31.1	Fairly steady; nearly two-dimensional	Primarily fixed
28.0	Fairly steady; nearly two-dimensional	Primarily fixed; some transitory
24.5	Quite unsteady; approaching two-dimensional	Primarily transitory; some fixed
21.0	Firmly attached to one wall; separation zones on other wall	Transitory
16.8	Unsteady but not violent	
14.0	Quite steady	Small zones of transitory
7.0	Very smooth; minor end disturbances	No separation apparent

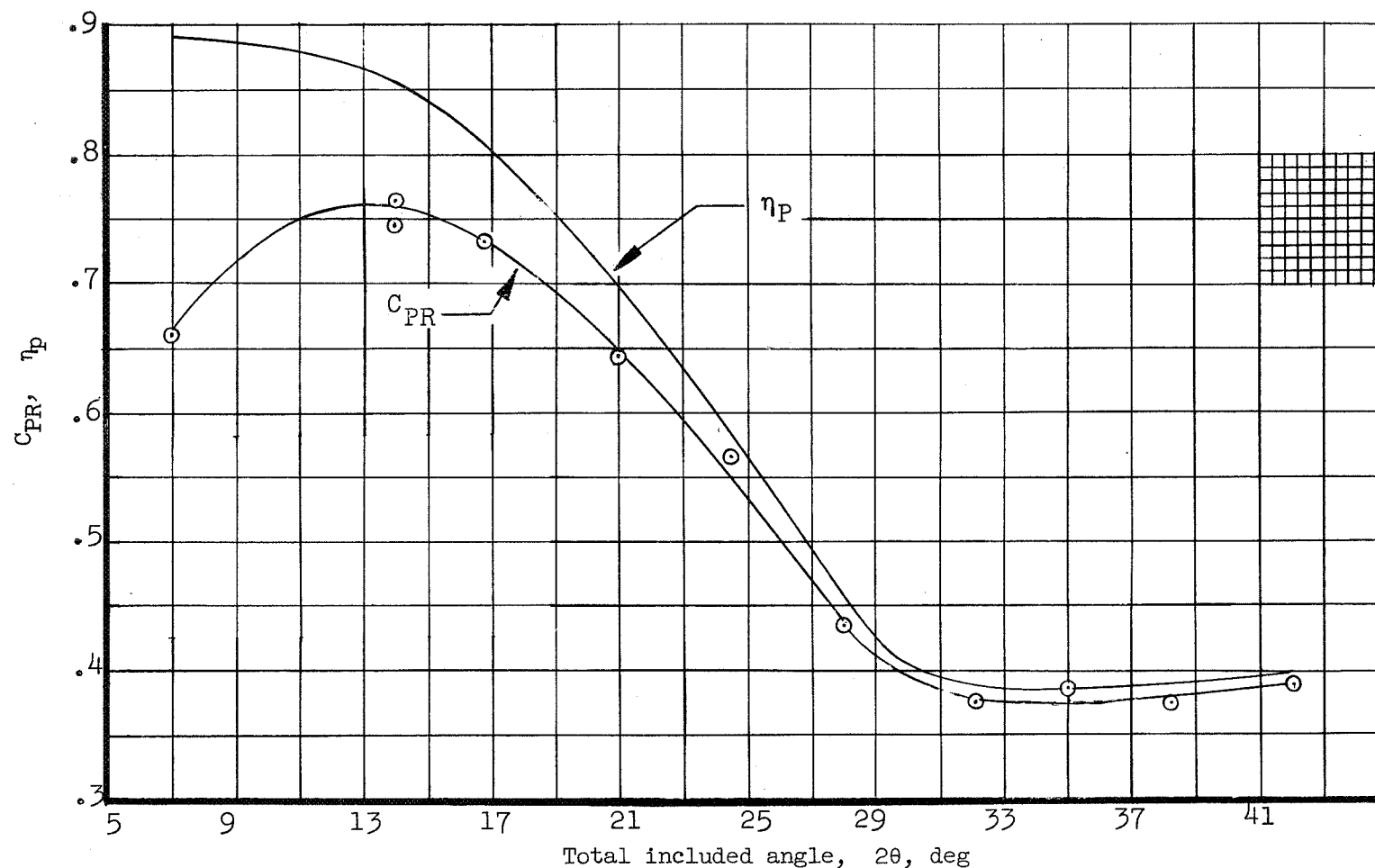


Figure 19.- Vaneless diffuser pressure recovery and effectiveness. See table given in figure 18 for description of flows at angles marked by data points. Constant inlet conditions. $L/W_1 \approx 8.0$; $W_1 = 3.00$ inches; $R_{W_1} \approx 2.4 \times 10^5$.

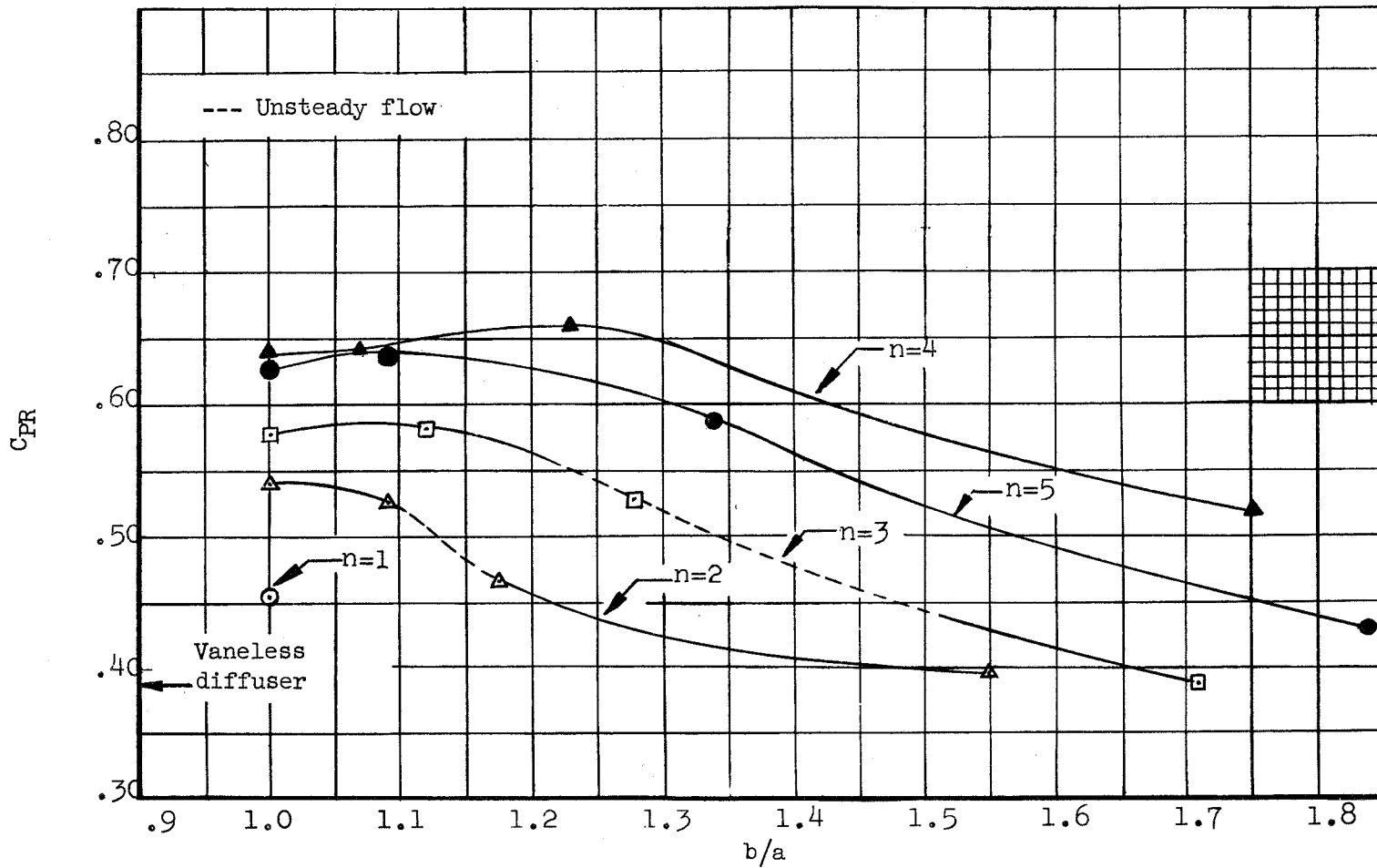
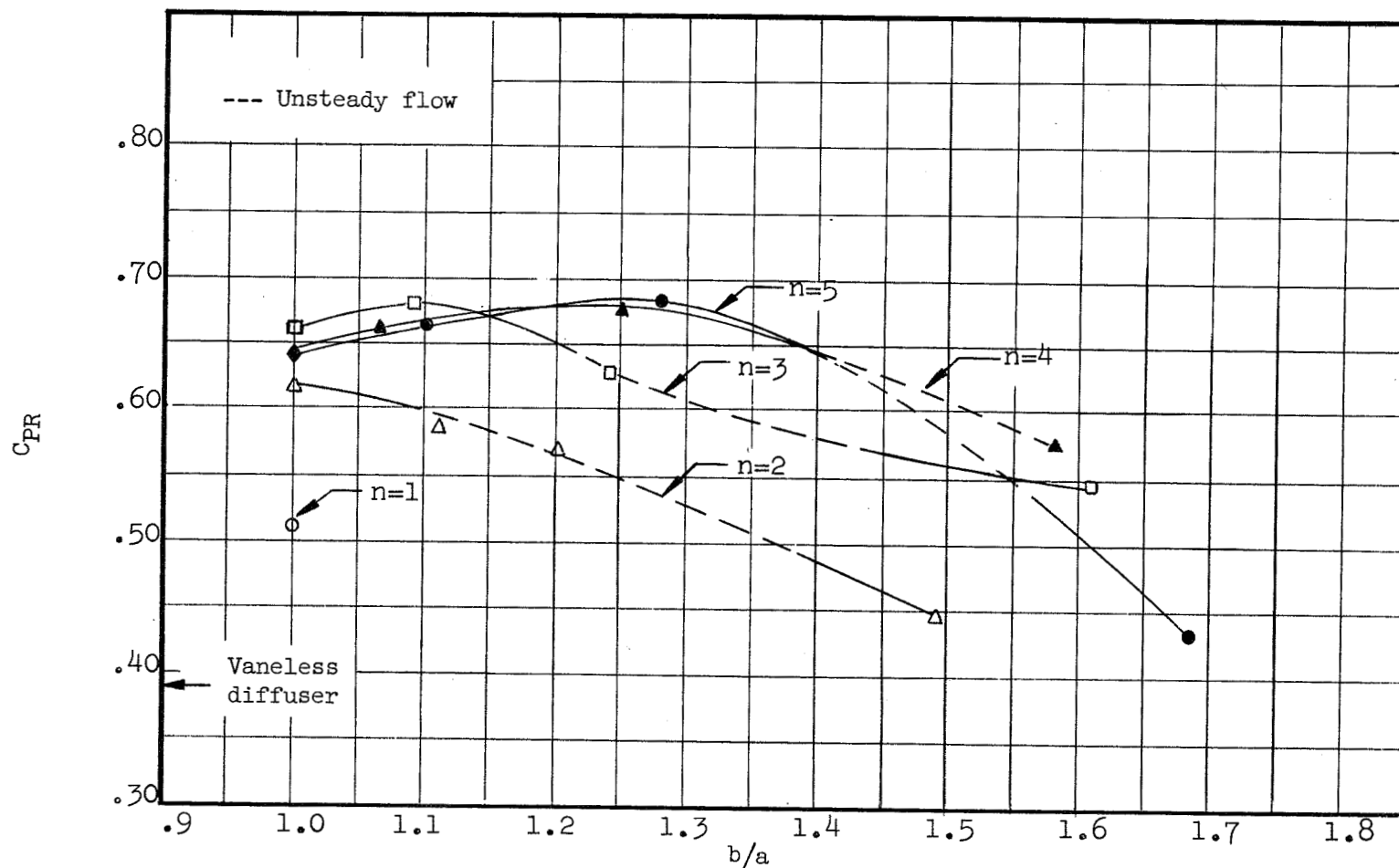
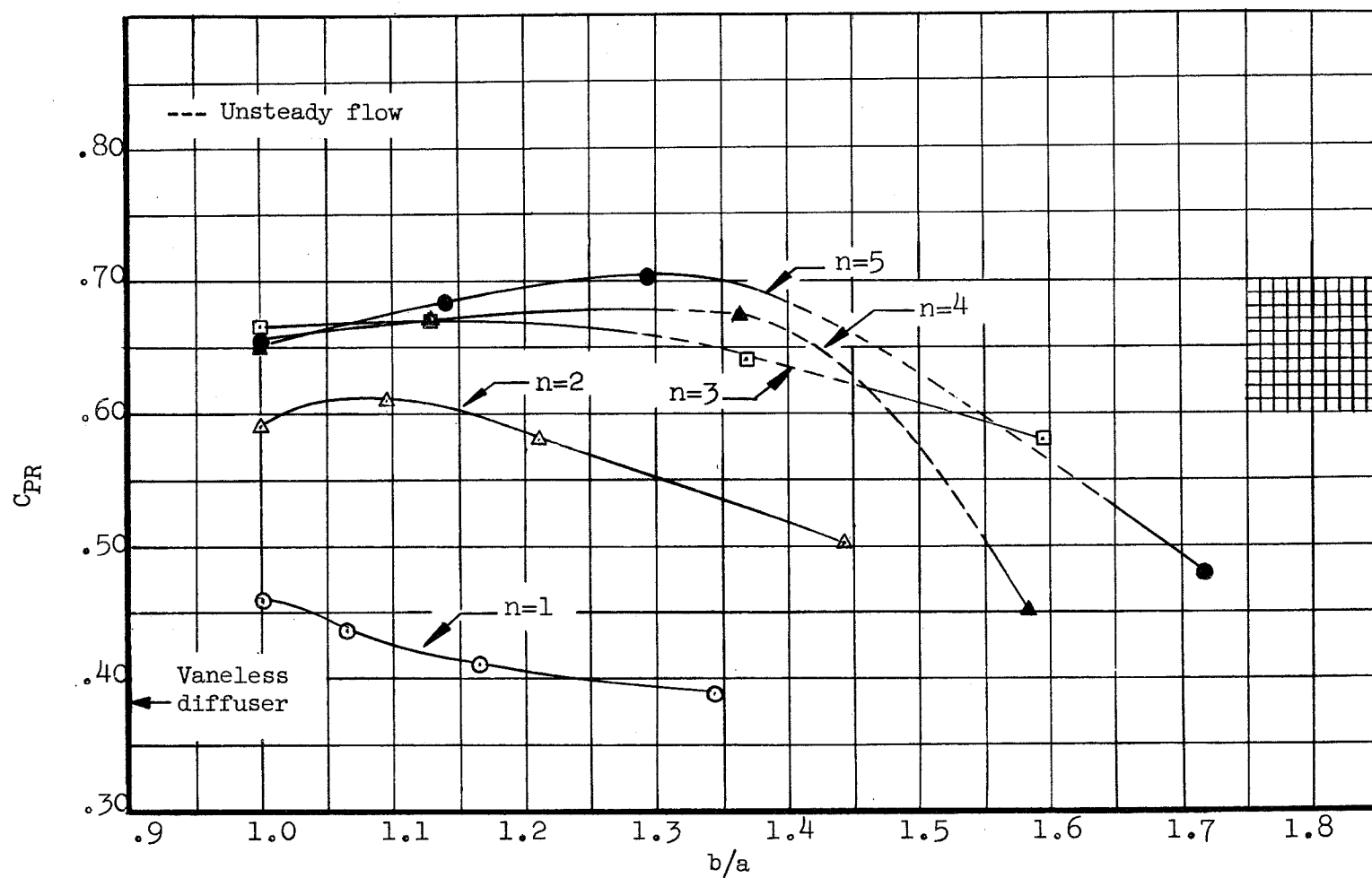
(a) $f = 3.00$ inches.

Figure 20.- Pressure recovery plotted against b/a ratio for vane. $2\theta = 42.0^\circ$;
 $W_1 = 3.00$ inches; $L/W_1 \approx 8.0$; $R_{W_1} \approx 2.4 \times 10^5$; $a = \frac{W_1}{n+1}$; $\alpha = \frac{2\theta}{n+1}$.



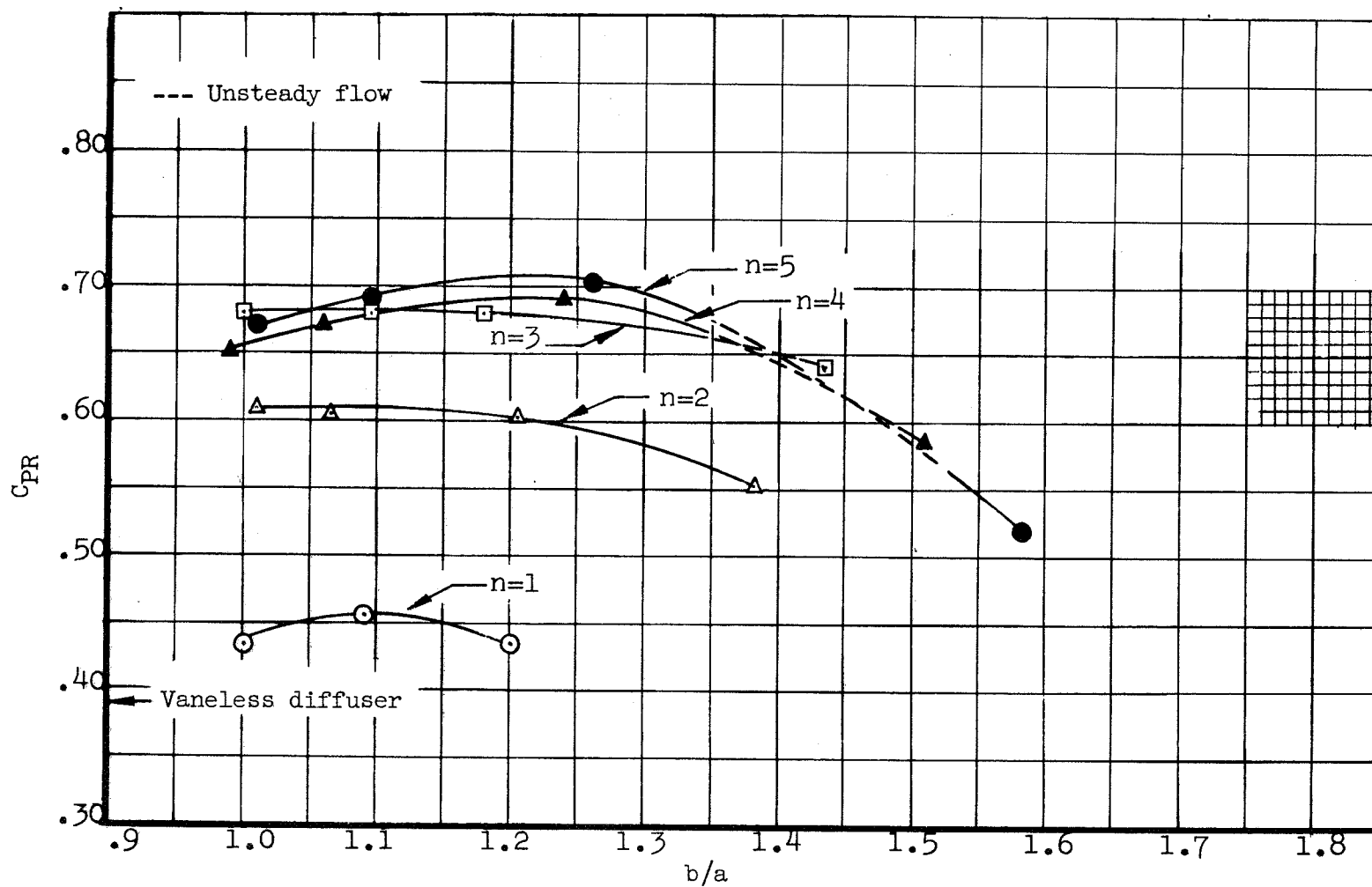
(b) $f = 6.00$ inches.

Figure 20.- Continued.



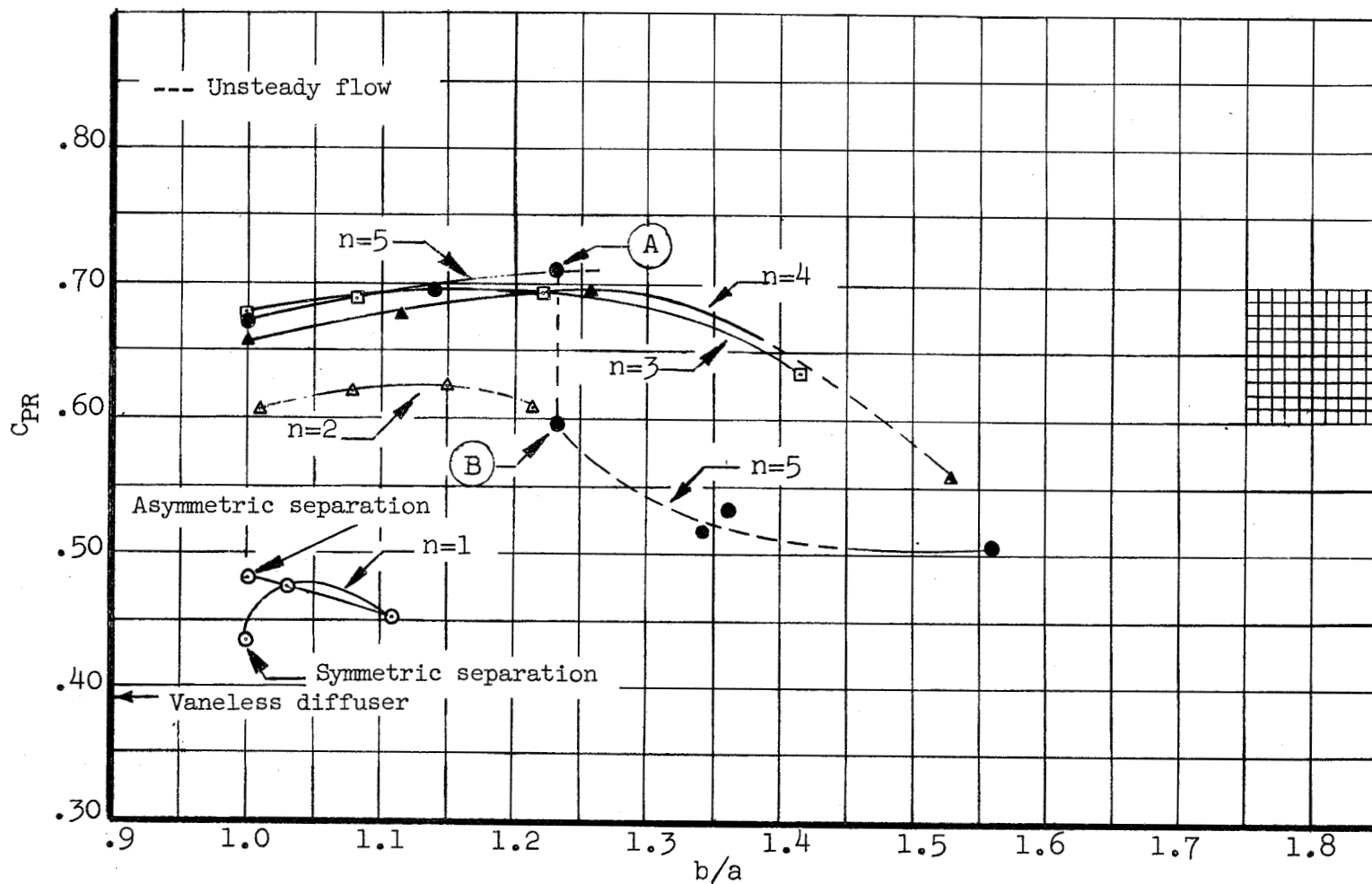
(c) $f = 9.00$ inches.

Figure 20.- Continued.



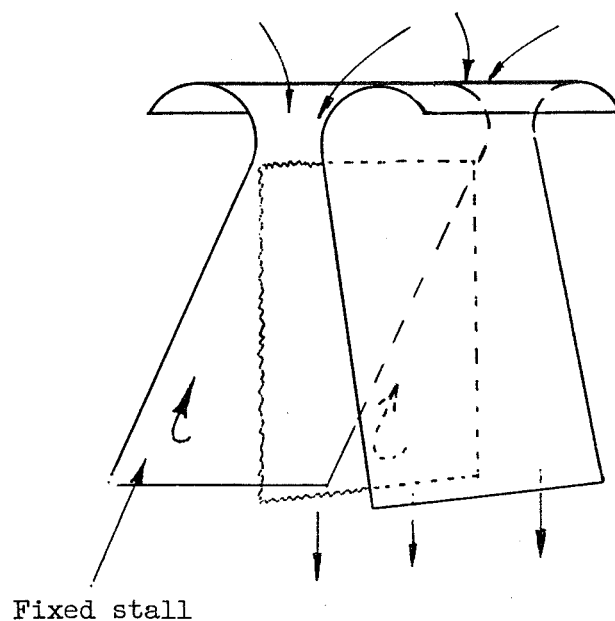
(d) $f = 12.0$ inches.

Figure 20.- Continued.

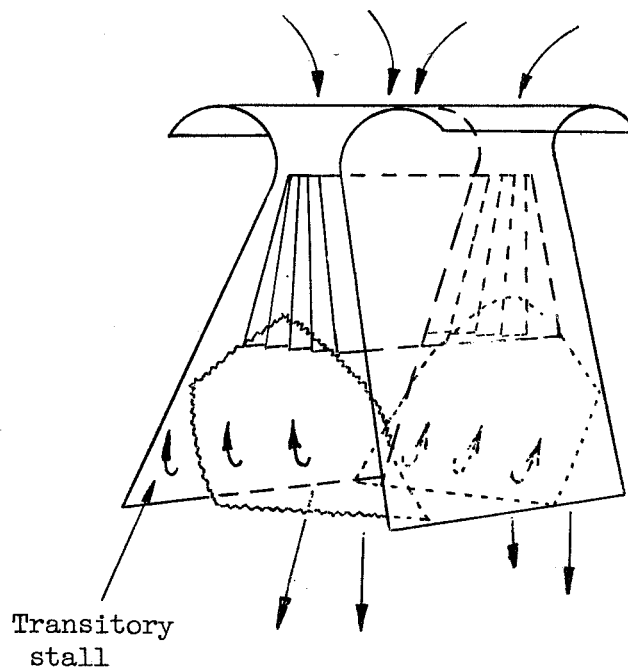


(e) $f = 15.0$ inches.

Figure 20.- Concluded.



(a) Unvaned diffuser: steady flow; two-dimensional fixed stall; poor recovery.



(b) A near-optimum vaned diffuser: steady flow; symmetric transitory stall with some fixed stall; good recovery.

Figure 21.- Comparison of separation patterns. $2\theta = 42.0^\circ$.

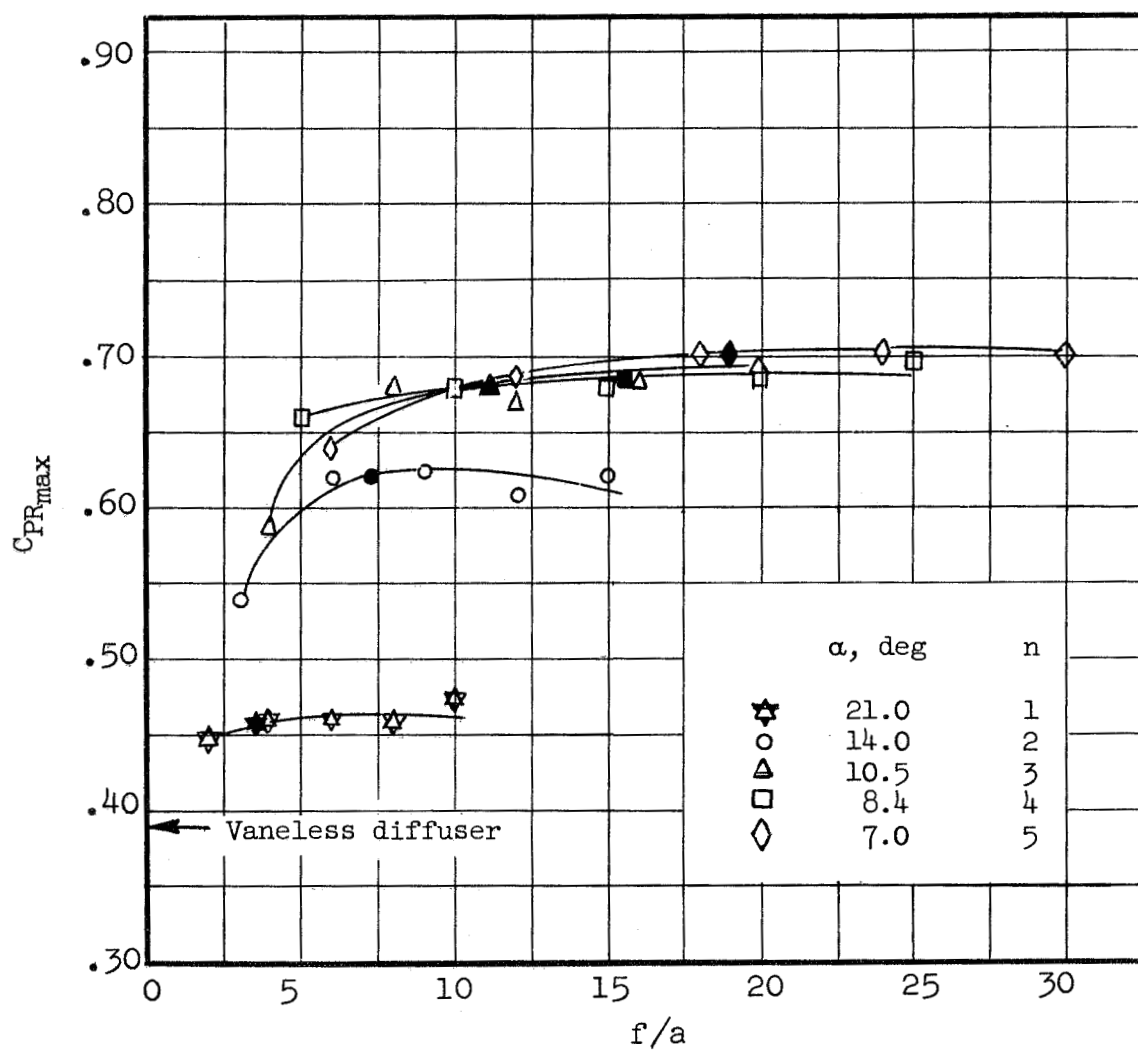


Figure 22.- Pressure recovery at optimum vane location. $2\theta = 42.0^\circ$;
 $W_1 = 3.00$ inches; $L/W_1 \approx 8.0$; $R_{W_1} \approx 2.4 \times 10^5$; $a = \frac{W_1}{n+1}$; $\alpha = \frac{2\theta}{n+1}$.
 Solid symbols indicate $(f/a)_{as}$ for high turbulence from figure 3.

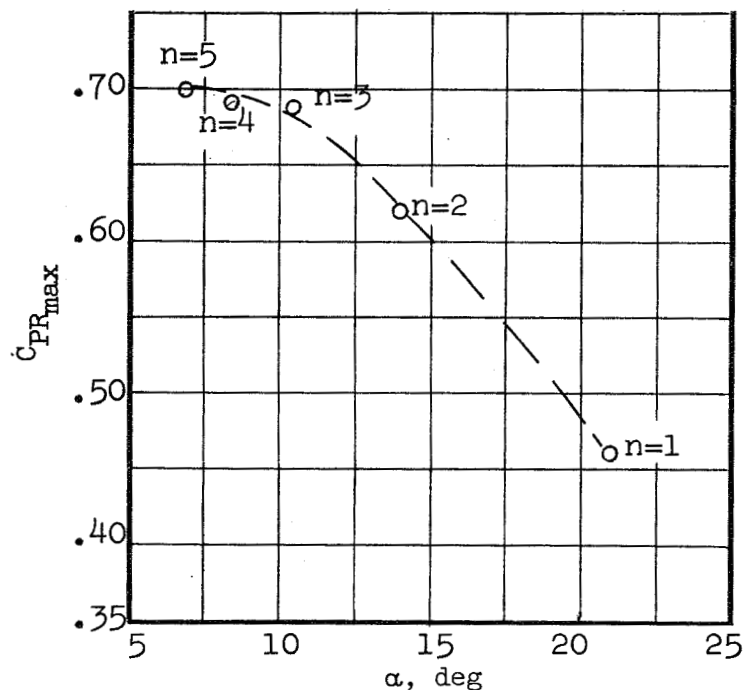


Figure 23.- Pressure-recovery coefficient plotted against vane angle. $2\theta = 42.0^\circ$; $W_1 = 3.00$ inches; $L/W_1 \approx 8.0$; $R_{W1} \approx 2.4 \times 10^5$; $a = \frac{W_1}{n+1}$; $\alpha = \frac{2\theta}{n+1}$; $f = 15.0$ inches; $1.05 < b/a < 1.7$; α is a discrete variable.

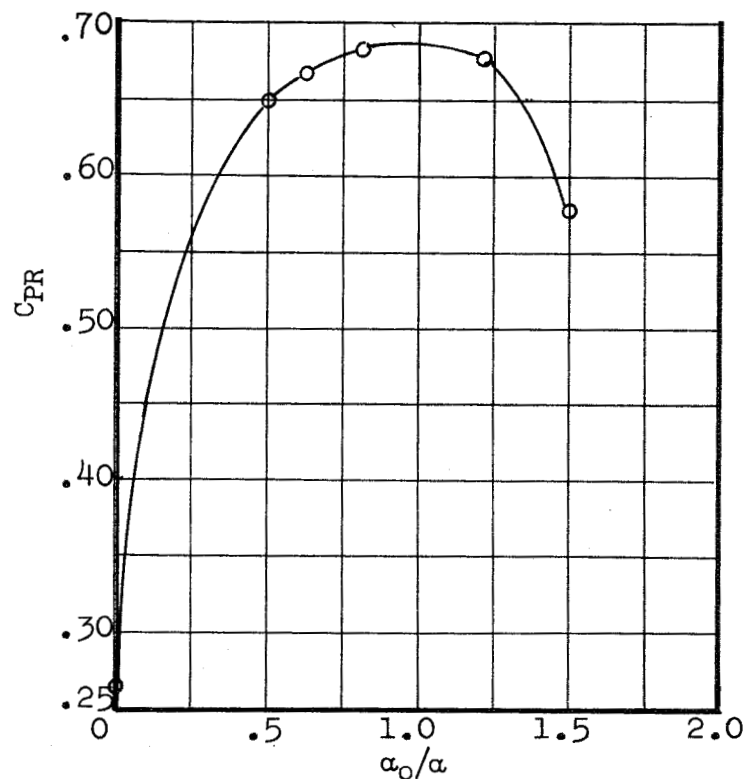


Figure 24.- Pressure-recovery coefficient plotted against relative vane angle. $2\theta = 42.0^\circ$; $W_1 = 3.00$ inches; $L/W_1 \approx 8.0$; $R_{W1} \approx 2.4 \times 10^5$; $f = 15.0$ inches; $n = 5$; $b/a = 1.01$; $a = \frac{W_1}{n+1} = 0.5$ inch.

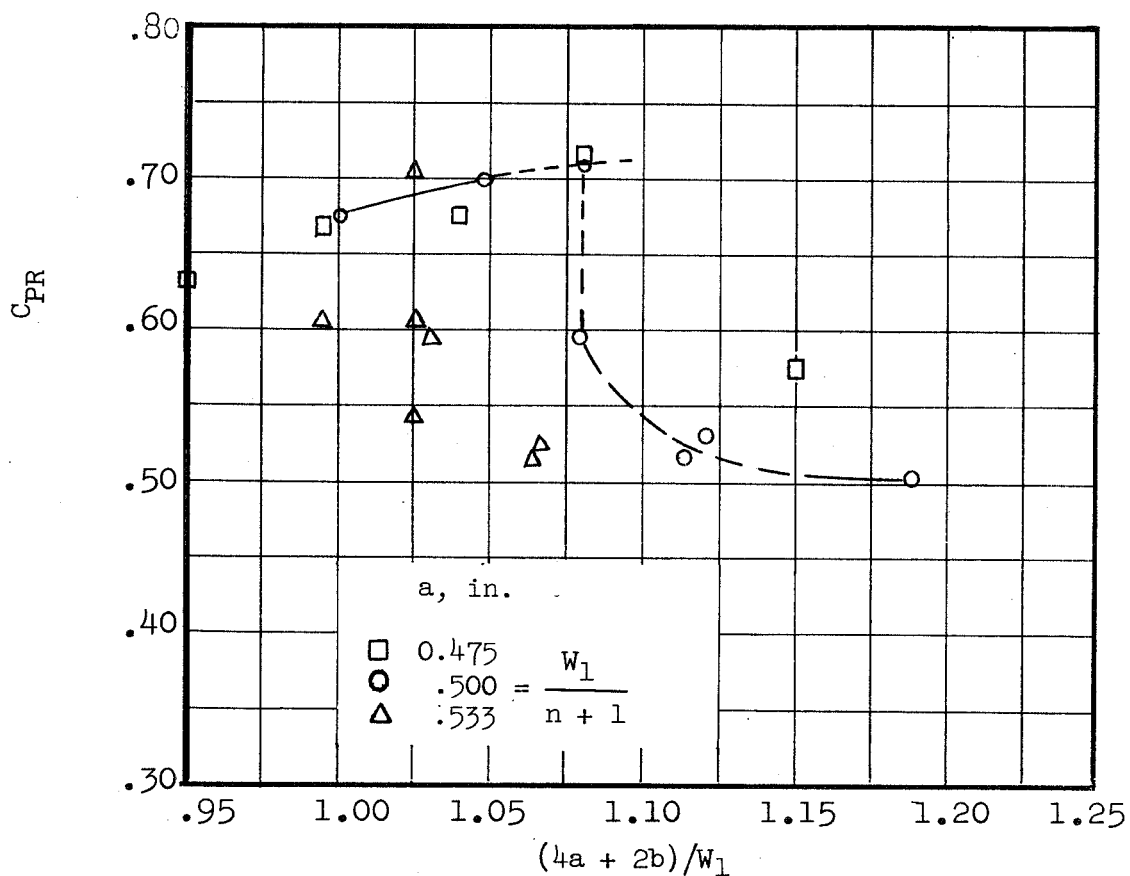
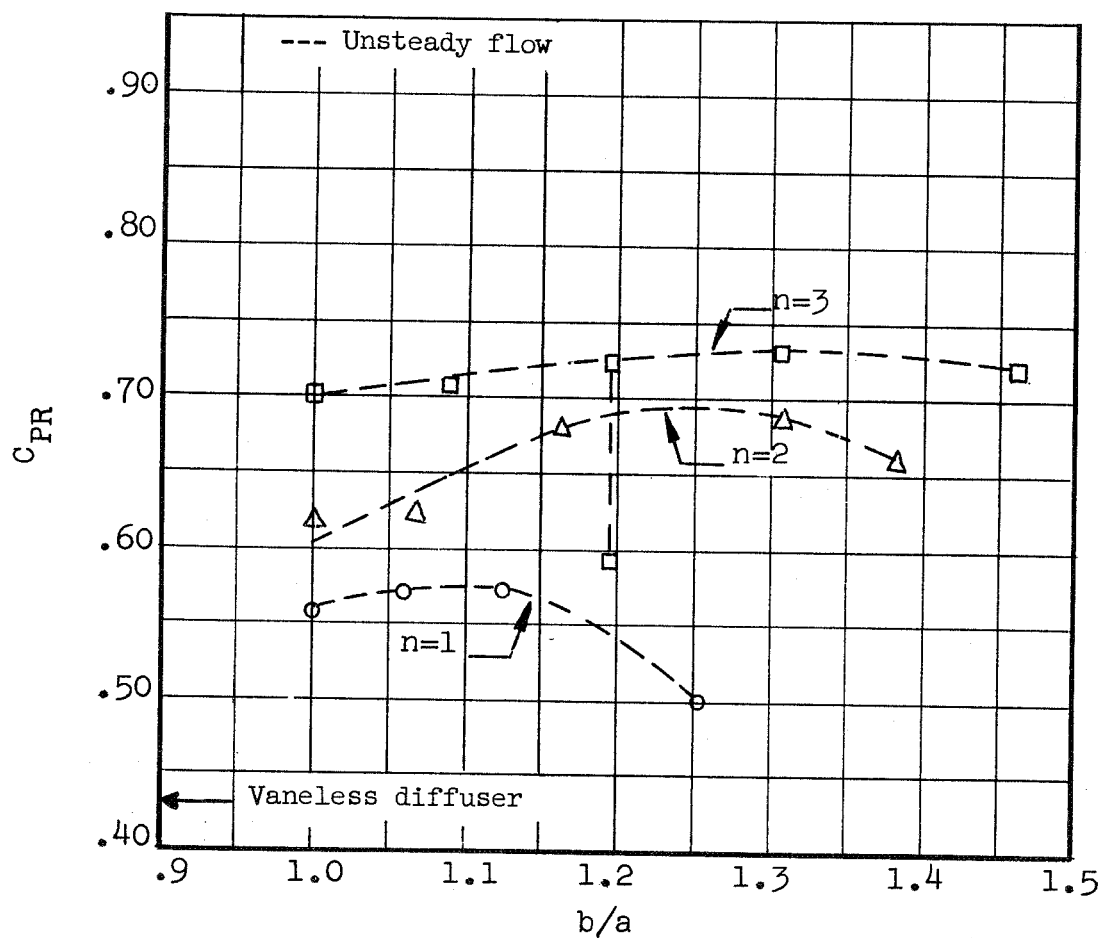


Figure 25.- Pressure-recovery coefficient plotted against ratio of vane inlet area to diffuser inlet area. $2\theta = 42.0^\circ$; $W_1 = 3.00$ inches; $L/W_1 \approx 8.0$; $f = 15.0$ inches; $n = 5$; $\alpha = 7.0^\circ$; $R_{W_1} \approx 2.4 \times 10^5$.

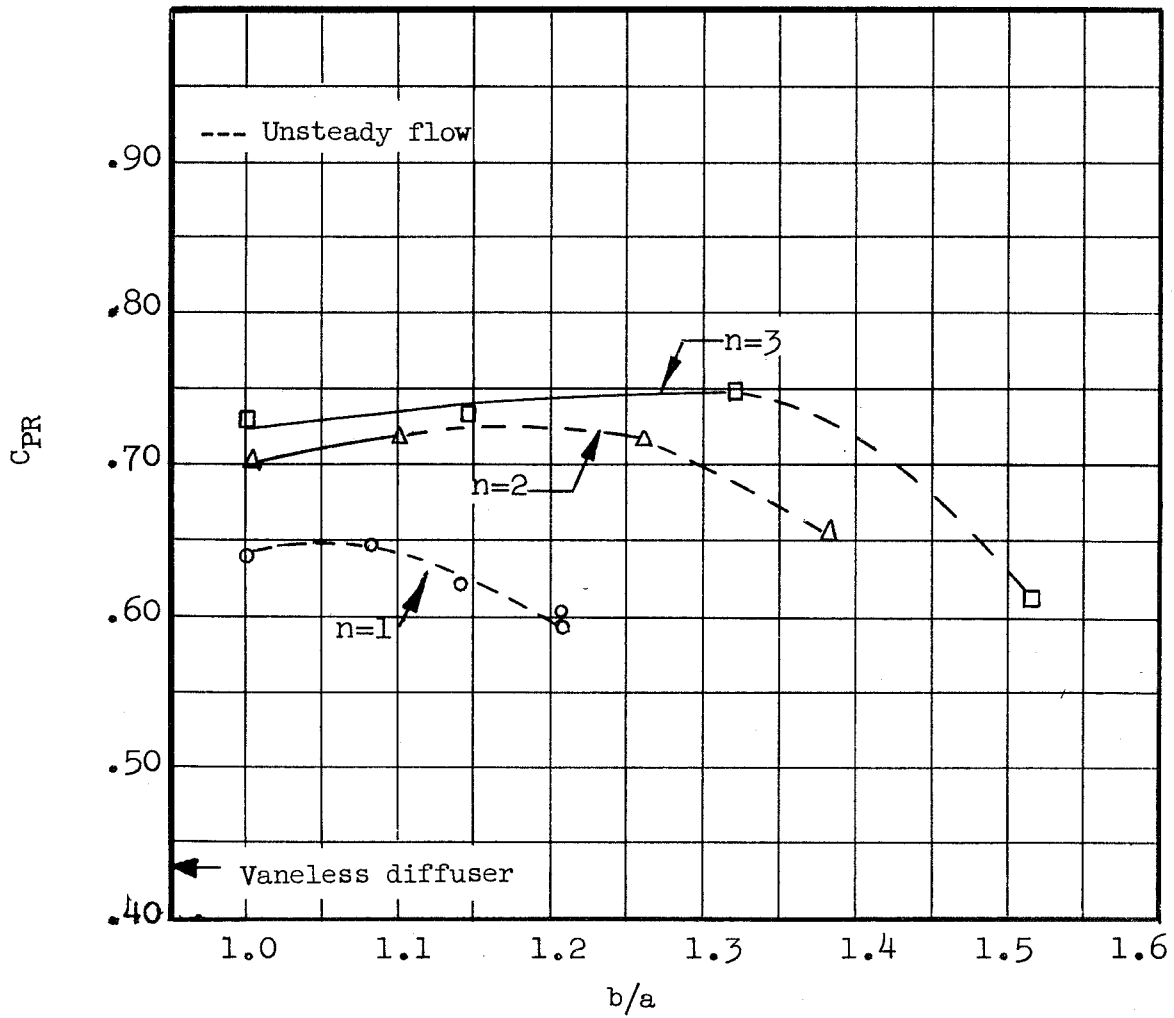


(a) $f = 3.00$ inches.

Figure 26.- Pressure-recovery plotted against b/a ratio for vane.

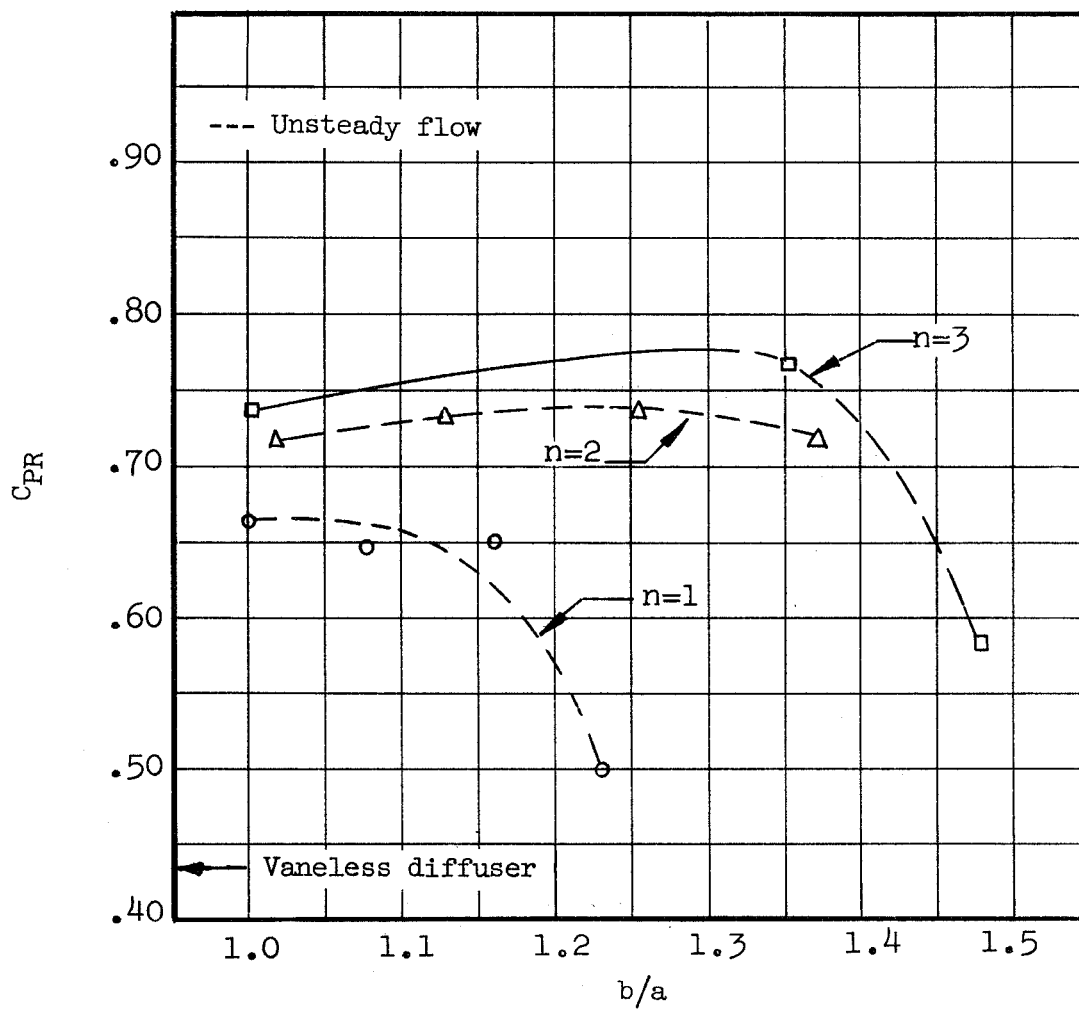
$2\theta = 28.0^\circ$; $W_1 = 3.00$ inches; $L/W_1 \approx 8.0$; $R_{W1} \approx 2.4 \times 10^5$;

$f = 3.00$ inches; $a = \frac{W_1}{n+1}$; $\alpha = \frac{2\theta}{n+1}$.



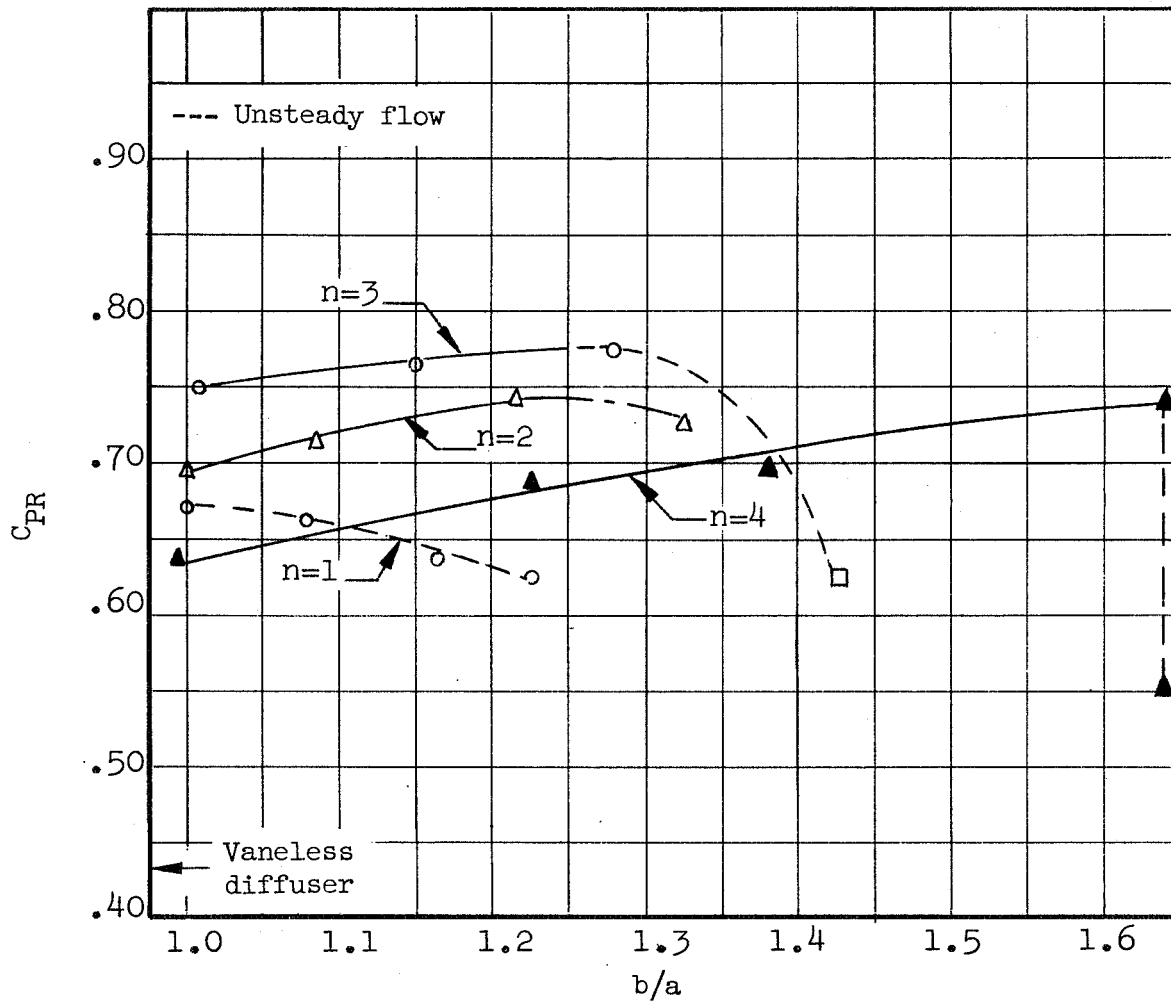
(b) $f = 6.0$ inches.

Figure 26.- Continued.



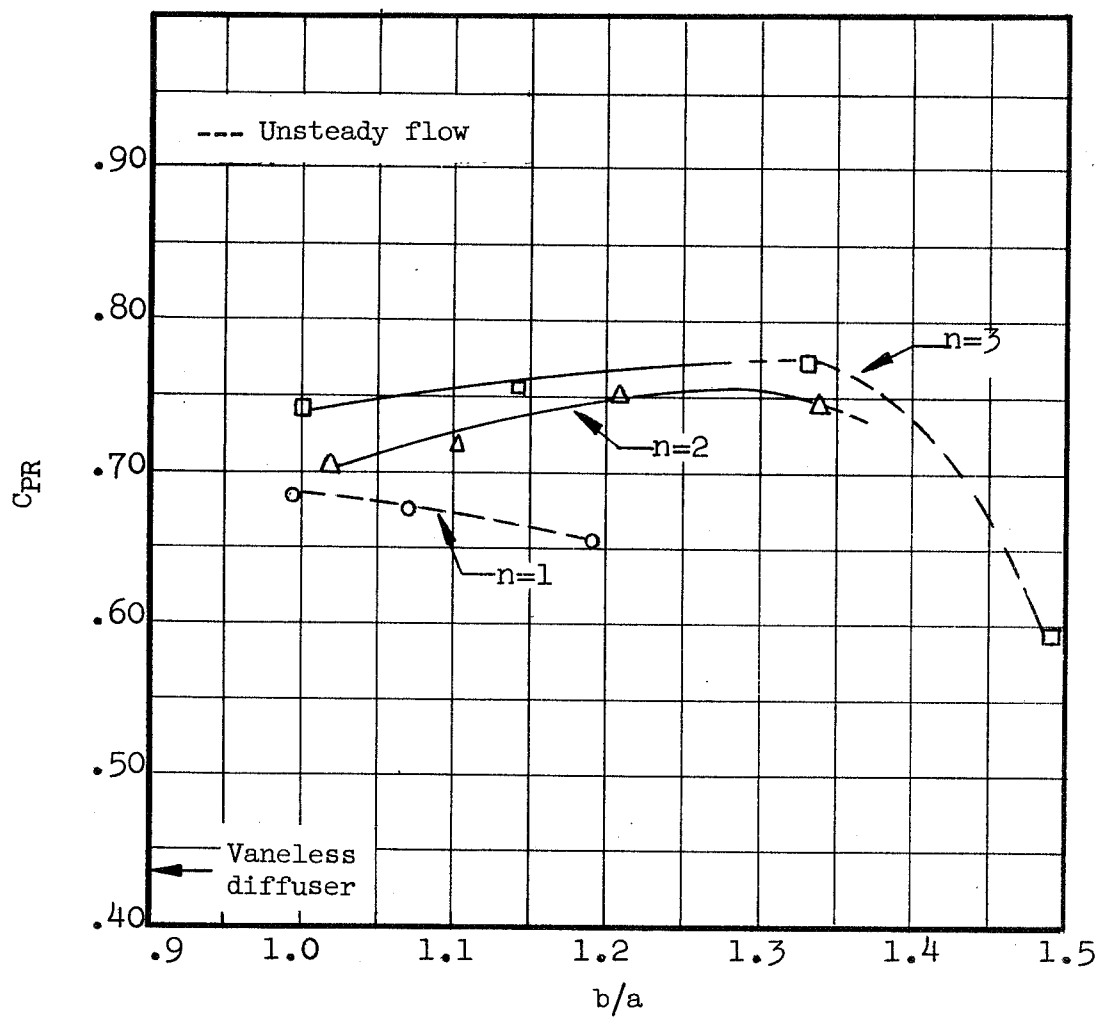
(c) $f = 9.0$ inches.

Figure 26.- Continued.



(d) $f = 12.0$ inches.

Figure 26.- Continued.



(e) $f = 15.0$ inches.

Figure 26.- Concluded.

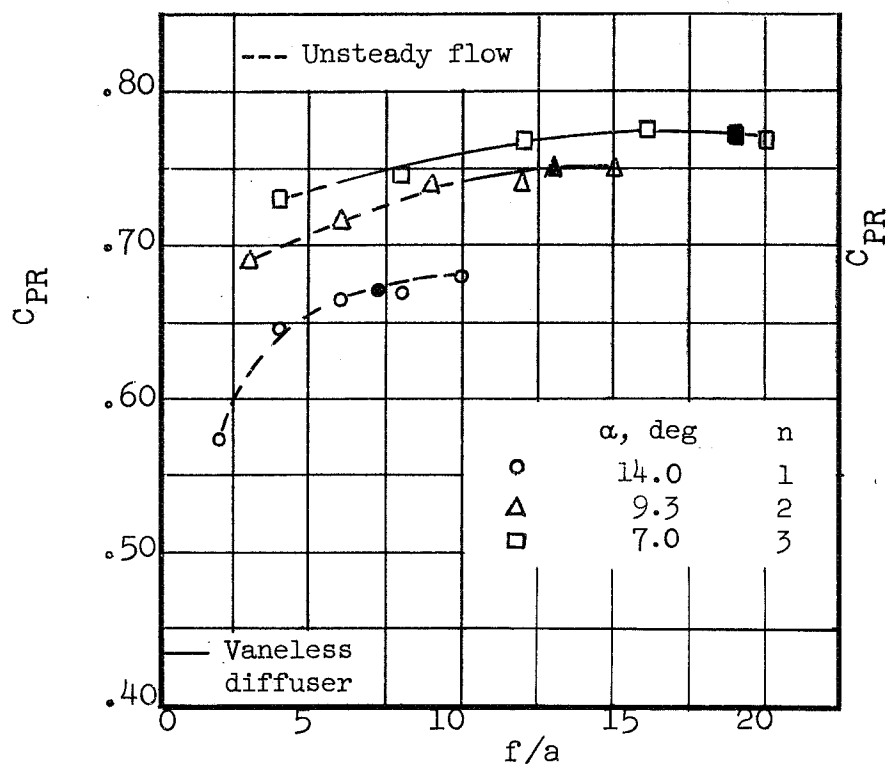


Figure 27.- Pressure-recovery coefficient at optimum vane location. $2\theta = 28.0^\circ$; $W_1 = 3.00$ inches; $L/W_1 \approx 8.0$;

$$R_{W1} \approx 2.4 \times 10^5; a = \frac{W_1}{n+1}; \alpha = \frac{2\theta}{n+1}.$$

Solid symbols indicate high turbulence $(f/a)_{as}$ from figure 4.

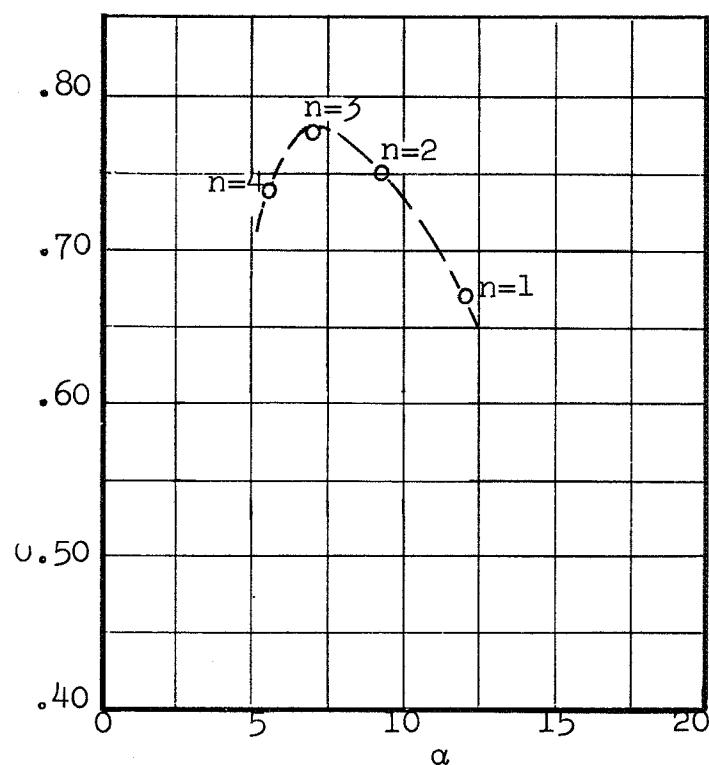


Figure 28.- Pressure-recovery coefficient plotted against vane angle. $2\theta = 28.0^\circ$; $W_1 = 3.00$ inches; $L/W_1 \approx 8.0$;

$$R_{W1} \approx 2.4 \times 10^5; a = \frac{W_1}{n+1}; \alpha = \frac{2\theta}{n+1};$$

$f = 12.0$ inches; $b/a \approx 1.2$; α is a discrete variable.

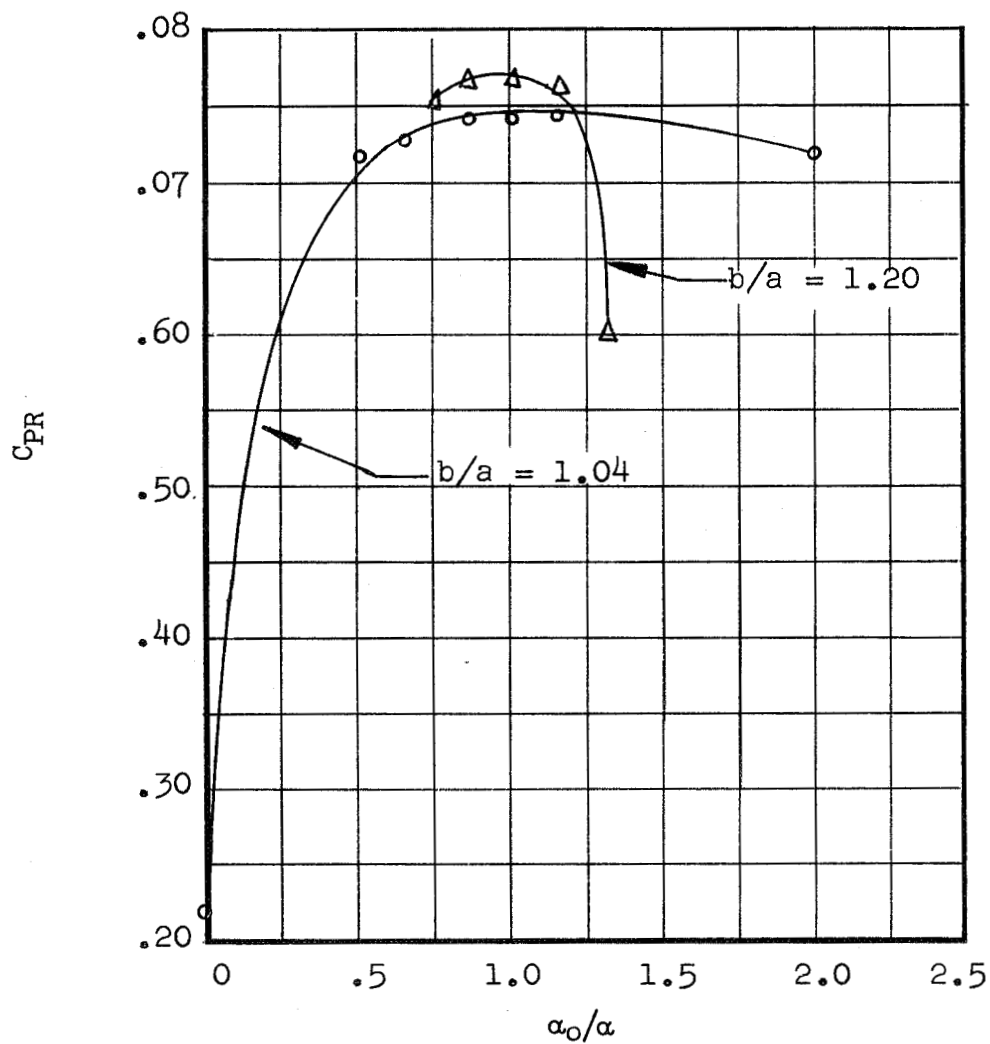


Figure 29.- Pressure-recovery coefficient plotted against relative vane angle. $2\theta = 28.0^\circ$; $W_1 = 3.00$ inches; $L/W_1 \approx 8.0$; $R_{W_1} \approx 2.4 \times 10^5$; $f = 12.0$ inches; $n = 3$; $a = \frac{W_1}{n + 1} = 0.75$ inch.

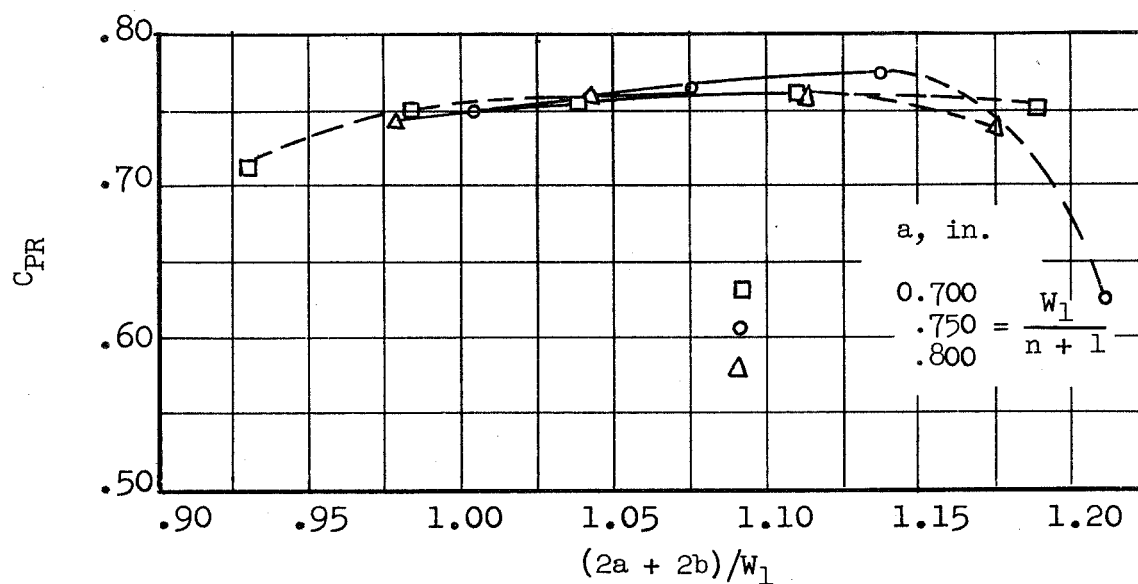


Figure 30.- Pressure-recovery coefficient plotted against ratio of vane inlet area to diffuser inlet area. $2\theta = 28.0^\circ$; $W_1 = 3.00$ inches; $L/W_1 \approx 8.0$; $R_{W_1} \approx 2.4 \times 10^5$; $f = 12.0$ inches; $n = 3$; $\alpha = 7.0^\circ$.

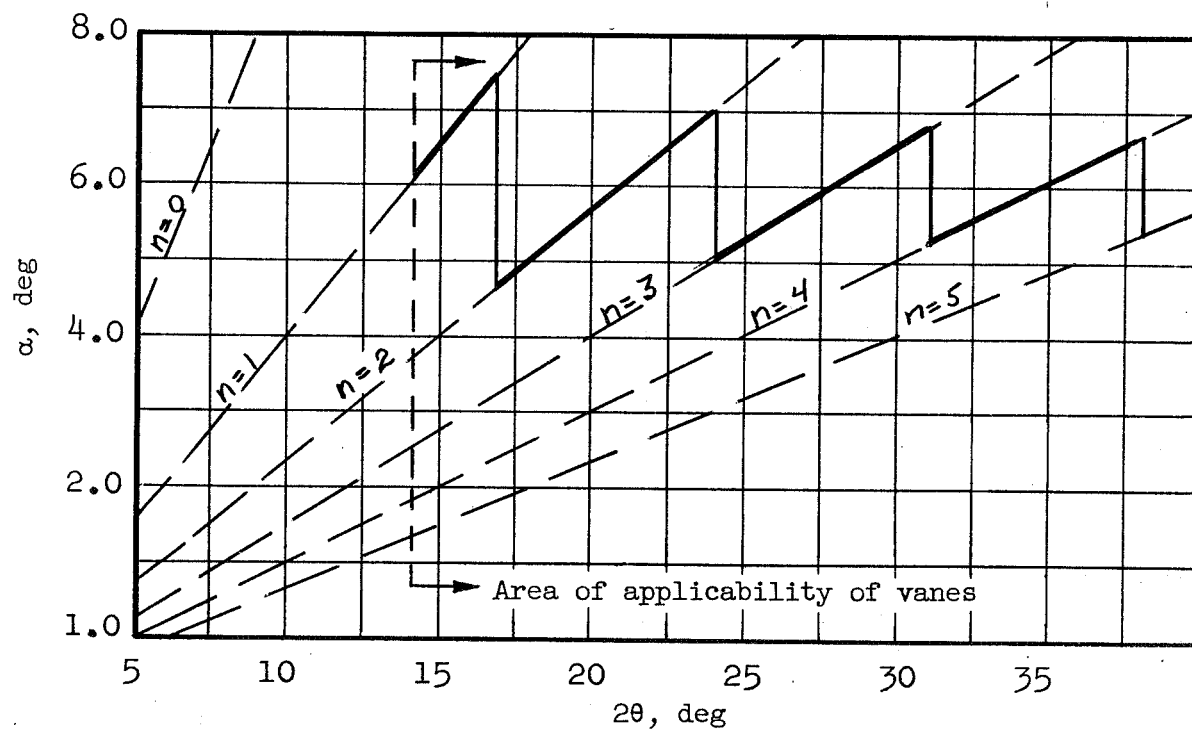


Figure 31.- Curve of vane angle nearest 7.0° . $\alpha = \frac{2\theta}{n + 1}$.

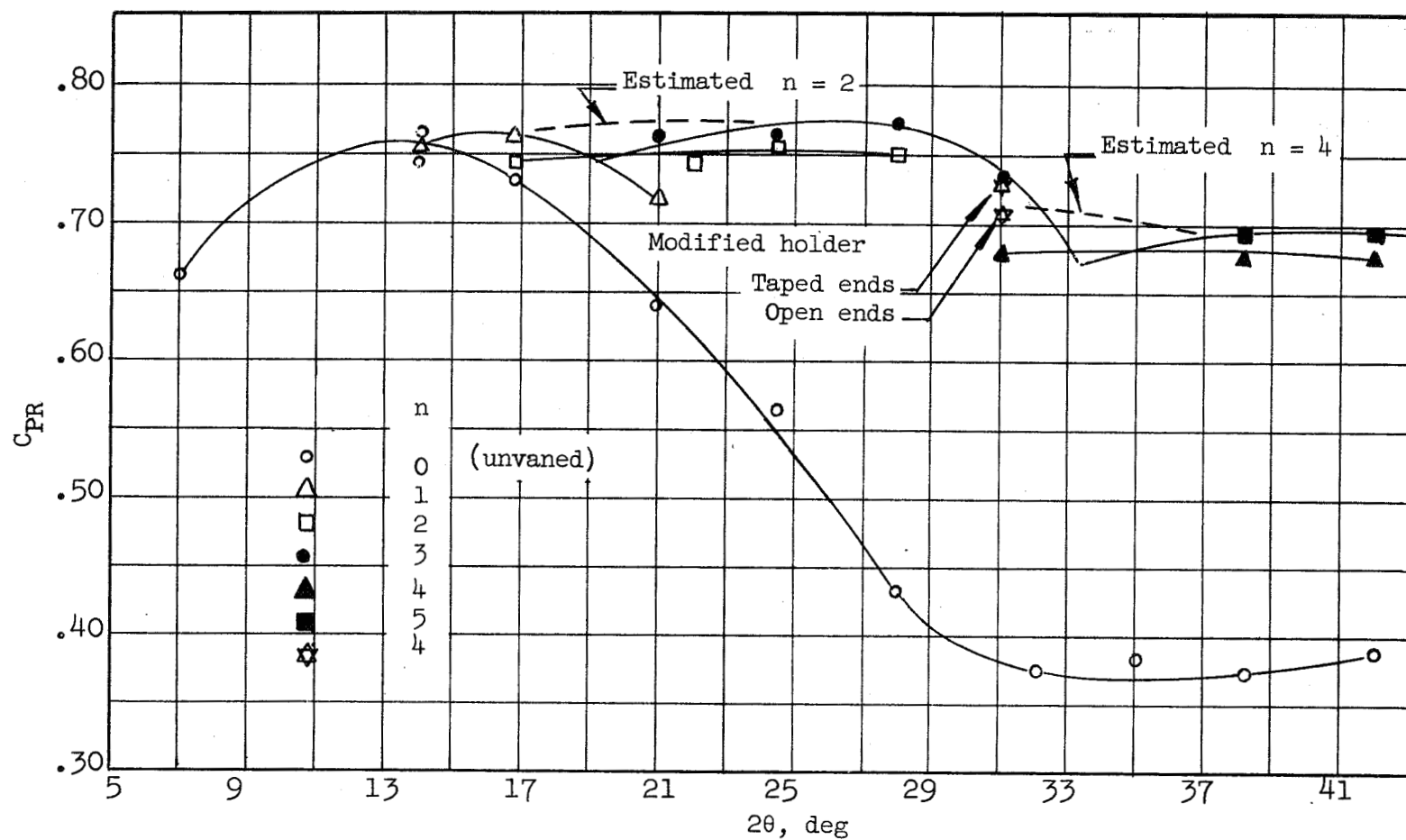


Figure 32.- Pressure-recovery coefficient plotted against diffuser total included angle.

$$W_1 = 3.00 \text{ inches}; L/W_1 \approx 8.0; R_{W_1} \approx 2.4 \times 10^5; a = \frac{W_1}{n+1}; \alpha = \frac{2\theta}{n+1}; b/a \approx 1.2.$$

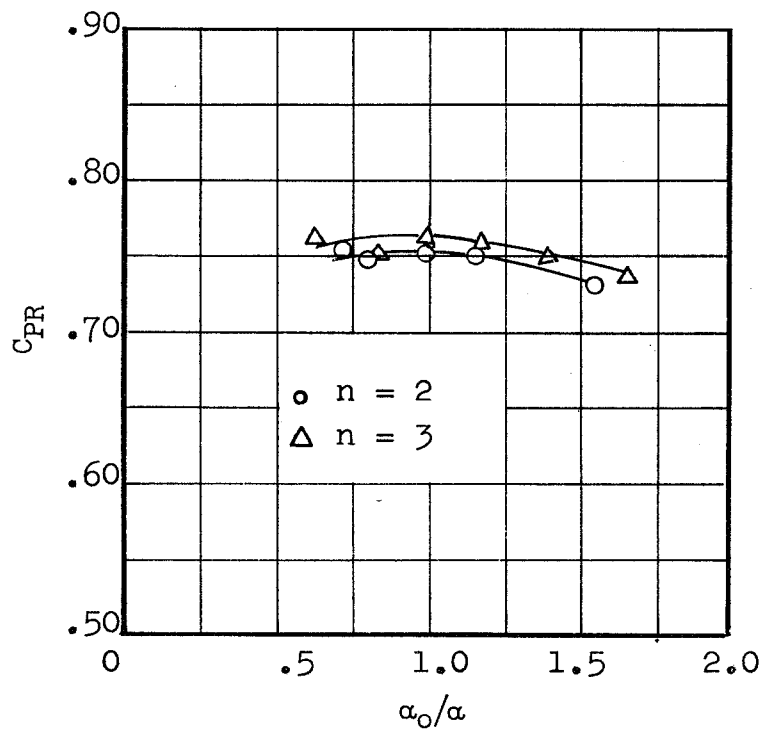


Figure 33.- Pressure-recovery coefficient plotted against relative vane angle. $2\theta = 24.5^\circ$; $W_1 = 3.00$ inches; $L/W_1 \approx 8.0$; $R_{W_1} \approx 2.4 \times 10^5$; $f = 15.0$ inches; $b/a = 1.2$; $a = \frac{W_1}{n+1}$.

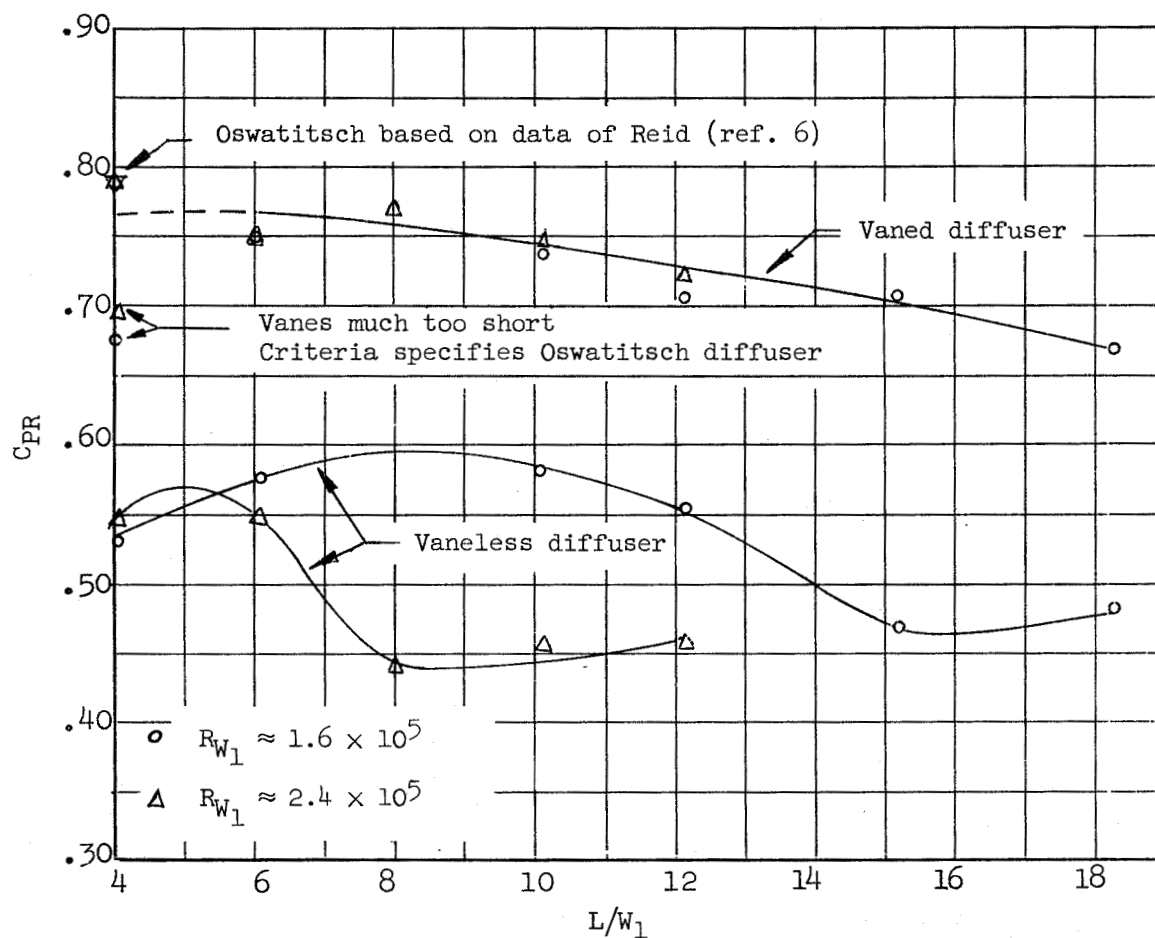
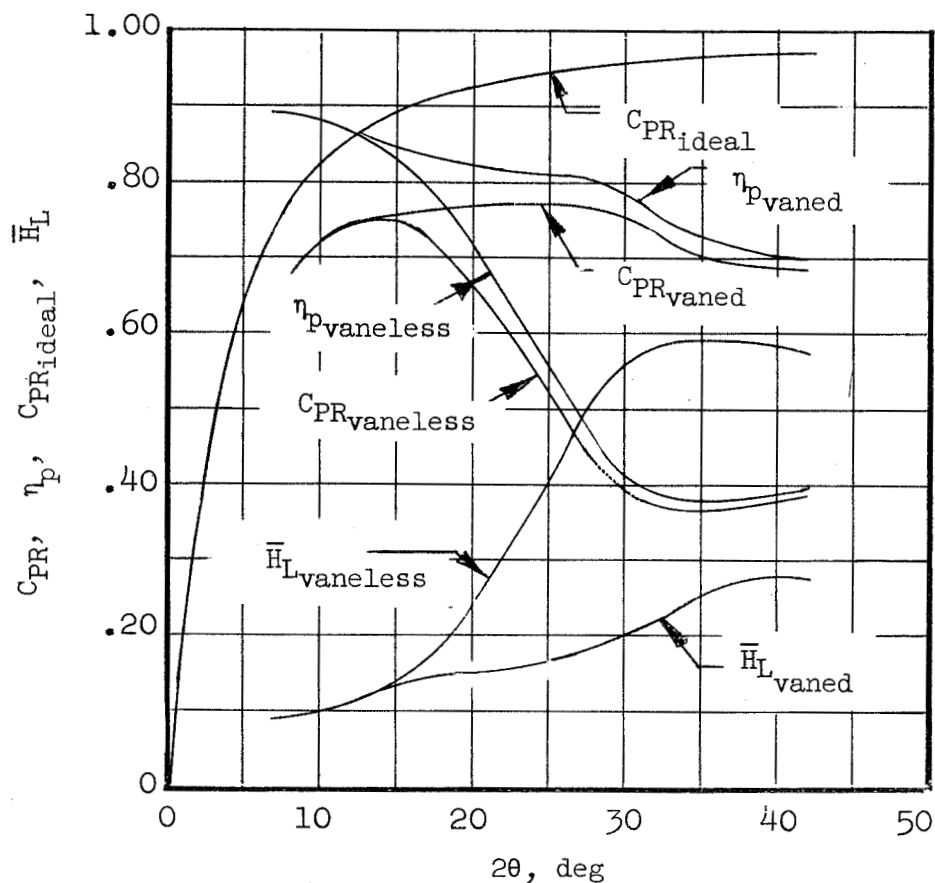
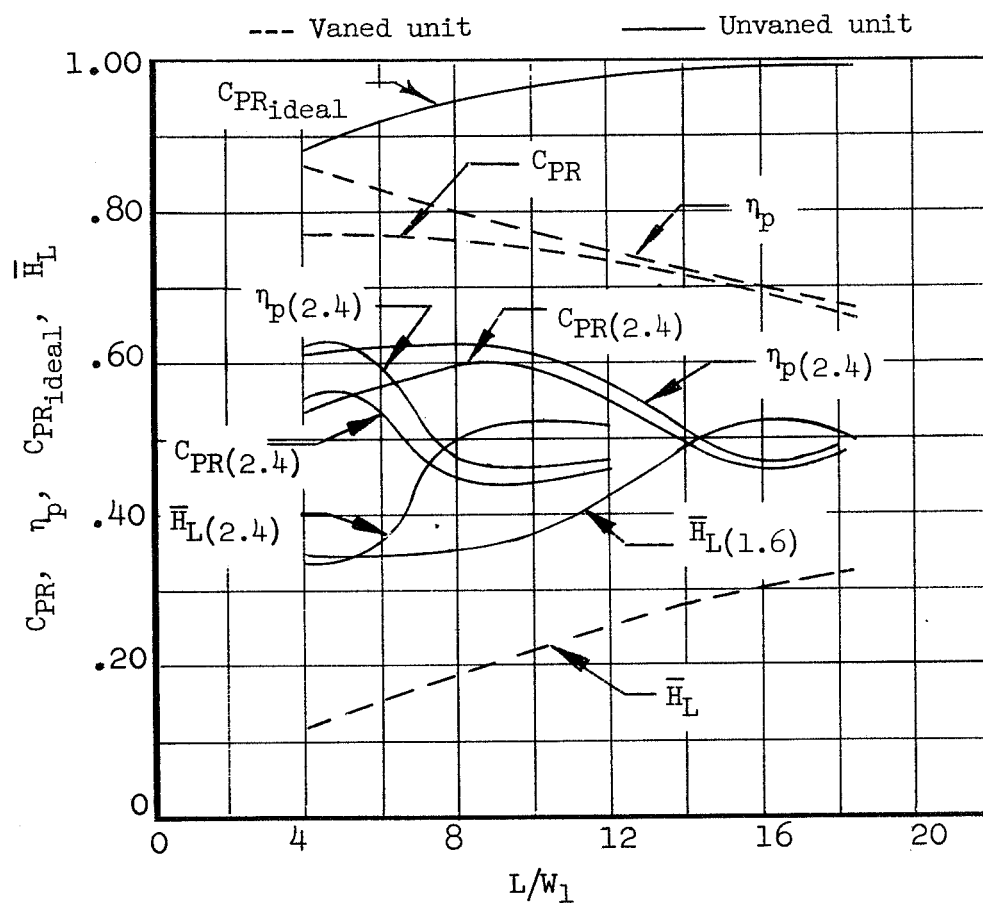


Figure 34.- Pressure recovery coefficient plotted against diffuser length ratio. $2\theta = 28.0^\circ$; $L \approx 24.0$ inches; vanes selected by design criteria.



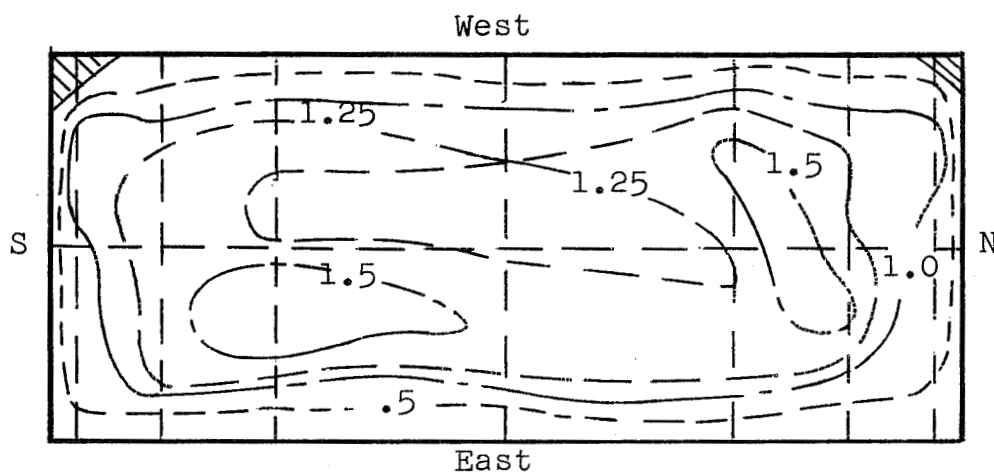
(a) Constant inlet conditions. $W_1 = 3.00$ inches; $L/W_1 \approx 8.0$;
 $R_{W1} \approx 2.4 \times 10^5$.

Figure 35.- Diffuser performance curves for vaned and unvaned units.
 Vanes selected by design criteria.

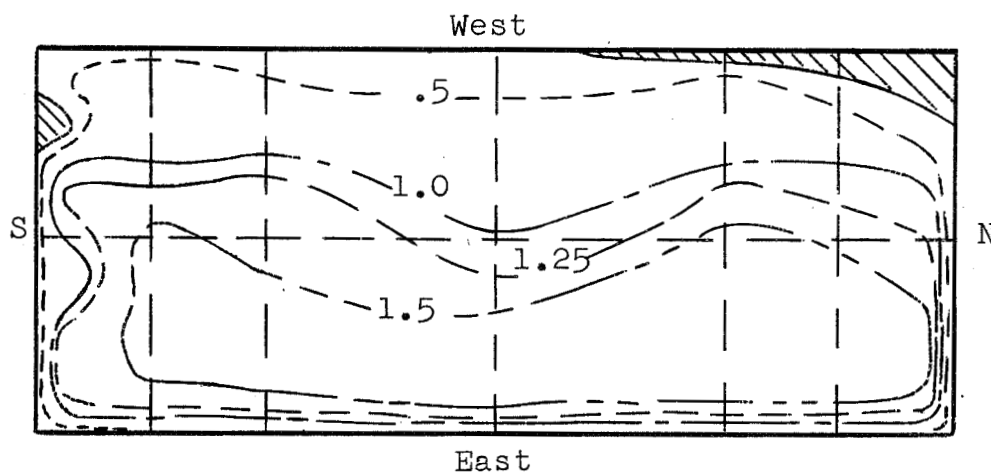


(b) Two inlet conditions. $2\theta = 28.0^\circ$; $L \approx 24$ inches; $() = R_{W1} \times 10^{-5}$.

Figure 35.- Concluded.

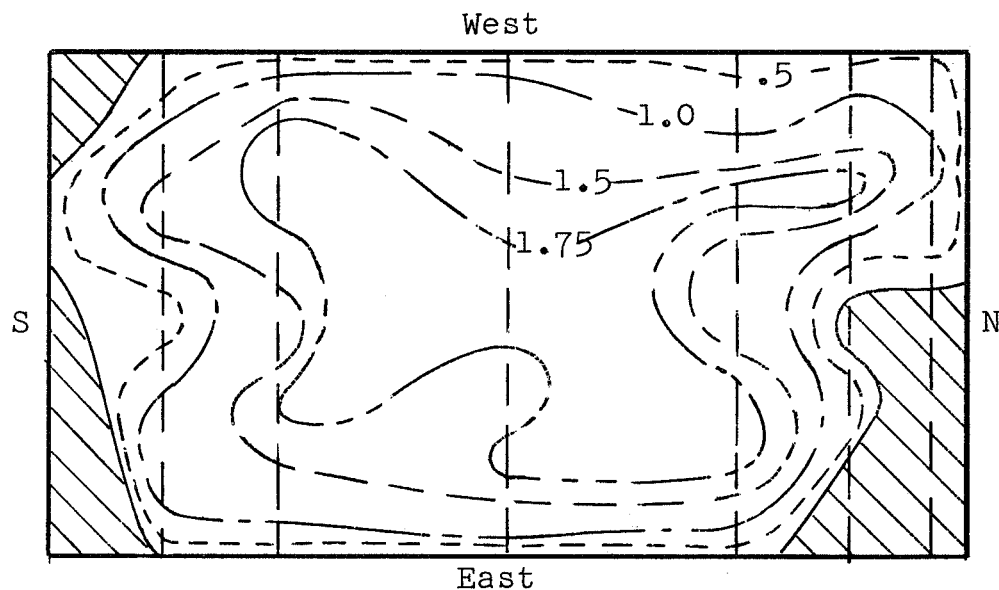


(a) With vanes. $n = 1$; $f = 15$ inches.

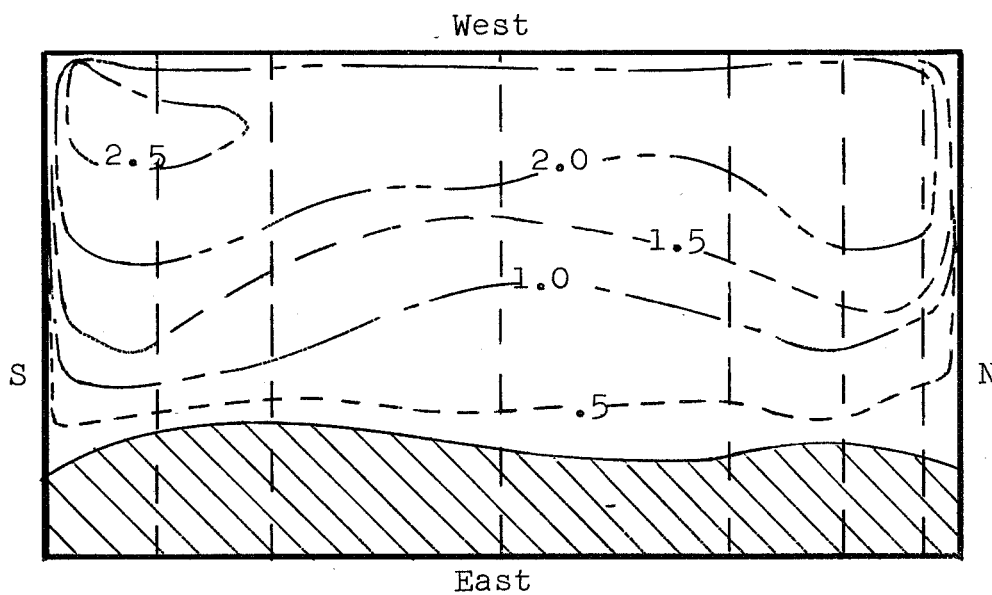


(b) No vanes.

Figure 36.- Dimensionless exit velocity contours V_2/V_{21} at $2\theta = 16.8^\circ$.
View looking upstream.

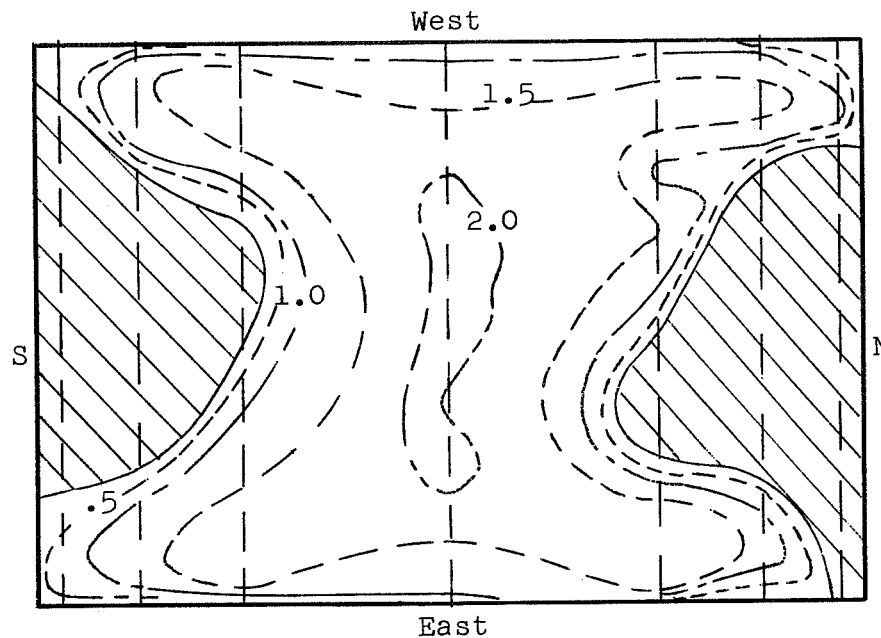


(a) With vanes. $n = 3$; $f = 15$ inches.

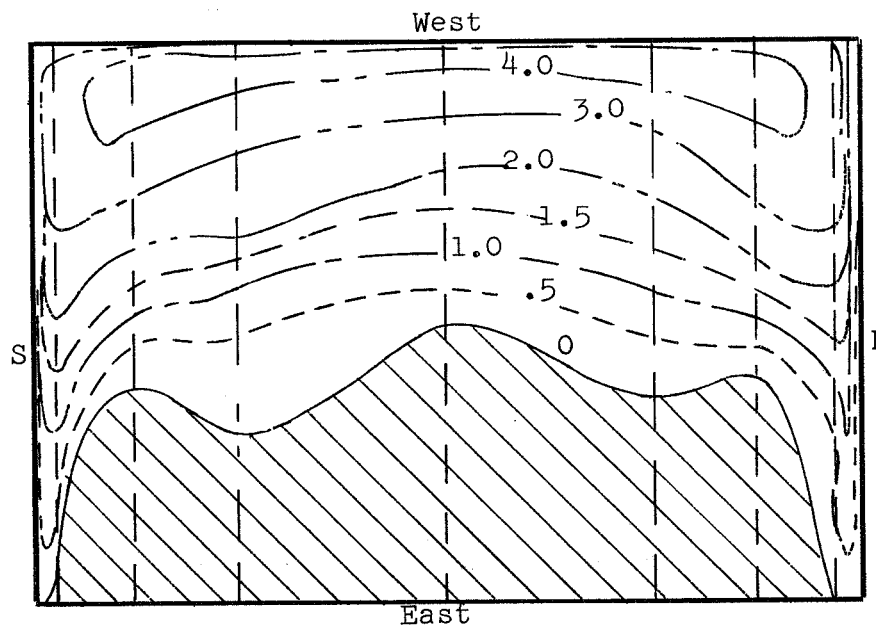


(b) No vanes.

Figure 37.- Dimensionless exit velocity contours V_2/V_{2i} at $2\theta = 24.5^\circ$.
View looking upstream.

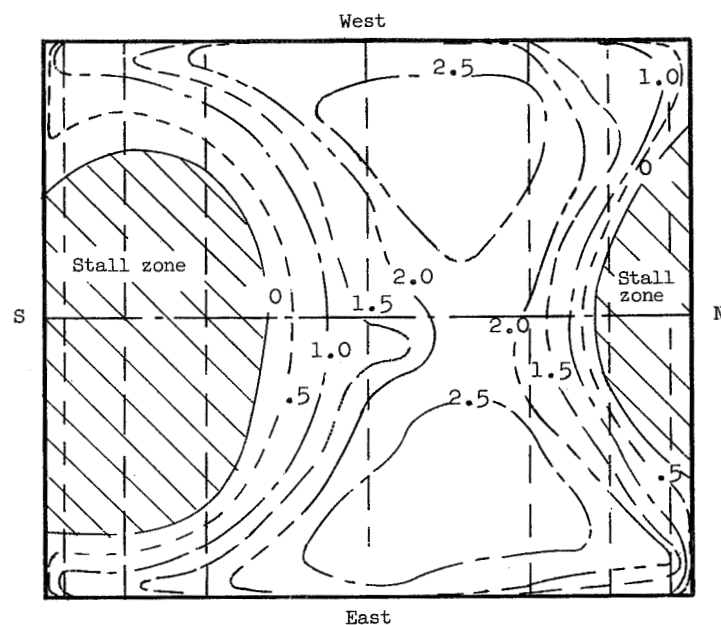
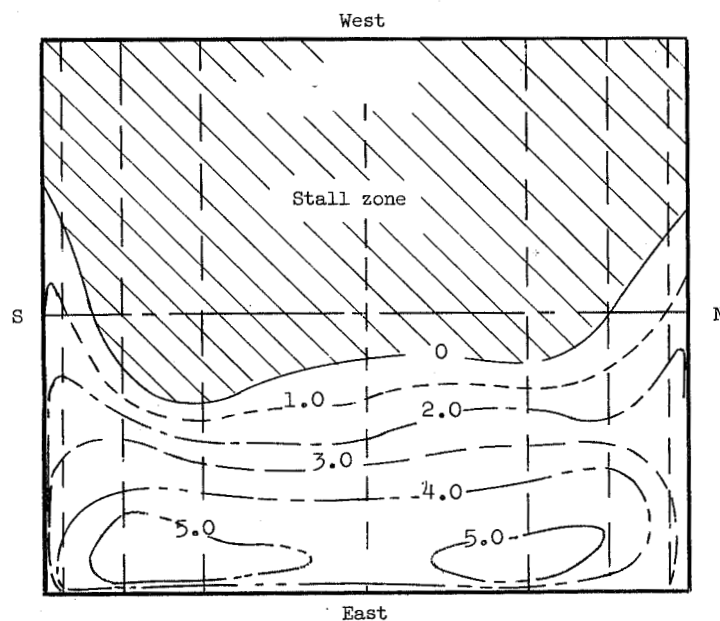


(a) With vanes. $n = 4$; $f = 15$ inches. Modified holders, taped ends.



(b) No vanes.

Figure 38.- Dimensionless exit velocity contours V_2/V_{2i} at $2\theta = 31.10^\circ$.
View looking upstream.

(a) With vanes. $n = 5$; $f = 9$ inches.

(b) No vanes.

Figure 39.- Dimensionless exit velocity contours V_2/V_{2i} at $2\theta = 42.0^\circ$.
View looking downstream.